PNL-6800 Pt. 4
UC-408

17

Pacific Northwest Laboratory Annual Report for 1988 to the DOE Office of Energy Research

Part 4 Physical Sciences
March 1989

Prepared for the U.S. Department of Energy
under Contract DE-AC06-76RLO 1830

Pacific Northwest Laboratory
Operated for the U.S. Department of Energy
by Battelle Memorial Institute

Battelle

DISCLAIMER

PACIFIC NORTHWEST LABORATORY
operated by
BATTELLE MEMORIAL INSTITUTE
for the
UNITED STATES DEPARTMENT OF ENERGY
under Contract DE-AC06-76RLO 1830

Printed in the United States of America
Available from
National Technical Information Service
United States Department of Commerce
5285 Port Royal Road
Springfield, Virginia 22161

NTIS Price Codes
Microfiche A01

Printed Copy

Pages	Price Codes
001-025	A02
026-050	A03
051-075	A04
076-100	A05
101-125	A06
126-150	A07
151-175	A08
176-200	A09
201-225	A10
226-250	A11
251-275	A12
276-300	A13

PNL-6800, Pt. 4
UC-408

Pacific Northwest Laboratory Annual Report for 1988 to the DOE Office of Energy Research

Part 4 Physical Sciences

L. H. Toburen and Staff

March 1989

Prepared for
the U.S. Department of Energy
under Contract DE-AC06-76RLO 1830

Pacific Northwest Laboratory
Richland, Washington 99352

PREFACE

This 1988 Annual Report from Pacific Northwest Laboratory (PNL) to the U.S. Department of Energy (DOE) describes research in environment, safety and health conducted during fiscal year 1988. The report again consists of five parts, each in a separate volume.

The five parts of the report are oriented to particular segments of the PNL program. Parts 1 to 4 report on research performed for the DOE Office of Health and Environmental Research in the Office of Energy Research. Part 5 reports progress on all research performed for the Assistant Secretary for Environment, Safety and Health. In some instances, the volumes report on research funded by other DOE components or by other governmental entities under interagency agreements. Each part consists of project reports authored by scientists from several PNL research departments, reflecting the multidisciplinary nature of the research effort.

The parts of the 1988 Annual Report are:

Part 1: Biomedical Sciences		
Program Manager: J. F. Park		D. L. Felton, Report Coordinator and Editor
Part 2: Environmental Sciences		
Program Manager: R. E. Wildung		S. G. Weiss, Report Coordinator and Editor G. P. O'Connor, Editor
Part 3: Atmospheric Sciences		
Program Manager: C. E. Elderkin		C. E. Elderkin, Report Coordinator E. L. Owczarski, Editor
Part 4: Physical Sciences		
Program Manager: L. H. Toburen		L. H. Toburen, Report Coordinator K. A. Parnell, Editor
Part 5: Environment, Safety, Health, and Quality Assurance		
Program Managers: L. G. Faust W. T. Pennell J. M. Selby		L. G. Faust and W. T. Pennell, Report Coordinators S. K. Ennor, Editor

Activities of the scientists whose work is described in this annual report are broader in scope than the articles indicate. PNL staff have responded to numerous requests from DOE during the year for planning, for service on various task groups, and for special assistance.

Credit for this Annual Report goes to the many scientists who performed the research and wrote the individual project reports, to the program managers who directed the research and coordinated the technical progress reports, to the editors who edited the individual project reports and assembled the five parts, and to Ray Baalman, editor in chief, who directed the total effort.

Members of the Scientific Advisory Committee, established in 1985, are:

Dr. Franklin I. Badgley	University of Washington
Dr. Leo K. Bustad	Washington State University
Dr. Franklin Hutchinson	Yale University
Dr. Albert W. Johnson	San Diego State University
Dr. J. Newell Stannard	University of Rochester; University of California, San Diego

W. J. Bair
T. S. Tenforde
Environment, Health and Safety
Research Program

Previous reports in this series:

Annual Report for:

1951	HW-25021, HW-25709
1952	HW-27814, HW-28636
1953	HW-30437, HW-30464
1954	HW-30306, HW-33128, HW-35905, HW-35917
1955	HW-39558, HW-41315, HW-41500
1956	HW-47500
1957	HW-53500
1958	HW-59500
1959	HW-63824, HW-65500
1960	HW-69500, HW-70050
1961	HW-72500, HW-73337
1962	HW-76000, HW-77609
1963	HW-80500, HW-81746
1964	BNWL-122
1965	BNWL-280, BNWL 235, Vol. 1-4; BNWL-361
1966	BNWL-480, Vol. 1; BNWL-481, Vol. 2, Pt. 1-4
1967	BNWL-714, Vol. 1; BNWL-715, Vol. 2, Pt. 1-4
1968	BNWL-1050, Vol. 1;, Pt. 1-2; BNWL-1051, Vol. 2, Pt. 1-3
1969	BNWL-1306, Vol. 1;, Pt. 1-2; BNWL-1307, Vol. 2, Pt. 1-3
1970	BNWL-1550, Vol, 1;, Pt. 1-2; BNWL-1551, Vol. 2, Pt. 1-2
1971	BNWL-1650, Vol. 1;, Pt. 1-2; BNWL-1651, Vol. 2, Pt. 1-2
1972	BNWL-1750, Vol. 1;, Pt. 1-2; BNWL-1751, Vol. 2, Pt. 1-2
1973	BNWL-1850, Pt. 1-4
1974	BNWL-1950, Pt. 1-4
1975	BNWL-2000, Pt. 1-4
1976	BNWL-2100, Pt. 1-5
1977	PNL-2500, Pt. 1-5
1978	PNL-2850, Pt. 1-5
1979	PNL-3300, Pt. 1-5
1980	PNL-3700, Pt. 1-5
1981	PNL-4100, Pt. 1-5
1982	PNL-4600, Pt. 1-5
1983	PNL-5000, Pt. 1-5
1984	PNL-5500, Pt. 1-5
1985	PNL-5750, Pt. 1-5
1986	PNL-6100, Pt. 1-5
1987	PNL-6500, Pt. 1-5

CONTENTS

Analytical Studies

Chernobyl Database Management

The Chernobyl Database project is developing and maintaining an information system to provide researchers with data relating to the Chernobyl nuclear accident of April 1986. The system is the official United States repository for Chernobyl data, and includes a bibliography and diverse quantitative measurements with supporting information. Use of information contained in this system presents an opportunity for researchers to evaluate predictions of historical risk, transport, and deposition models previously based on laboratory experiments, computer simulations, and limited measurement data.

Project staff have used structured systems analysis techniques to analyze, design, and document the system. Measurement data have been obtained and will be solicited in the future from domestic and foreign organizations. A committee of database advisors, representing a spectrum of potential users, reviews data to determine research usefulness and to develop approaches for standardizing data in the system. Researchers can retrieve data via on-line menus and forms or by requesting information from project staff. The analysis, design, and user interface is implemented. In subsequent years, project staff will continue to obtain and load data, enhance quality and standardization of data, publicize the system, and support researcher requests.

Chernobyl Database

F. Carr, Jr., J. R. Williams, J. A. Mahaffey, J. K. Soldat, L. L. Cadwell, E. A. Lepel, and J. M. McClelland

The work performed on the Chernobyl Database project during fiscal year 1988 has included acquiring publications for the database library, adding 30,000 sample measurements to the database, developing a user interface to allow researchers to access the database via a series of menus and forms, and soliciting database users.

A collection of publications containing information about Chernobyl and the Chernobyl accident has been assembled to form a library. Information pertaining to documents and the organizations which published them has been incorporated into the database. Approximately 130 publications reside in the library and computerized bibliography, half collected this past year. Many publications have been obtained through an advisory committee which provides technical expertise and guidance to the project.

Four major data sets have been added this past year to the sample measurements, which are stored electronically. These are from the Brookhaven National Laboratory, the U.S. Environmental Protection Agency, Stone and Webster, and Commissariat A L'Energie Atomique (France). These data sets, along with the data entered previously, are being standardized to aid in the reporting and selection capabilities of the database. Table 1 shows the number of samples obtained from each data set entered. Tables 2, 3, and 4 show the distribution of these samples by media and geographic location. Table 5 shows the number of measurements by isotope. The total in Table 5 differs from the totals in Tables 1, 2, and 3 because samples may have multiple isotopic analyses.

TABLE 1. Breakdown of Samples by Data Set Source

Data Set Source	Number of Samples
EG&G Idaho, Inc.	7,067
Department of Social and Health Services (Washington State)	454
Environmental Protection Agency (Domestic)	6,301
Environmental Protection Agency (Foreign)	3,806
Brookhaven National Laboratory	38
Stone and Webster	9,407
Commissariat A L'Energie Atomique (France)	20,463
Total	47,536

A user interface has been developed to allow researchers to use the database via selections from menus and forms. It allows inexperienced computer users to view data.

Poster and slide presentations indicated the developmental approach, content, and functioning of the Chernobyl Database. The poster was

presented at the Health Physics Society and Radiation Research Society meetings. Slides were presented and the database was demonstrated to scientific representatives of various governmental agencies. As a result, 25 requests for information about the database have been received. Of these, 10 requests have resulted in on-line user access to the database.

TABLE 2. Breakdown of Samples by Media

Media	Number of Samples
Air	25,746
Animal	4,212
Earth	7,190
Human	710
Vegetation	6,950
Water	2,381
Other	264
Unknown	83
Total	47,536

TABLE 3. Number of Samples by Country

Country	Number of Samples
Austria	2,318
Belgium	1,230
Bulgaria	74
Canada	109
China	480
Czechoslovakia	33
Denmark	1,179
Finland	4,445
France	3,381
Germany, FR	3,096
Germany, GDR	57
Greece	1,959
Greenland	7
Hong Kong	1
Hungary	1,841
Ireland	40
Israel	86
Italy	4,494
Japan	1,496
Korea	12
Luxembourg	9
Netherlands	801
Norway	433
Poland	454
Portugal	28
Rumania	32
Spain	143
Sweden	3,644
Switzerland	1,318
Turkey	112
United Kingdom	4,745
United States	7,418
USSR	1,555
Yugoslavia	238
Other	268
Total	47,536

TABLE 4. Breakdown of Samples by State for Data Recorded in the United States

State	Number of Samples	State	Number of Samples
AK	95	NC	149
AL	281	ND	103
AR	112	NE	134
AZ	73	NH	110
CA	232	NJ	114
CO	121	NM	105
CT	95	NV	159
DC	16	NY	450
DE	76	OH	291
FL	205	OK	96
GA	67	OR	110
HI	88	PA	370
IA	94	RI	71
ID	214	SC	117
IL	107	SD	84
IN	95	TN	218
KS	93	TX	199
KY	64	UT	73
LA	48	VA	116
MA	62	VT	74
MD	44	WA	692
ME	105	WI	107
MI	118	WV	71
MN	130	WY	74
MO	119	Unknown	402
MS	109		
MT	66	Total	7,418

TABLE 5. Breakdown of Sample Counts by Isotope

Isotope	Number of Samples
Alpha	233
Antimony	107
Barium	2,712
Beta	4,617
Bismuth	260
Cerium	596
Cesium	14,009
Cobalt	333
Hydrogen	503
Iodine	17,502
Lanthanum	674
Molybdenum	378
Neptunium	210
Niobium	182
Potassium	1,301
Radium	238
Radon	358
Rhodium	267
Ruthenium	3,100
Strontium	1,032
Tellurium	2,220
Thorium	453
Uranium	378
Zinc	263
Zirconium	783
Other	6,204
Total	58,913

Measurement and Dosimetry

Supercritical Fluid Analytical Methods

Supercritical fluids are providing the basis for new and improved methods across a range of analytical technologies. New methods are being developed to allow the detection and measurement of compounds that are incompatible with conventional analytical methodologies. Characterization of process and effluent streams for synfuel plants requires instruments capable of detecting and measuring high-molecular-weight compounds, polar compounds, or other materials that are generally difficult to analyze. The purpose of this program is to develop and apply new supercritical fluid techniques for extraction, separation, and analysis. These new technologies will be applied to previously intractable synfuel process materials and to complex mixtures resulting from their interaction with environmental and biological systems.

Supercritical Fluid Analytical Methods

R. D. Smith, B. W. Wright, and H. R. Udseth

Chromatographic methods combined with mass spectrometry (MS) compose a nearly ideal analytical approach for characterizing complex mixtures. At Pacific Northwest Laboratory (PNL), supercritical fluid methods are being developed for materials where conventional gas or liquid chromatographic (LC) methods and existing mass spectrometric methods are inadequate (see references following this article). The advantages of supercritical fluid chromatography (SFC) accrue from the nature of supercritical fluids. The solvating properties of supercritical fluid mobile phases approach those of liquid phases, yet solute diffusivity typically remains one to two orders of magnitude higher. These properties allow high separation efficiencies to be realized while exploiting the variable and often high solvating power of the supercritical fluid. Consequently, SFC can separate thermally labile and nonvolatile solutes [a procedure not possible with gas chromatography (GC)] and can do so with higher efficiencies.

The SFC-MS combination, based upon expansion of the fluid directly into the mass spectrometer ion source, is increasingly practiced in a number of laboratories. The SFC restrictor largely dictates SFC-MS performance and currently defines the range of applicability. Several commercial SFC-MS interfaces are now available. Chemical ionization (CI) has been shown to produce detection limits which are generally superior to electron ionization (EI) because the latter necessitates high dilution of the expanded fluid to the requisite low pressures for EI. Greater sensitivity, compared to EI, in combination with "EI-like" spectra, can be obtained by CO_2 charge exchange under CI conditions.

A major advantage of SFC-MS is the tremendous selectivity possible. The use of high-resolution MS can further enhance this capability to resolve components of the same nominal molecular weight, to aid identification, and to eliminate background complications. Figure 1 illustrates the simultaneous high-resolution MS detection of nine organophosphorus insecticides from the single capillary SFC separation.

One possible approach to truly universal detection we are currently exploring is based upon the change in the speed of sound in a fluid mixture. In the vicinity of a fluid's critical point and in practice for any substantially compressible fluid, any change in fluid composition results in a substantial change in the speed of sound (the speed of sound *approaches zero* at a fluid's critical point). In the region of high dilution relevant to SFC, elution of an analyte results in a shift in the speed of sound that is linearly related to analyte concentration in the fluid. To test this concept in our laboratory, a high-pressure ultrasonic detection cell having a volume too large for practical SFC detection (~2 mL) was constructed. Figure 2 shows the experimental arrangement, which used a lock-in amplifier to measure the phase shift or attenuation between sending (excitor) and receiving (pickup) piezoelectric crystals. Our initial experiments have resulted in detection limits of $\sim 10^{-7}$ M for naphthalene in CO_2. Of course, gradient programming methods would necessitate the use of a reference cell or other method to correct for changes in the speed of sound for the pure mobile phase. Since detection limits are largely determined by the precision of temperature and pressure control, substantial improvements may be feasible. Very small-volume detectors, perhaps fabricated using modern microelectronic methods to form an interdigital electrode array of transducers, should give adequate detection limits for capillary SFC. Such a detector would be

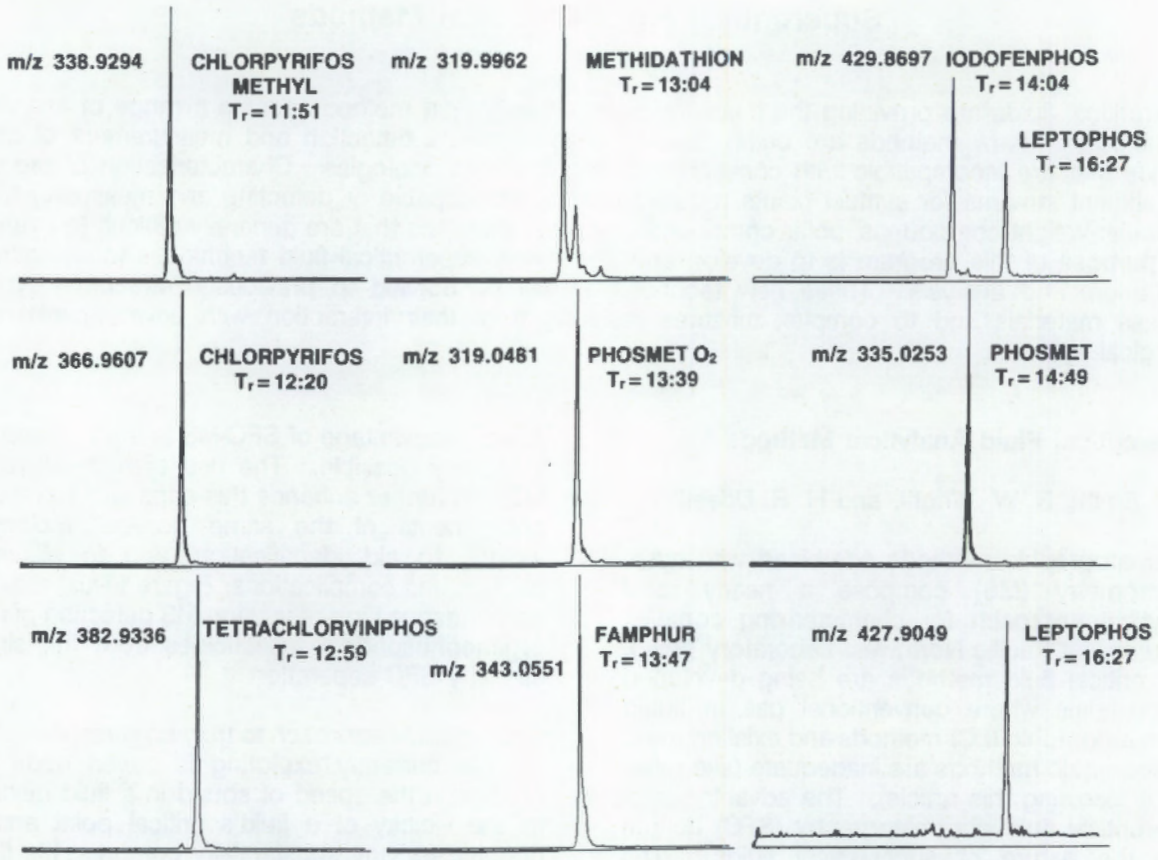

FIGURE 1. Selected Ion Chromatograms for Nine Organophosphorus Insecticides Obtained Using High-Resolution MS to Allow Enhanced Selectivity in Detection

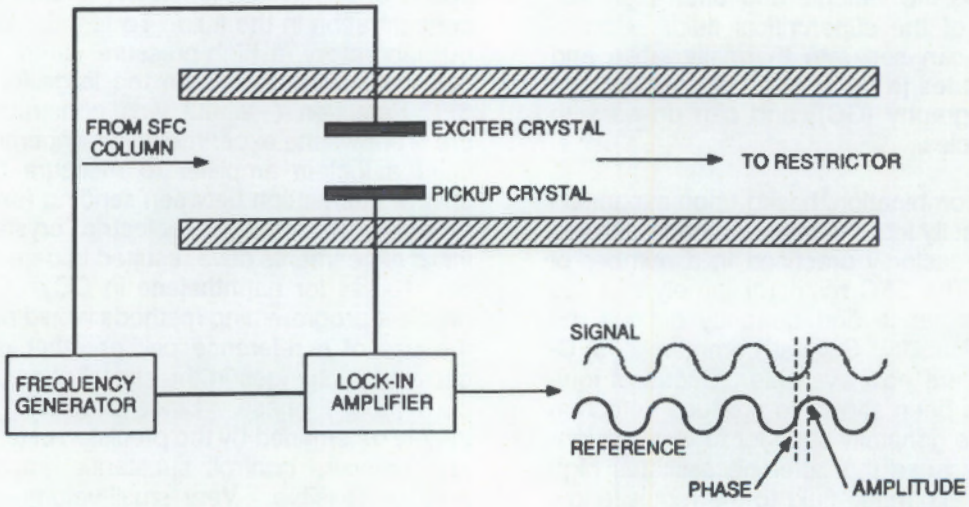

FIGURE 2. An Arrangement for a Universal Detector for SFC. Detection can be based upon either attenuation of the ultrasonic waves or with greater sensitivity by measurement of the phase shift due to changes in the speed of sound.

universal and potentially quite sensitive, but would have to be manufactured in a manner to allow easy replacement of the ideally inexpensive detection cell.

The development of the high flow rate (HFR) interface for SFC-MS (Smith and Udseth 1987) has allowed some of the difficulties associated with the transfer of higher molecular weight and lower volatility samples to be overcome. This system also allows the use of either packed microbore (high-performance LC-type) or larger-diameter dynamic range limitations. This design also permits optimum CI ion source operation largely independent of SFC flow rate and the choice of CI reagents, along with operation under isobaric or pressure-programmed conditions.

Ionic polyether antibiotics, known as ionophores, are used commercially to combat coccidiosis, a protozoan infestation of the intestine, in poultry, cattle, sheep, and swine. These compounds are able to form lipid-soluble complexes with cations, providing a transport mechanism for cations across lipophilic membranes. The mass spectra and structures for two thermally labile ionophores (which decompose above ~100°C) obtained following capillary SFC using a CO_2/2-propanol mobile phase are shown in Figures 3 and 4. Abundant protonated molecular ions were produced for these compounds (Figures 3 and 4a).

The abundant fragment ion at m/z 922 in the mass spectrum shown in Figure 4a corresponds to the loss of 1,3-propanediol from the protonated molecule. By increasing the restrictor heater temperature from 145°C (Figure 4a) to 300°C (Figure 4b), an increase in lower molecular weight fragment ions and a decrease in the relative intensity of the protonated molecule were obtained. This allows the degree of fragmentation to be controlled and produces increased information for structural identification. Even when analyzed using the capillary column, the chromatographic peaks for these ionophore compounds exhibited substantial tailing, reflecting their highly polar nature. Improved chromatography should be obtainable by using a more inert capillary column.

The HFR interface for SFC-MS is useful for obtaining high-quality (high signal-to-noise ratio for protonated molecules) CI mass spectra of thermally labile, high molecular weight, biologically active molecules of low volatility. The system can be operated with alcohol-modified fluids, using either packed microbore or capillary columns for chromatography. Work is continuing toward optimization of the HFR SFC-MS system for analysis of these types of biologically significant molecules.

References

Kalinoski, H. T., and R. D. Smith. 1988. "Pressure Programmed Microbore Column Supercritical Fluid Chromatography-Mass Spectrometry for the Determination of Organophosphorus Insecticides." *Anal. Chem.* 60:529.

Kalinoski, H. T., H. R. Udseth, E. K. Chess, and R. D. Smith. 1987. "Capillary Supercritical Fluid Chromatography-Mass Spectrometry." *J. Chromatogr.* 394:3.

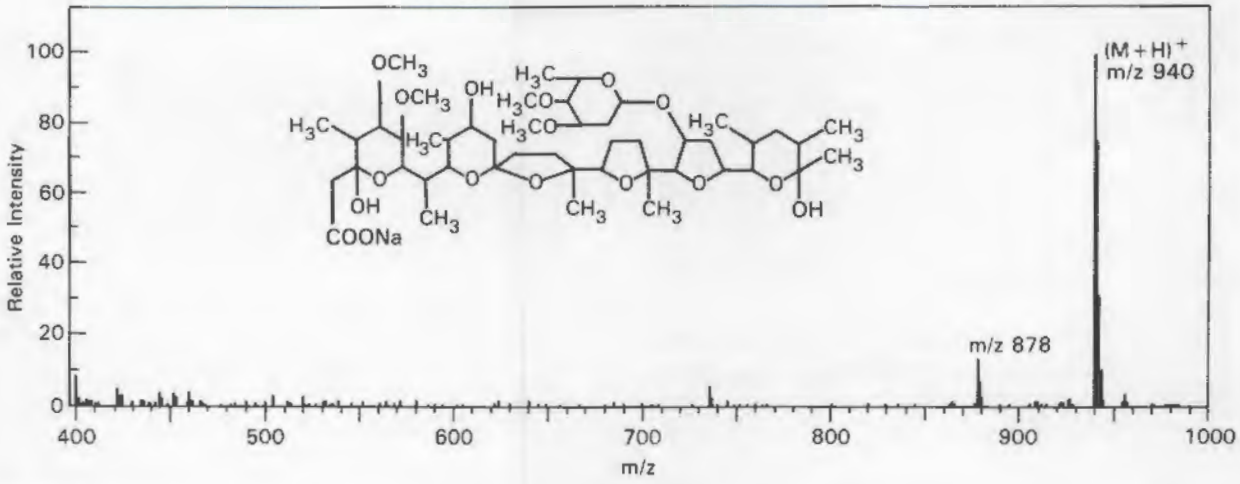

FIGURE 3. Positive Ion 2-Propanol CI Mass Spectrum of a Polyether Antibiotic Inophore (inset) Obtained Following SFC

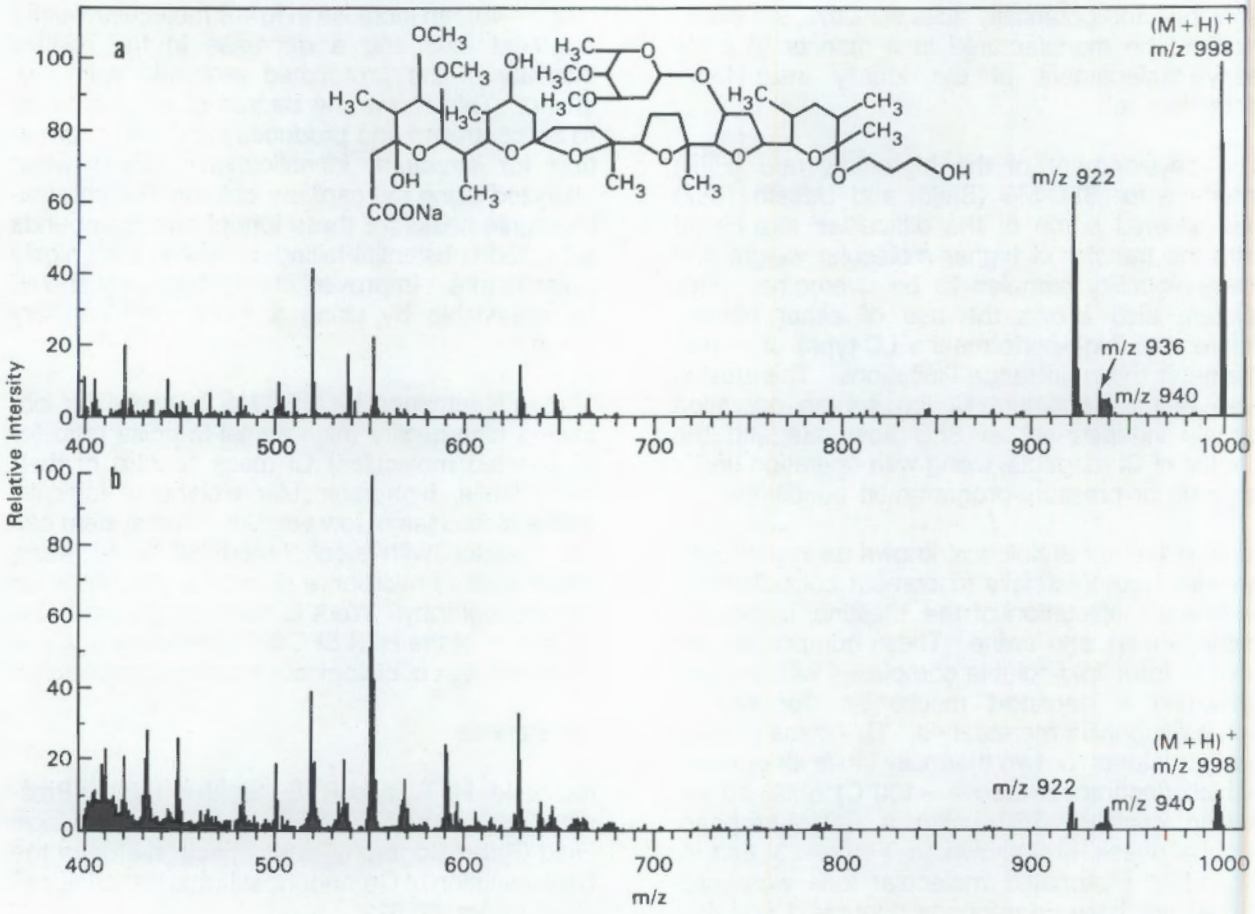

FIGURE 4. Positive Ion 2-Propanol CI Mass Spectra of a Polyether Antibiotic Ionophore (inset) Obtained at a) Low and b) High Restrictor Heater Temperatures

Kalinoski, H. T., H. R. Udseth, B. W. Wright, and R. D. Smith. 1987. "Analytical Applications of Capillary Supercritical Fluid Chromatography-Mass Spectrometry." *J. Chromatogr.* 400:307.

Smith, R. D., W. D. Felix, J. C. Fjeldsted, and M. L. Lee. 1982. "Capillary Column Supercritical Fluid Chromatography/Mass Spectrometry." *Anal. Chem.* 54:1883.

Smith, R. D., J. C. Fjeldsted, and M. L. Lee. 1982. "Direct Fluid Injection Interface for Capillary Supercritical Fluid Chromatography-Mass Spectrometry." *J. Chromatogr.* 247:231.

Smith, R. D., H. T. Kalinoski, and H. R. Udseth. 1987. "Fundamentals and Practice of Supercritical Fluid Chromatography-Mass Spectrometry." *Mass Spectrom. Rev.* 6:640.

Smith, R. D., H. T. Kalinoski, H. R. Udseth, and B. W. Wright. 1984. "Rapid and Efficient Capillary Column Supercritical Fluid Chromatography with Mass Spectrometric Detection." *Anal. Chem.* 56:2476.

Smith, R. D., and H. R. Udseth. 1983a. "Direct Mass Spectrometric Analysis of Supercritical Fluid Extraction Products." *Sep. Sci. Technol.* 18:245.

Smith, R. D., and H. R. Udseth. 1983b. "Mass Spectrometry with Direct Supercritical Fluid Injection." *Anal. Chem.* 55:2266.

Smith, R. D., and H. R. Udseth. 1983c. "New Method for the Direct Analysis of Supercritical Fluid Coal Extraction and Liquefaction." *Fuel* 62:466.

Smith, R. D., and H. R. Udseth. 1984. "Direct Supercritical Fluid Injection Mass Spectrometry of Mycotoxins." *Biomed. Mass Spectrom.* 10:577.

Smith, R. D., and H. R. Udseth. 1987. "A Mass Spectrometer Interface for Microbore and High Flow Rate Capillary Supercritical Fluid Chromatography with Splitless Injection." *Anal. Chem.* 59:13.

Smith, R. D., and H. R. Udseth. 1988. "High Efficiency Separation Techniques." *Chem. Brit.* 24:350.

Smith, R. D., B. W. Wright, and H. T. Kalinoski. 1986. "Supercritical Fluid Chromatography-Mass Spectrometry (SFC-MS)." In *Progress in HPLC: Volume 4 1985-1986; Supercritical Fluid Chromatography*, eds. H. Parvez, M. Yoshioka, and S. Parvez. V. N. U. Science Press, Holland.

Smith, R. D., B. W. Wright, and H. R. Udseth. 1984. "Supercritical Methods in Analytical Chemistry." In *Anal. Spectros. Sym. Ser.*, ed. W. S. Lyon, Vol. 19, p. 375. Elsevier Scientific Publishing Co., Amsterdam, The Netherlands.

Wright, B. W., H. R. Udseth, E. K. Chess, and R. D. Smith. 1988. "Supercritical Fluid Chromatography and Supercritical Fluid Chromatography/Mass Spectrometry for Analysis of Complex Hydrocarbon Mixtures." *J. Chromatogr. Sci.* 28:228.

Development of Capillary Electrophoresis-Mass Spectrometry

R. D. Smith, J. A. Loo, C. J. Barinaga, and H. R. Udseth

The chemical analysis of complex mixtures continues to pose tremendous challenges. Gas chromatography-mass spectrometry (GC-MS) has become established as the definitive technique for the analysis of many compound mixtures due to its high selectivity and excellent sensitivity. The two independent dimensions of information provided by the high-resolution separations of capillary GC and the mass spectra permit rapid detection and identification of most amenable compounds with an extremely high degree of confidence. Unfortunately, only a small fraction of the compounds of possible interest to many areas of research or having practical importance can be addressed by GC-MS. This limitation results from the necessity of a minimal vapor pressure and thermal stability of the analyte in both the chromatographic separation and transport through the mass spectrometer interface (where gas-phase electron impact or chemical ionization methods are used almost exclusively).

Capillary zone electrophoresis (CZE) is a form of free zone electrophoresis and one of several capillary electrophoresis formats conducted in small diameter capillaries and capable of ultra-high-resolution separations. Capillary zone electrophoresis separations obtaining more than 10^6 theoretical plates in less than 20 min have been demonstrated. Separations are based on differences in the electrophoretic mobilities of analytes. Electro-osmotic flow of the buffer medium makes it an elution technique which resembles chromatography. Thus CZE provides high-resolution separations and selectivities which can be manipulated by changing the electrophoretic medium (i.e., typically pH and buffer composition as well as equilibria with migrating micellar phases). Capillary zone electrophoresis is amenable to broad compound classes with application limited only by the necessity for solubility in the buffer and a non-zero net electrophoretic mobility. This technique is limited to small capillary diameters (generally <100-μm i.d.) to suppress convection caused by a radial temperature gradient through the electrophoretic medium from Joule heating. This allows the high efficiencies resulting from the nearly flat flow profile provided by electro-osmosis to be realized. The major limitations of CZE are related to the sensitivity and range of application possible with on-column detection methods [ultraviolet (UV) and fluorescence].

We have recently developed an improved electrospray ionization interface for capillary zone electrophoresis-mass spectrometry (CZE-MS). Our initial interface employed a vacuum-deposited metal film at the exit of the capillary to make an electrical contact with the eluting buffer and establish the electrospray field gradient (Olivares et al. 1987). This interface had several attractive features including negligible dead volume and avoidance of a nebulizing gas with the attendant problems (Bruins, Covey, and Henion 1987). We were able to demonstrate high-efficiency separations in excess of 10^5 theoretical plates with detection limits in the attomole range (Smith et al. 1988) using this interface for selected compounds.

This initial interface design did, however, impose significant limitations on the range of capillary electrophoretic (CE) separations that could be performed. The flow rates typically used were near the minimum at which a stable electrospray could be generated so that separations with low

electro-osmotic velocity (i.e., CZE with surface-modified capillaries, gel-filled capillaries, etc.) could not be performed. Since the buffer solution was directly electrosprayed, constraints were placed on its composition. Aqueous solutions could not be electrosprayed, nor could high-ionic-strength solutions. Since many CZE separations are optimally performed in aqueous solutions at high ionic strength, it was necessary to compromise the separations by the addition of organic solvents and the reduction of ionic strength to utilize the interface. Unfortunately, the use of a lower-ionic-strength buffer also lowers the maximum sample size that can be utilized without degrading separation efficiency decreasing the sensitivity of the method. The vacuum deposition of a metal film CZE electrode was also a tedious process. In addition, the vapor-deposited metal film had poor adhesion characteristics and a limited lifetime.

To circumvent these limitations, a new interface that does not require a metalized tip was designed and developed. In the new approach the electrical contact at the column exit is made through a flowing liquid sheath. Figure 1 shows a schematic illustration of one version of the liquid sheath electrode interface. The capillary and the sheath liquid are brought together via a Teflon® tee outside the probe body (not shown). The capillary protrudes slightly from the stainless steel tube (~0.3 mm) so that a positive flow of liquid from the sheath is necessary to make electrical contact. An auxiliary gas flow can be delivered through these tubes to flow over the tip in the direction of the electrospray.

The principal advantage of this interface is that it allows operation over a much broader range of electrophoresis conditions. The sheath flow can be readily varied in both composition and volume. Thus, the composition of the electrosprayed solution, which is the mixture of the sheath and the capillary eluant, can be readily varied independently of the separation buffer. If the buffer is aqueous, an organic solvent, such as methanol or acetonitrile, can be added in the desired amount at the capillary terminus. If the ionic strength of the buffer is too high, it can be effectively diluted by the sheath liquid at the terminus. Some additional benefits also accrue in this design. The removal of any metal contact eliminates any possibility of electrochemical processes involving the analyte and reduces the likelihood of a corona discharge. (Such discharges are most readily generated from micro protrusions on metal surfaces.) The sheath liquid can also be used for postcolumn derivatization, to mix reagent ions into the electrospray plume, and to introduce a calibration compound.

Figure 2 shows an example of an electrospray ionization spectra for a previously intractable buffer solution. Figure 2a is the negative ion spectra [the addition of oxygen as done by others (Whitehouse et al. 1985) is needed to suppress discharges] and 2b is the positive ion spectra from an aqueous solution of 0.05-M sodium dodecylsulfate (SDS). The solution cannot be electrosprayed directly, but the addition of 5 μL/min of isopropanol through the sheath produces a stable, well-behaved electrospray. Details of the interface design and performance have been published elsewhere (Smith, Barinaga, and Udseth 1988).

®Teflon is a registered trademark of E. I. du Pont de Nemours and Co., Wilmington, Delaware.

References

Bruins, A. P., T. R. Covey, and J. D. Henion. 1987. "Ion spray Interface for Combined Liquid Chromatography/Atmospheric Pressure Ionization Mass Spectrometry." *Anal. Chem.* 59:2642.

Olivares, J. A., N. T. Nguyen, C. R. Yonker, and R. D. Smith. 1987. "On-Line Mass Spectrometric Detection for Capillary Zone Electrophoresis." *Anal. Chem.* 59:1230.

Smith, R. D., C. J. Barinaga, and H. R. Udseth. 1988. "Improved Electrospray Ionization Interface for Capillary Zone Electrophoresis-Mass Spectrometry." *Anal. Chem.* 60:1948.

Smith, R. D., J. A. Olivares, N. T. Nguyen, and H. R. Udseth. 1988. "Capillary Zone Electrophoresis Mass Spectrometry Using an Electrospray Ionization Interface." *Anal. Chem.* 60:436.

Whitehouse, C. M., R. N. Dreyer, M. Yuamashita, and J. B. Fenn. 1985. "Electrospray Interface for Liquid Chromatographs and Mass Spectrometers." *Anal. Chem.* 57:675.

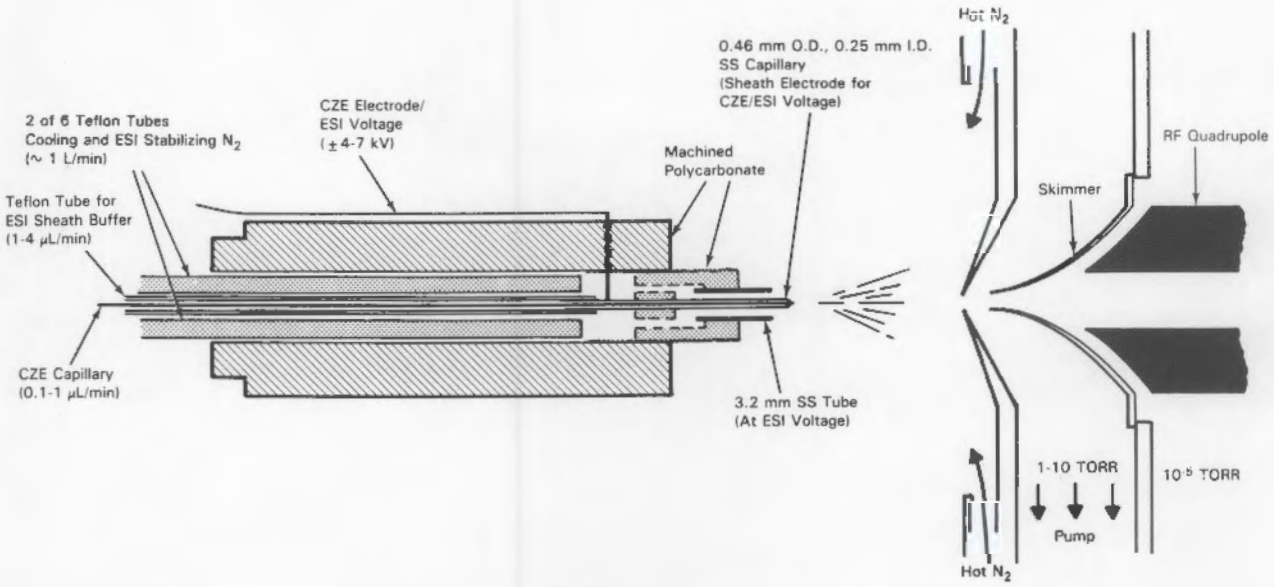

FIGURE 1. Schematic Illustration of the CZE-MS Interfaces Utilizing a Liquid Sheath Electrode (not to scale)

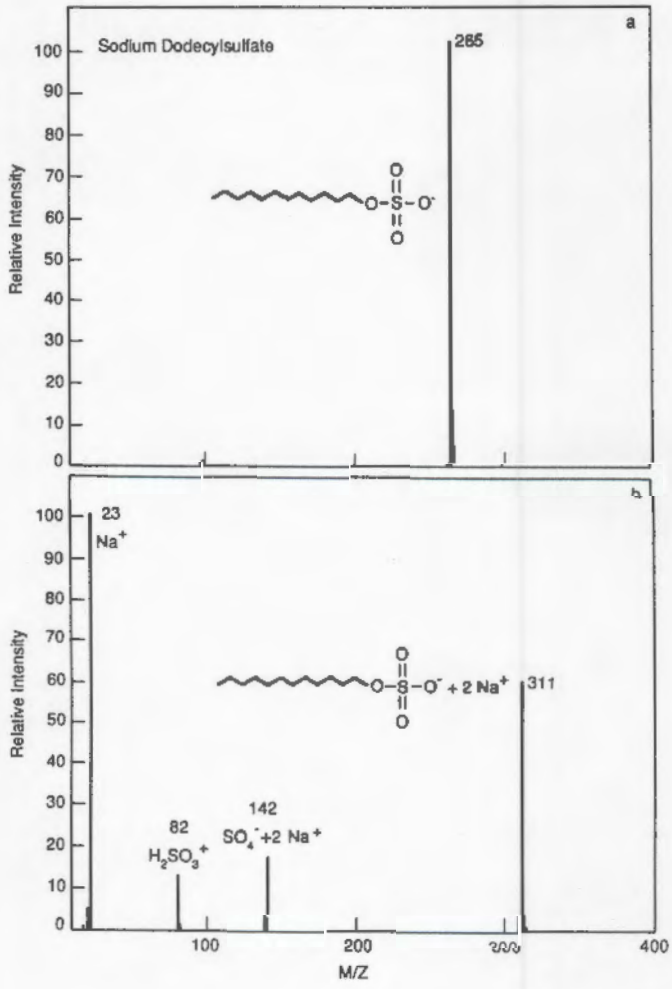

FIGURE 2. Electrospray Ionization Mass Spectra of Aqueous Solutions of Sodium Dodecylsulfate Obtained in the a) Negative and b) Positive Ion Modes

Lasers in Environmental Studies

High-resolution lasers have properties which allow them to address extremely difficult problems in trace isotope analysis, problems which previously had no solution or required very large and expensive instrumentation such as accelerator mass spectrometry. In prior years this program has shown how double-resonance ionization mass spectrometry (DRIMS) with single-mode continuous wave (cw) lasers can provide analytical methodology for the measurement of rare isotopes at abundances of less than 1 part in 10^{12} with respect to other isotopes of the same element. Measurements on the isotope ^{90}Sr were begun in this year as a full test case for these techniques. Also, the development of the graphite furnace source for the atomization of real environmental samples has continued.

Double-Resonance Ionization Spectroscopy of ^{90}Sr

B. A. Bushaw and G. K. Gerke

The isotope ^{90}Sr is an environmentally important radionuclide generated in nuclear power and weapons cycles. Its high yield from fission processes, strong incorporation into bone material, and radioactive half-life, which nearly matches the biological (bone) half-life, require extremely sensitive measurement capabilities. However, current nuclear counting methods are difficult, requiring chemical separation and a long waiting period for the grow-in and subsequent counting of the ^{90}Yb daughter. Even with this approach the measurement capabilities are generally deficient, not being able to reach the detection limits given by regulatory guidelines. This, coupled with background levels of 10^{-10} to 10^{-13} abundance with respect to stable strontium isotopes and its spectroscopic and chemical similarity to the previously studied barium isotopes, make ^{90}Sr an ideal candidate for full demonstration of the cw-DRIMS technique on environmentally important species.

The excitation scheme uses two single-frequency ring dye lasers; the first dye laser is tuned to the 460.7 nm resonance line and the second dye laser then populates Rydberg levels (n = 12 to 15) of the atoms. This excitation pathway can be saturated (transferring as much as 30% to 50% of the atomic population into the Rydberg state) without focusing the laser beams and thus provides good spatial overlap with the atomization source. The Rydberg atoms are then ionized with a cw-CO_2 laser. Coincidence with the $4d^2\ ^1D_2$ auto-ionizing level allows saturation of the photoionization step. Since the ionization step is carried out with an auxiliary laser independent of the resonance excitation lasers, saturation of the ionization step does not significantly degrade the selectivity of the resonance steps.

Figure 1 shows spectra of resonance excitation to the 5s14d $^1D_2$ Rydberg state for a sample containing approximately 1 part-per-million ^{90}Sr with respect to the stable isotopes (50-fg ^{90}Sr spiked into a sample containing 50-ng total Sr). The upper trace was recorded with the mass spectrometer turned off and shows the spectrum for the naturally occurring isotopes. The mass 87 isotope exhibits hyperfine splitting due to the I = 9/2 nuclear spin. The even isotopes (84, 86, and 88) which have no nuclear spin exhibit single peaks and a regular progression with spacings of ~250 MHz due primarily to the mass effect. The lower trace shows the spectrum with the mass spectrometer tuned to mass 90 (and signal integration period increased by a factor of 10) to measure the isotope shift for ^{90}Sr. The observed shift is only -5 MHz from the predominant mass 88 isotope. This is due to the filling of a nuclear neutron shell in going from mass 88 to 90--the large volume shift almost exactly counterbalances the normal mass shift. Under these circumstances a laser selectivity of only ~100 is observed, due primarily to the -225 MHz shift in the first resonance. Several other $^1S_0$ and $^1D_2$ Rydberg states have been investigated as shown in Table 1. Unfortunately, they all show similarly small 88 to 90 isotope shifts of 10 MHz or less. An overall selectivity (laser + mass spectrometer) of 10^9 is achieved under these circumstances. While this is useful for many measurements on real samples, it is not sufficient to reach background levels. In an effort to improve the laser selectivity, we will study states with doubly excited configurations where the promotion of both 5s electrons to higher p and d orbitals should increase the volume shift even further. It is hoped that the increased volume shift for these states will place spectral position of the ^{90}Sr

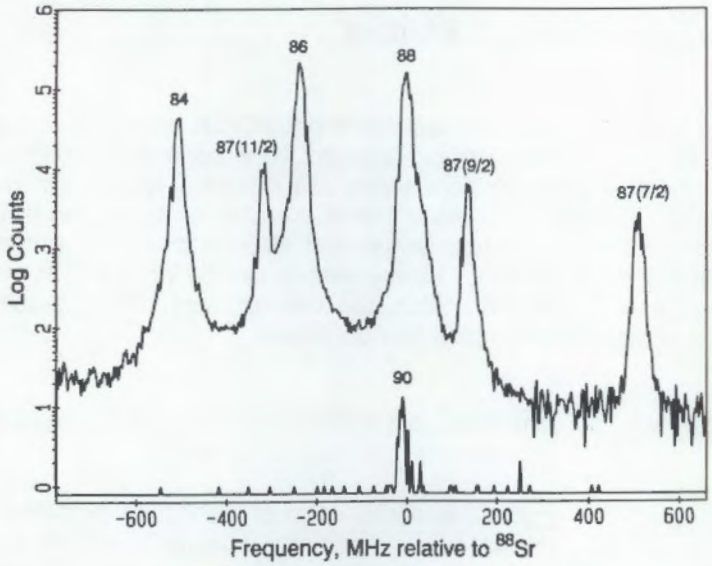

FIGURE 1. Double-Resonance Excitation Spectrum of the 5s14d $^1D_2$ Rydberg State of Strontium. The sample contained 50 ng of natural strontium (as aqueous nitrate) and was spiked with 50 fg of ^{90}Sr. The upper trace was recorded without mass selection and shows the spectrum for the naturally occurring isotopes. The lower trace is selected for mass 90 and shows the isotope shift of ^{90}Sr with respect to natural isotopes.

isotope approximately halfway between the 86 and 88 isotopes. If states with 88 to 90 shifts of greater than 50 MHz can be found, the laser selectivity will be sufficient for measurement at background level abundances.

TABLE 1. Frequency Shifts Between Strontium 90 - 88 in Rydberg States

State	Shift, MHz
5s13s $^1S_0$	-7.0
5s15s $^1S_0$	0.6
5s12d $^1D_2$	-5.0
5s13d $^1D_2$	-10.2
5s14d $^1D_2$	-5.4

Graphite Furnace Characterization

B. A. Bushaw, M. E. Geusic, and J. T. Munley

During fiscal year 1987 this program demonstrated detection limits of 10^{-17} g for barium isotopes using a graphite furnace atomization source (Bushaw and Gerke 1988). While these are the best detection limits that have been demonstrated for these types of measurements, they are still limited by an overall atom detection efficiency of 0.05%. The single largest factor in this efficiency was transport of atoms from the furnace to the laser ionization region, estimated at 5%. Original studies were carried out with graphite tubes with an aspect ratio of 8 (2-mm diameter x 16-mm length). Center loading of samples into these tubes produced an atomic beam controlled by the aspect ratio of the tube, with beam divergence of ~20 degrees full width at half maximum (FWHM). Also, half of the sample is lost out of the rear of the double-ended tubes.

During fiscal year 1988, new furnace geometries have been investigated to improve the transport properties. The furnace assembly was mounted on a rotational feedthrough into the vacuum system so that the angular distribution of the furnace output could be measured by scanning the atomic beam across a small aperture at the entrance to a quadruple mass spectrometer. Figure 1 shows typical results for two different tube designs. It can be seen that the atomic beam divergence decreases with increasing tube-aspect ratio, to as little as 6 degrees FWHM with a length-to-diameter ratio of 15. Further improvements are minimal because of local pressure buildup within small diameter tubes--pressures must be kept low enough for the mean free path to be greater than the dimensions of the tube to prevent collisional broadening of the atomic beam. Also, very small diameter tubes are difficult to load and exhibit unacceptable memory effects when dealing with routine repetitive loadings. In light of these measurements, we have settled on a single-ended tube geometry with an aspect ratio of 10 (1.5-mm bore x 15-mm length). This geometry improves the transport efficiency by a factor of ~8 up to 40% and should lower detection limits into the subattogram range. Measurements on samples containing less than 10,000 atoms of the isotope of interest should be possible.

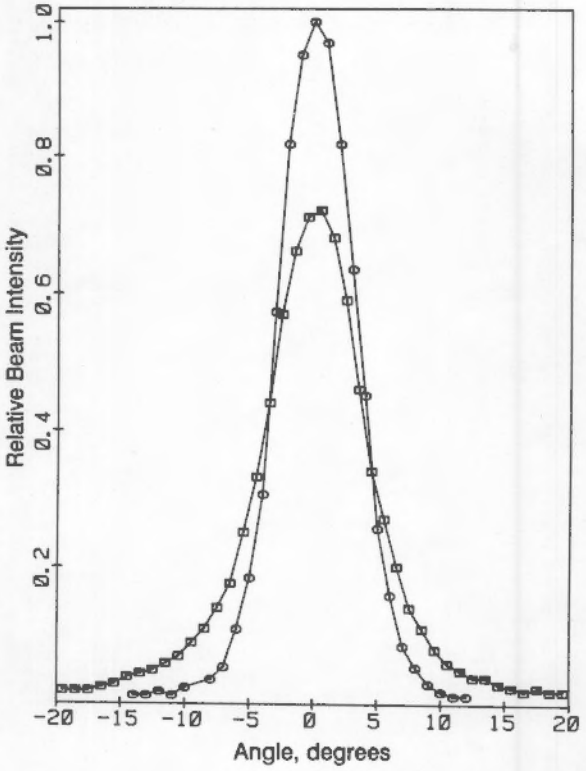

FIGURE 1. Atomic Beam Distribution Measured from Graphite Tube Furnaces. Squares are for a tube with an aspect ratio of 8 and the circles for an aspect ratio of 15.

Reference

Bushaw, B. A., and G. K. Gerke. 1988. "Lasers in Analytical Chemistry." In *Physical Sciences*, part 4 of *Pacific Northwest Laboratory Annual Report for 1987 to the DOE Office of Energy Research*, PNL-6500 Pt. 4, pp. 19-21, Pacific Northwest Laboratory, Richland, Washington.

Laser Measurements of ^{210}Pb

The goal of this project is to determine the correlation between radon exposure and the ratio of ^{210}Pb:^{208}Pb in the body. In order to measure at or near background levels, an analytical procedure capable of measuring ^{210}Pb in the presence of a 10^{10} excess of natural isotopes is being developed. The approach uses high-resolution continuous-wave (cw) laser ionization techniques coupled with mass spectrometry to provide the requisite selectivity and sensitivity sufficient for dealing with small samples.

Laser Spectroscopy of Pb

B. A. Bushaw, G. K. Gerke, and T. J. Whitaker

One of the first requirements for high-resolution studies involving double-resonance excitation to Rydberg states is simply knowing the energies of the states. For Pb, many of these are not known with sufficient accuracy for natural linewidth limited spectroscopy. Thus, we used a moderate-resolution pulsed laser system to map out the Rydberg series to an accuracy of 0.05 cm^{-1}. The first of two N_2 laser-pumped dye lasers was frequency doubled to the 283.3-nm resonance of Pb, while the second dye laser was scanned over the violet region of spectrum. This scheme mimics that used in the high-resolution studies with cw lasers. The Rydberg atoms were observed through ionization via absorption of a third photon, as shown in Figure 1. Those with long lifetimes (n>30) could also be observed by drifting out of the field-free excitation region into a field ionization region, as shown in Figure 1b. Six different Rydberg series have been observed and the strong [3/2,1/2],2 series has been detected out to principle quantum number n = 75. However, the region of primary interest for ^{210}Pb analyses is between n = 15 and n = 17. These states are important because further excitation with a CO_2 laser results in ionization just above the threshold, and transition probabilities are still large enough to saturate Rydberg generation without focusing of cw dye lasers.

High-resolution studies were begun after a new single-frequency ring dye laser was installed. It was converted to frequency-doubled operation and found to perform adequately, producing more than 1 mW at 283.3 nm. The laser has been incorporated into the laboratory's frequency measurement and stabilization systems. A measurement of the absolute frequency of the resonance line with this system has already resolved a discrepancy between the Massachusetts Institute of Technology and National Institute of Standards and Technology wavelength and energy-level monographs. First studies were directed at measuring the isotopic shifts and selectivity in the resonance line. This was accomplished with single-resonance experiments, photoionizing directly out of the resonance state with an ultraviolet Ar ion laser. This scheme is somewhat inefficient due to trapping by metastable states, but is sufficient for spectroscopic studies with microgram-sized samples. The shifts in the resonance line observed for the natural isotopes are shown in Figure 2. Note that the 1.5% abundant ^{204}Pb isotope is still several orders of magnitude above the tails from other isotopes. Measurements of the shifts agree (to within 0.4% for all components) with prior studies by the group at Karlsruhe (Thompson et al. 1983). The principal interference for ^{210}Pb, which occurs at +3974 MHz (with respect to ^{208}Pb), is the ^{207}Pb F = 3/2 component, located at +3019 MHz. The 955-MHz separation between the two should provide an isotopic selectivity of ~1000.

Preliminary results have also been attained in high-resolution double-resonance excitation to Rydberg states. The reduction in linewidth has been studied and it is estimated that the overall laser selectivity will exceed 10^8. When coupled with the mass spectrometer selectivity (~10^5), the overall selectivity requirements of the program should be reached easily. Measurements of the isotope shifts in the candidate Rydberg states (n = 15 to n = 17) are currently underway.

Reference

Thompson, R. C., M. Anselment, K. Bekk, S. Goring, A. Hanser, G. Meisel, H. Rebel, G. Schatz, and B. A. Brown. 1983. "High-Resolution Measurements of Isotope Shifts and Hyperfine Structure in Stable and Radioactive Lead Isotopes." *J. Phys. G* 9:443-458.

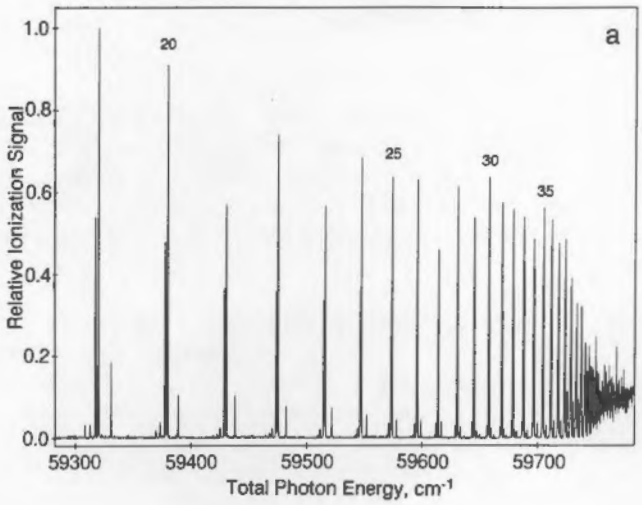

FIGURE 1. a) Even-Parity Rydberg Series of Pb at 0.3 cm^{-1} Resolution b) High-Lying Members of the Series Were Detected with Drifted Field Ionization

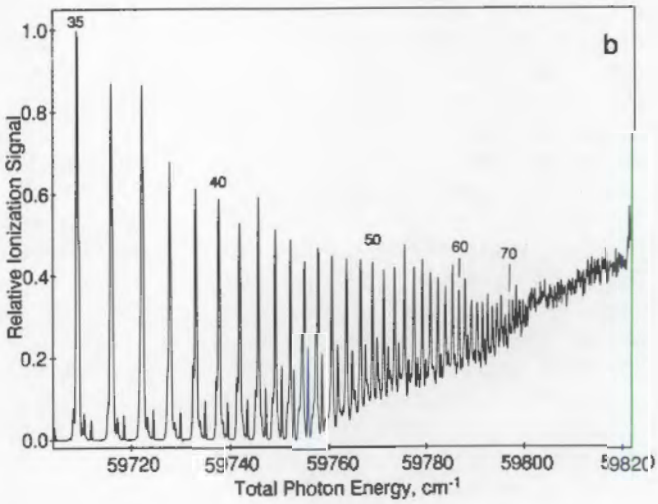

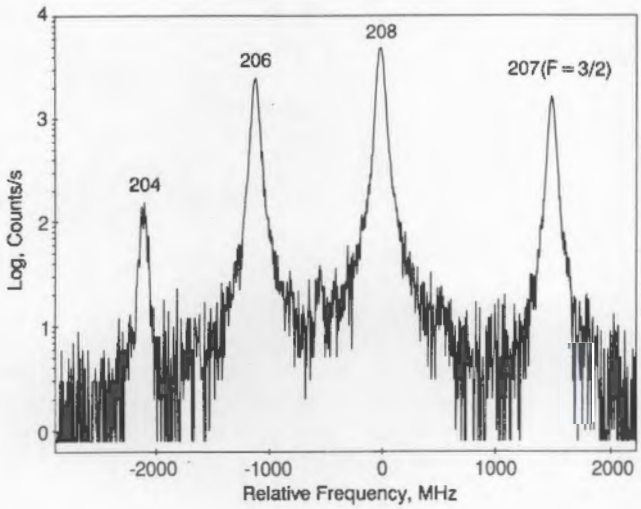

FIGURE 2. High-Resolution (full scan of ~0.3 cm^{-1}) Spectrum Showing Isotopic Structure in the Resonance Line of Pb. The ^{207}Pb F = 1/2 hyperfine component is off scale at -10,150 MHz.

DNA Adducts as Indicators of Health Risks

The objective of this program is to develop specific analytical methods for the determination of adducts formed in mammals by the reaction of carcinogenic compounds with cellular DNA. The DNA adducts are closely associated with the formation of cancerous cells, and their concentrations are thought to be related to the amount of exposure to carcinogenic chemicals. This program is developing mass spectrometric methods for analysis of adducts that may be applied toward health studies of human exposure to carcinogens.

Determination of Adducts of Polycyclic Aromatic Hydrocarbons to DNA

R. M. Bean, B. L. Thomas, E. K. Chess,
D. A. Dankovic, J. Pavlovich,[a] D. B. Mann,
G. A. Ross, C. G. Edmonds, and D. L. Springer

Metabolites of carcinogenic organic compounds have the ability to bond with deoxyribonucleic acids (DNA) to form DNA adducts. These species are retained for relatively long periods of time in the body, and are thought to be associated with the formation of cancer. Analysis of DNA for adducts may therefore provide an estimate of individual exposure to carcinogens. Methods currently being used for analysis of DNA adducts have been reviewed by Wogan and Gorelick (1985). In general, the currently available methods suffer either from a lack of sufficient sensitivity for environmental screening or from a lack of qualitative specificity. Although data on humans are sparse, we may expect, allowing for initial rapid decay after environmental exposure, adduct levels of 0.1 to 0.01 ng/mg of DNA. The objective of this project is to develop methods for the analysis of DNA adducts that will permit identification and quantitation of adducted polycyclic aromatic hydrocarbon (PAH) metabolites at environmental levels. Included within this objective is the preparation and characterization of DNA adducts to be used as analytical standards.

Several approaches to the analysis of DNA adducts are being undertaken. A primary analytical approach is to isolate the bound metabolites by cleaving the covalent bonds that attach them to the purine or pyrimidine bases of the DNA, and then to treat them with reagents that will increase their separability and their sensitivity to gas chromatography/mass spectrometry (GC/MS) detection. However, analysis of the metabolites while still bound to the nucleic acid base (as adducted nucleosides or nucleotides) would afford more specific information about the nature of the adduction process and its relation to carcinogenesis. Thus, separation and detection methods that do not require cleavage of the metabolite from the DNA bases are also being explored. These methods involve liquid chromatography and capillary electrophoresis, using fluorescence, chemiluminescence, or electrospray mass spectrometry detection.

Preparation of Analytical Standards. One of the limitations inherent in the direct analysis of adducts has been the lack of analytical standards. In initial experiments, we prepared nucleotide adducts of benzo[a]pyrene (BaP) in nanogram quantities with calf thymus DNA, using microsomal preparations to afford the adduction process. The microsomal method produced experimental artifacts, and did not produce adducts in the microgram quantities required for analytical study. A method using intact rat hepatocytes, developed in our Biology and Chemistry Department, appears to be a satisfactory method for obtaining the required quantities of a variety of PAH adducts (Dankovic et al. 1987). The products from this *in vitro* method seem to very closely approximate the adduct distributions found from *in vivo* studies of adducts. The significance of this result is that for the first time, research quantities of many different adducts can be prepared from adducting hydrocarbons and pure DNA. At the present time, about 5 μg adducted BaP, 1.5 μg adducted fluoranthene, 200 ng dibenz[a,h]anthracene, and 110 ng 7,12-dimethylbenz[a]anthracene have been used for study. The rate of metabolism of each hydrocarbon by the hepatocyte system is different; hence, the incubation conditions require preliminary experiments before microgram-scale experiments can be successfully conducted.

GC/MS of Derivatized Metabolites. Upon treatment with hydrochloric acid, the adducting moiety from PAH adducts is liberated as a tetrahydrotetrahydroxy compound (tetrol) that is subject to derivatization by a number of agents prior to analysis by GC/MS. The BaP tetrol forms a

(a) Oregon State University (NORCUS student)

tetramethyl ether as well as a tetraacetate that is detectable by selected ion monitoring (SIM) mass spectrometry at the picogram level (Bean et al. 1987). A principal research problem is to prepare these derivatives reliably, in good yield, and at the concentrations required with background noise sufficiently low for unambiguous identification. Although we have extended the sensitivity of the permethylation method to 10 pg of tetrol (Bean et al. 1987), we have not yet been able to do so reliably and without unacceptable accompanying chemical noise. During a study of the mass spectral properties of derivatives of BaP metabolites (Chess et al. 1988), we found that the methyl ether derivatives of several PAH tetrols produce a unique spectrum resulting from a reverse Diels-Alder (RDA) cleavage. This cleavage is not observed with PAH acetate or trifluoroacetate derivatives, which fragment by other mechanisms. We have recently found that the trimethylsilyl derivative of BaP tetrol also undergoes the RDA cleavage to yield a fragment ion of 404 amu that has very little interference in the single ion chromatogram. The derivative is more readily and reliably prepared than the corresponding methyl ethers, and unoptimized detection levels are approaching the 1 pg level.

Detection of Intact Adduct by Chemiluminescence. Chemiluminescence is a powerful and specific detection method that has been recently applied to the analysis of a number of PAH compounds (Sigvardson and Birks 1983). It has been shown recently that amino-PAH compounds are particularly sensitive to this detection technique, with detection limits 1 to 2 orders of magnitude lower than fluorescence detection (Sigvardson, Kennish, and Birks 1984). The structures of DNA adducts formed from PAH compounds comprise both a fluorescent hydrocarbon moiety and an aromatic amine linkage. Thus, preliminary studies were conducted to determine if these compounds are amenable to specific detection by chemiluminescence. The chemiluminescence response we are investigating depends on electronic excitation of the analyte by the reaction between an aryl oxalate and hydrogen peroxide. A variety of oxalates can be used for the reaction, each giving different light intensities and durations that are pH dependent. Although in principle the reaction is simple, from a practical standpoint the process is more difficult because of need for compatibility between separation column eluant and post-column reagents and solvents, the mechanical arrangements for reagent metering, and the short time required between post-column mixing and detection. For these experiments, bis-(2,4,6-trichlorophenyl) oxalate was used with hydrogen peroxide to initiate chemiluminescence response from a synthetic BaP-guanosine adduct and the response compared with fluorescence detection. The experiments were conducted without a separation column. The results of these preliminary experiments indicate that the adduct does exhibit a strong chemiluminescence response under the conditions used that is comparable in intensity with fluorescence. It is very likely that the chemiluminescence response can be increased substantially by increasing oxalate concentration, choosing a more responsive oxalate, and optimizing solvent, pH, and post-column mixing conditions. Further chemiluminescence studies are planned.

Separation of Adducts by Capillary Zone Electrophoresis. Electrophoretic separation of high molecular weight compounds in silica capillaries filled with buffer solutions has several advantages that lend themselves well to the analysis of adducts. Capillary zone electrophoresis (CZE) separation efficiencies can be high for molecules with higher molecular weights since mobility depends mainly on charge. Furthermore, electro-osmotic flow is relatively frictionless, resulting in essentially "plug" flow for the separated analyte. The PAH-adducted nucleotides and nucleosides are sufficiently polar to give good electrophoretic mobility with excellent separation efficiency. Figure 1 shows an electropherogram of BaP-guanosine adduct at pH = 10.7. Good separations can also be obtained at acid pH. In our studies, detection was by laser fluorescence. Although detection wavelength was not optimized for these experiments, it appears that about 100 attomoles can be detected under the conditions used. We have found that the use of a mixed solvent/buffer system as the mobile phase is critical to good performance. If water alone is used, several peaks appear, presumably because of hydrolysis under the strongly acidic or basic conditions of the separation. A principal problem with CZE is the small sample capacity. The column must be very small in diameter to avoid overheating the column. Only about 10 nL of sample can be applied to the column, giving an overall detection level of 10 pg/mL using fluorescence detection.

The next step in this technology will be to interface the CZE system with a mass spectrometer. Normal mass spectrometric analysis is not sensitive enough to detect femtogram quantities of analyte. An electrospray interface, pioneered at PNL (Olivares et al. 1987) and winner of an R&D-100 award (Special Report 1988), has been demonstrated to be capable of detecting femtogram

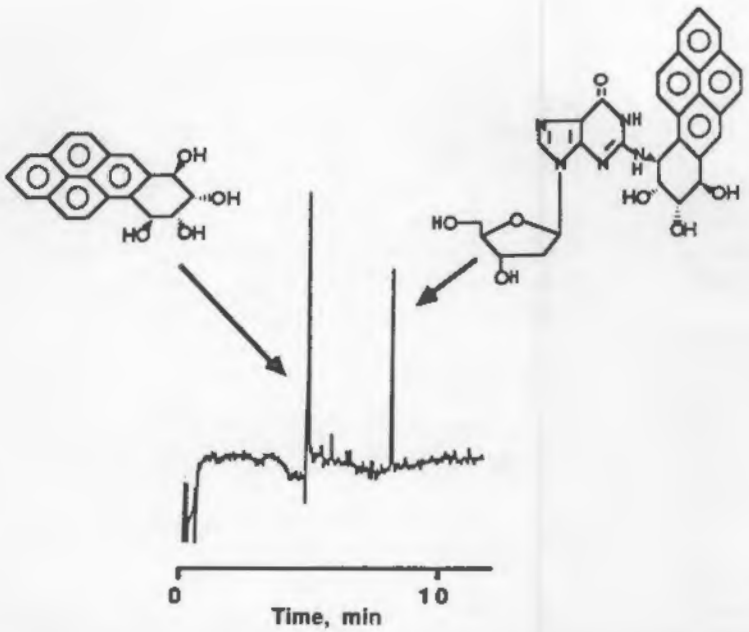

FIGURE 1. Capillary Electropherogram of a Mixture of a BaP-Tetrol (peak on left, 3 attomole), and BaP-Guanosine Adduct (720 attomole). Separation conducted with a 1.5 m x 100 μm inner diameter column at 35 KV, using 1:1 phosphate buffer (pH 10.7):acetonitrile as mobile phase. In our studies, detection was by laser fluorescence. Sample injection volume, 9 nL.

quantities of certain polypeptide analytes. Research is being conducted to interface CZE with a new triple-quadruple atmospheric-inlet mass spectrometer recently acquired for this and other biochemical studies.

Another refinement of the CZE approach to adduct analysis will be an investigation of the CZE and mass spectrometric properties of the BaP-nucleotide adduct (containing a phosphate moiety). The nucleotide should be more amenable to electrospray ionization than the nonphosphorylated nucleoside. Procedures for isolation of the BaP-nucleotide from a synthetic DNA-adduct sample were researched this past summer by a NORCUS graduate student supported by this project, J. G. Pavlovich. Although the phosphate-containing adduct was not isolated in pure form, the work is being continued by Mr. Pavlovich at Oregon State University under the direction of Professor D. F. Barofsky, also partially supported by this project during fiscal year 1988.

Investigation of Nonclassical DNA Adducts. We are engaged in an Exploratory Research Project to identify forms of hydrocarbon adducts that do not exhibit the behavior of "classical" adducts formed through normal diolepoxide addition to DNA bases. A number of researchers (Shen, Fahl, and Jefcoate 1980; Ashurst and Cohen 1982) have reported that when radiolabeled BaP adducts are isolated by the conventional method, 1/3 to 1/2 of the radiolabeled nucleoside material is not recovered as the classical adduct. We have examined this "nonclassical" adduct material by treating it with 0.12 N HCl to release it from the residual DNA structure. This process was followed by solid reverse-phase adsorption of the hydrolyzed product. Reverse-phase chromatography of this material revealed that in addition to tetrols, from 10% to 33% of the nonclassical material had retention times consistent with BaP-3,6-quinone and BaP-6,12-quinone. We have confirmed the presence of these quinones with mass spectrometry. Quinones are not found in the nonclassical fraction unless the acid hydrolysis step is performed, leading us to believe that the appearance of quinones after acid treatment results from cleavage of covalent bonds to the DNA structure. Formation of nonclassical structures may be a consequence of a competing adduct-formation mechanism, as suggested by Cavalieri and Rogan (1985). The project will continue through fiscal year 1989 to confirm these results and to investigate the nature of the quinone-precursor structure.

References

Ashurst, S. W., and G. M. Cohen. 1982. "The Formation of Benzo[a]pyrene-Deoxyribonucleoside Adducts *In Vivo* and *In Vitro*." *Carcinogenesis* 3:267-273.

Bean, R. M., E. K. Chess, B. L. Thomas, D. L. Springer, D. B. Mann, and D. J. Hendren. 1987. Abstracts of the *Eleventh International Symposium on Polynuclear Aromatic Hydrocarbons*, Gaithersburg, Maryland.

Cavalieri, E. L., and E. G. Rogan. 1985. "Polycyclic Hydrocarbons and Carcinogenesis." ACS Symposium Series 283, ed. R. G. Harvey, pp. 289-305. American Chemical Society, Washington, D.C.

Chess, E. K., B. L. Thomas, D. J. Hendren, and R. M. Bean. 1988. "Derivatized Mass Spectral Characteristics of Metabolites of Benzo[a]Pyrene." *Biomed. Environ. Mass Spectrom.* 15:485-493.

Dankovic, D.A., D. L. Springer, B. L. Thomas, D. B. Mann, and R. M. Bean. 1987. "Preparation of DNA Adducts for Chromatin and Chemical Characterization Studies, Using Freshly Isolated Rat Hepatocytes." In *Proceedings of the DOE Contractor Conference on Chemical Research*, Monterey, California.

Olivares, J. A., N. T. Nguyen, C. R. Yonker, and R. D. Smith. 1987. "On-Line Mass Spectrometric Detection for Capillary Zone Electrophoresis." *Anal. Chem.* 59:1230-1232.

Shen, A. L., W. E. Fahl, and C. F. Jefcoate. 1980. "Metabolism of Benzo[a]pyrene by Isolated Hepatocytes and Factors Affecting Covalent Binding of Benzo[a]pyrene Metabolites to DNA in Hepatocyte and Microsomal Systems." *Arch. Biochem. Biophys.* 204:511-523.

Sigvardson, K. W., and J. W. Birks. 1983. "Peroxyoxalate Chemiluminescence Detection of Polycyclic Aromatic Hydrocarbons in Liquid Chromatography." *Anal. Chem.* 55:432-435.

Sigvardson, K. W., J. M. Kennish, and J. W. Birks. 1984. "Peroxyoxalate Chemiluminescence Detection of Polycyclic Aromatic Amines in Liquid Chromatography." *Anal. Chem.* 56:1096-1102.

Special Report of the R&D 100 Winners. 1988. R&D 100, Des Plaines, Illinois, p. 7.

Wogan, G. N., and N. J. Gorelick. 1985. "Chemical and Biochemical Dosimetry of Exposure to Genotoxic Chemicals." *Environ. Health Perspec.* 62:5-18.

Biological Effectiveness of Radon Alpha Particles

The increase in biological effectiveness observed when animals are exposed to radon daughters at reduced dose rates is a major concern in establishing exposure limits. Since this effect is parallelled by an increase in transformation in some cell lines exposed to neutrons at low dose rate, the critical events may involve the initiation step of carcinogenesis. In order to study the details of the time dependence of transformation and to test alternative biophysical models of the dose-rate effect, an irradiation system which will greatly reduce the stochastic variation in energy deposition in individual cells exposed to low doses is being developed. This system will use alpha-particle microbeam irradiation and is expected to be in operation by mid fiscal year 1989.

Alpha-Particle Microbeam Irradiation

L. A. Braby and W. D. Reece

An increase in biological effectiveness with decreasing dose rate has been observed both for transformation in cells exposed to high linear energy transfer (LET) radiations (Hill, Han, and Elkind 1984) and for lung cancer in animals exposed to radon daughters in air (Cross et al. 1984). Due to the high LET of alpha particles emitted by radon daughters, the specific energy (the stochastic analog to dose) delivered to a cell nucleus by the passage of a single alpha particle is quite large, on the order of 0.4 Gy. Thus, at environmentally relevant doses, where the mean specific energy for all cell nuclei is a few centigray, the majority of the cell nuclei receive no irradiation and only a few are traversed by an alpha particle. Since the occurrence of a track in a given cell is a Poisson random variable, the probability of two or more tracks is extremely small. It must be those cells which experience two or more tracks which are responsible for any dose-rate effect on tumor initiation since cells experiencing only a single track have no information on the dose rate.

Several models incorporating alternative mechanisms for the production and repair of radiation damage have been proposed to account for the increase in transformation (Rossi and Kellerer 1986; Burch and Chesters 1986; Elkind and Hill 1986), but it is extremely difficult to test these models with conventional broad-beam irradiation since the majority of the cells exposed receive no damage or are damaged by a single particle track and cannot be involved in the dose-rate effect. We will overcome this problem by using a charged particle microbeam system to irradiate individual cells with a specified number of charged particle tracks at precisely controlled positions. This will allow split-dose experiments in which each cell receives exactly two alpha particles with a specified time between them. These experiments will eliminate the uncertainty and reliance on assumptions that are inherent in experiments where only a small fraction of the cells receive the combination of events that are to be tested.

Design of the microbeam irradiation system was begun two years ago using discretionary funding. This year, the design was completed, the major components were purchased, and much of the system was assembled. Study of transformation by alpha particles does not require a particle beam less than about 5 μm in diameter, so the radon initiative proposal was based on use of an inexpensive collimator utilizing laser-drilled holes. Additional discretionary funding has allowed us to incorporate a more versatile collimator based on eight individual knife edges which each can be positioned with 0.1-μm precision to construct two properly aligned rectangular holes. This collimator design minimizes slit-edge scatter and provides the flexibility needed to study the sensitivity of cells to single charged particles.

The microbeam irradiation system will utilize the 2-MV tandem accelerator at PNL to produce protons to 4 MeV and alpha particles to 6 MeV. The major components of the beam line are illustrated schematically in Figure 1. Since the accelerator beam is horizontal, a 90° bending magnet is used so that the dishes of cells can be irradiated in their normal horizontal position without disrupting the layer of medium covering the cells. The horizontal portion of the beam line includes the standard energy control slits, beam scanner, faraday cup, and vacuum pump. After the bending magnet, a second set of slits is used to fine tune the 90° magnet to eliminate any effect of energy drift. The beam then comes to a pair of concentric faraday cups with a 330-μm axial opening. These cups provide an indication of the beam focus, and the central one can be used to estimate the particle fluence rate through the collimator. The beam line, including a mounting system which provides two-dimensional

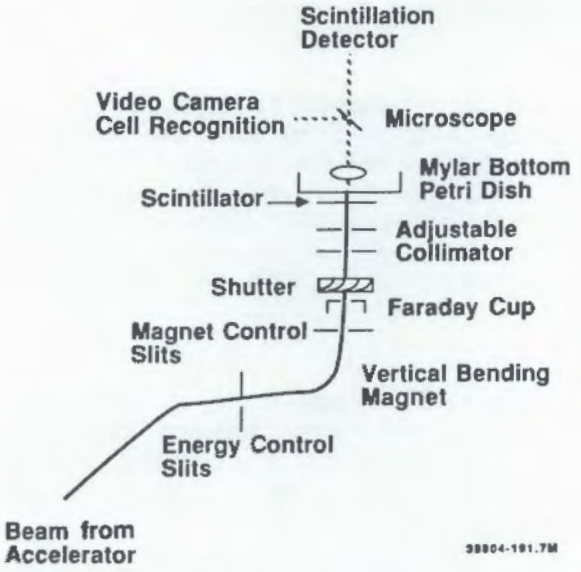

FIGURE 1. Schematic Diagram of Charged Particle Microbeam Irradiation System

positioning and angular adjustment of the components following the bending magnet, has been assembled and has been tested with an oxygen ion beam.

The collimator assembly and beam shutter will be assembled in a 35-cm section of vacuum line above the faraday cup. The shutter will consist of a beam stop mounted on a linear-motion feedthrough operated by a pneumatic cylinder and fast-acting electronically controlled valves. The eight knife edges which make up the collimator are mounted individually on custom linear-motion feedthroughs that are operated by compound micrometer screws and a lever system that gives approximately 5-to-1 mechanical advantage, as shown in Figure 2. The lever system is machined from a single piece of material so that there are no hinge points or sliding contacts to produce irregular motion. All critical components are made of stainless steel so that thermal expansion of the beam line and the knife-edge mounting rod cancel each other. This system gives resolution of 0.2 μm per division on the micrometer spindle, and has been tested using diffraction of a laser beam to determine reproducibility.

The charged particle beam will exit the vacuum system through a 330-μm-diameter aperture sealed by a 2-μm-thick plastic scintillator film. The light produced when a charged particle passes through this film will be collected by the microscope, which is also used to determine the

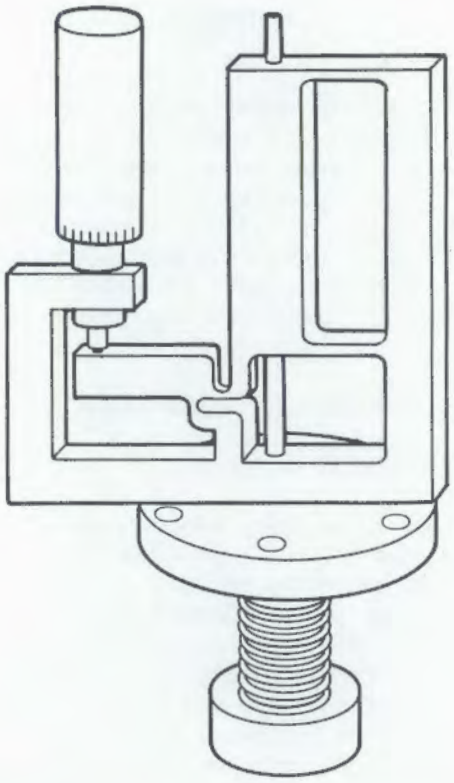

FIGURE 2. Split-Positioning System with Mechanical Linkage and Micrometer Screw to Provide 0.2 μm per Division Resolution

position of the cells relative to the collimator. A small computer will control the particle and beamline shutters and will use the light pulse data to control the dose to individual cells. The cells will be grown in special petri dishes with thin plastic film bottoms and stainless steel sides designed for precise positioning. The beam exit aperture and the dishes are designed so that the two plastic films are in contact, but the dish can be moved by a motorized positioning table so that the charged particle beam lines up with the desired part of the cell. The microscope is equipped for phase contrast imaging of cells in epi illumination so that no optical components are required on the accelerator side of the cells. This allows the collimator components to be mounted very near the plane of the cells, and to reduce the effects of the few scattered particles which are not stopped by the second collimator aperture.

The remaining components for the system are expected to be delivered early in fiscal year 1989 and we anticipate testing irradiation of individual cells soon thereafter.

References

Burch, P.R.J., and M. S. Chesters. 1986. "Neoplastic Transformation of Cells *In Vitro* at Low and High Dose Rates of Fission Neutrons: An Interpretation." *Int. J. Radiat. Biol.* 49:495-500.

Cross, F. T., R. F. Palmer, G. E. Dagle, R. H. Busch, and R. L. Buschbom. 1984. "Influence of Radon Daughter Exposure Rate, Unattachment Fraction, and Disequilibrium on Occurrence of Lung Tumors." *Radiat. Prot. Dos.* 7:381-384.

Elkind, M. M., and C. K. Hill. 1986. "Biophysical Models for the Role of Intracellular Repair in the Anomalous Enhancement of Neoplastic Transformation by Low Doses of Fission-Spectrum Neutrons at Low Dose Rates: Reply to the Letter to the Editor by P.R.J. Burch and M. S. Chesters." *Int. J. Radiat. Biol.* 50:181-183.

Hill, C. K., A. Han, and M. M. Elkind. 1984. "Fission-Spectrum Neutrons at a Low Dose Rate Enhance Neoplastic Transformation in the Linear, Low Dose Region (0-10 CGy)." *Int. J. Radiat. Biol.* 46:11-15.

Rossi, H. H., and A. M. Kellerer. 1986. "The Dose Rate Dependence of Oncogenic Transformation by Neutrons May Be Due to Variation of Response During the Cell Cycle." *Int. J. Radiat. Biol.* 50:353-361.

Physical Processes in Radiation Biology

Radiation Physics

The spatial pattern and interaction channels by which energy is deposited plays a dominant role in the subsequent chemical and biological processes leading to radiation damage in biological systems. For radiation of high linear energy transfer (LET), radiochemical and radiobiological models of radiation action rely on an accurate description of the physical processes which occur along the charged particle track. Our studies focus on investigation of the processes of ionization by charged particles which contribute to understanding of the initial spatial distributions of ionization that define the physical structure of a charged particle track, on the fate of the target atom/molecule which undergoes an ionizing event, and an incorporation of interaction cross sections into comprehensive Monte Carlo models of charged particle track structure.

During the past year the experimental studies have focused on determination of the mechanisms for multiple-ionization of atomic targets by fast ions and neutrals (H^+, H^0, He^{2+}, He^+, He^0, etc.). Emphasis was on separation of multiple ionization processes involved in direct ionization, charge-transfer ionization, and simultaneous ionization and charge transfer. Theoretical studies were undertaken with the Born Approximation and Binary Encounter Theory to develop reliable models of the single differential ionization cross sections for protons. Development of Monte Carlo track structure codes were directed toward investigation of energy deposition in cellular and subcellular structure of X-irradiated oocytes. This investigation of energy deposition distributions was undertaken to provide dosimetric insight into the interpretation of biological results obtained at the Lawrence Livermore National Laboratory.

Multiple Ionization of Atoms by Ion Impact

R. D. DuBois

In our efforts to understand energy deposition by fast charged particles traversing gaseous media, we have been studying the role that multiple target ionization plays in these collisions. This is because the occurrence of multiply ionizing collisions can significantly alter our understanding and modeling of radiation-induced damage. For example, if several electrons are ejected in a single collision, each of those electrons must be accounted for in a proper model. Also of potential concern is the possibility that the resultant multiply charged target ions will interact differently with their neighbors than would singly charged ions.

Thus, the goals for our multiple-ionization studies have been 1) to measure the relative importance of multiple target ionizations for various light-ion, target atom combinations and impact energies, 2) to identify the ionization channels (e.g., "pure" outer-shell ionization, electron capture or loss by the projectile, inner-shell ionization) responsible for multiple and single target ionizations, and 3) to obtain information about the interaction mechanism(s) leading to multiple ionizations. Information regarding these aspects is important in formulating theoretical treatments of multiple ionization and subsequently testing the theoretical results.

During the past year our multiple-ionization studies have concentrated on four topics: 1) an investigation of the mechanism(s) responsible for double ionization of helium in direct ionization processes by both bare and structured ions, 2) multiple ionizations of helium resulting from hydrogen and helium atom impact, 3) multiple ionizations of atoms resulting from He^+ impact, and 4) collecting preliminary data for multiple ionization of some simple molecules. Topics 1, 2, and 3 will be discussed below while topic 4 will appear in a following section.

Multiple Ionization Mechanisms.[a] The mechanisms leading to double ionization of helium were investigated by studying the projectile charge and impact velocity dependences of total-, single-, and double-ionization cross sections. This study was restricted to the "pure" ionization channel since this is the dominant channel for fast ion impact. "Pure" ionization means that any ionization resulting from electron-transferring

(a) This subsection is a summary of a paper published in *Physical Review A*, October 1988.

collisions was excluded. The projectile charge state and impact velocity dependences of cross sections measured in our laboratory and obtained from the literature were analyzed to identify whether the double ionization was a result of a single projectile-target interaction, two projectile-target interactions, or a combination of these two ionization mechanisms. Identifying the mechanism is important since a single projectile-target interaction implies using only a first order calculation to describe the cross sections, whereas two projectile-target interactions imply that the second Born term is required.

For high-energy, bare-ion impact, when the collision is perturbative (i.e., whenever Z/v is small), the signature for double ionization resulting from a single projectile-target interaction is a $(Z/v)^2\ln(v)$ dependence for both the single- and double-ionization cross sections. On the other hand, double ionization resulting from two projectile-target interactions will exhibit a $(Z/v)^4$ dependence while the total-ionization cross sections have a $(Z/v)^2\ln(v)$ dependence. Thus, evidence that double ionization occurs by a one-step interaction mechanism is a constant ratio of double ionization to single ionization, σ_2/σ_1, independent of projectile charge and impact velocity; for a two-step interaction mechanism, the ratio of the total-ionization cross section to the square root of the double-ionization cross section, $\sigma_T/\sqrt{\sigma_2}$, should increase slowly as ln(v). Also for a two-step interaction, σ_T and $\sqrt{\sigma_2}$ should have the same projectile charge state dependences.

Using data obtained from the literature and from measurements performed in our laboratory, the projectile charge and impact velocity dependences for "pure" total and double ionization of helium were studied for fully stripped ions ranging from protons to oxygen. From these dependences, the following conclusions can be drawn: 1) the two-step mechanism was found to be the dominant "pure" double-ionization mechanism for proton impact energies between approximately 0.1 and 0.5 MeV; 2) for heavier, fully stripped ions, this mechanism dominates above approximately 0.1 MeV/u and continues to dominate to higher impact energies than for protons (≈2 MeV/u for He^{2+} and >3 MeV/u for heavier ions); 3) the one-step mechanism will ultimately dominate for very high impact energies since it has a $v^{-2}\ln(v)$ dependence, whereas the two-step mechanism has a v^{-4} dependence; and 4) the total-ionization cross sections scale as Z^2 only for situations where the collision is perturbative, i.e., for small Z/v. Otherwise, the cross sections increase at a slower rate.

The same analysis was also performed using available partially stripped projectile ion data; but in this case, the interpretation is complicated since partially stripped projectiles interact with an effective nuclear charge which depends on the impact parameter. This average effective charge, Z_{eff}, was determined for partially stripped projectiles by scaling experimental cross sections for these ions to those obtained for fully stripped ion impact. For any given projectile, it was found that Z_{eff} obtained using the double-ionization cross section data was larger than Z_{eff} obtained using the total- (mostly single in this case) ionization cross section data. This occurred for all cases where the projectile contained most of its bound electrons, i.e., low charge state ions; for nearly fully stripped projectiles, the same Z_{eff} was obtained whether total- or double-ionization cross sections were used.

Since the partially stripped projectiles interact with different effective nuclear charges, the ratios $\sigma_T/\sqrt{\sigma_2}$ are affected. Conclusions about the mechanisms responsible for double ionization for structured ions could, therefore, be obtained for only a few cases. It appears that the two-step interaction mechanism dominates the double ionization of helium for He^+ impact between 0.05 and 0.5 MeV, but never dominates for H° and He° impact. This work indicates that the type of interaction mechanism responsible for "pure" double-(multiple) target ionization depends on the magnitude of Z/v, where Z is the nuclear charge for bare-ion impact, but is the *effective* charge for partially stripped ion impact.

Hydrogen and Helium Atom Impact. By installing a set of electrostatic deflection plates between the beam collimators, we have been able to remove all charged components from the incoming beam immediately prior to the interaction region. Doing so, cross sections for multiple ionization of helium have been accumulated for 0.15 to 0.4 MeV H° and 0.15 to 2 MeV He° impact. Some of the results for the "pure" ionization channel were discussed in the preceding section. In addition, the electron capture and loss channels were measured. Preliminary results for 150 to 400 keV H° impact are shown in Figure 1. Included for comparison are the measurements of Solov'ev et al. (1962), where the total single-, and total double-ionization cross sections were obtained. The present data are considerably smaller than their measurements. Included in the figure are total-ionization cross sections extracted from the present data and total electron-loss cross sections measured by Toburen et al. (1968). Efforts are in progress to extend

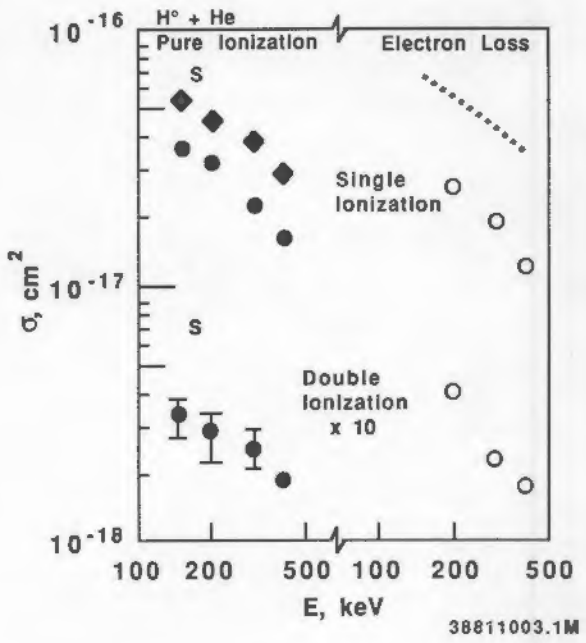

FIGURE 1. Preliminary Cross Sections for Ionization of Helium by Hydrogen Atom Impact. Total ion production cross section: ♦, present work. Single- and double-ionization cross sections for ionization and electron-loss channels: •, o, present work. Total single- and total double-ionization cross sections: S, Solov'ev et al. Total electron-loss cross sections: ---, Toburen et al.

---

the H° energy range and to confirm the absolute cross sections.

These H° and He° data, when combined with our earlier H^+, He^{2+}, and He^+ measurements, will provide a complete picture of ionization occurring as a 2 MeV H^+ or He^{2+} ion slows down in a gaseous media. In particular, these data provide information about the source of electrons that are observed in our electron-emission studies.

Multiple Ionization of Atoms by He^+ Impact. Several years ago our multiple-ionization studies were initiated with measurements for 15 to 100 keV H^+ and He^+ impact (DuBois 1984). A year ago, the He^+ energy range was extended to 2 MeV, and, in addition to the "pure" ionization and electron-capture channels, data for the electron-loss channels were accumulated. These data provide information about the sources of free electrons observed for He^+ impact on He, Ne, Ar, and Kr targets. For example, as illustrated in Figure 2, the "pure" ionization channels generally dominate in the production of free electrons. But, for low impact energies, the electron-capture channels play a significant, if not a dominant, role. Note that for free electrons to be emitted as a result of electron capture by the projectile, at least a two-electron transition is required; whereas for "pure" ionization, only a single-electron transition is necessary.

As the projectile energy increases, electron loss from the incoming He^+ ion becomes important. Our coincidence measurements indicate that this electron loss often results in ionization of the target as well. As a result, as shown in Figure 2, for higher impact energies, the electron-loss channels play a major role in the production of free electrons. Thus, modeling these collisions requires following the stripped projectile, the fast stripped projectile electron, as well as any ejected target electrons that may result.

References

DuBois, R. D. 1984. "Electron Production in Collisions Between Light Ions and Rare Gases: The Importance of the Charge-Transfer and Direct-Ionization Channel." *Phys. Rev. Lett.* 52:2348-2351.

Solov'ev, E. S., R. N. Il'in, V. A. Oparin, and N. V. Federenko. 1962. "Ionization of Gases by Fast Hydrogen Atoms and by Protons." *J. Expltl. Theoret. Phys.* (USSR) 42:659-668. English translation *Sov. Phys.* JETP 15:459-464.

Toburen, L. H., M. Y. Nakai, and R. A. Langley. 1968. "Measurements of High-Energy Charge-Transfer Cross Sections for Incident Protons and Atomic Hydrogen in Various Gases." *Phys. Rev.* 171:114-122.

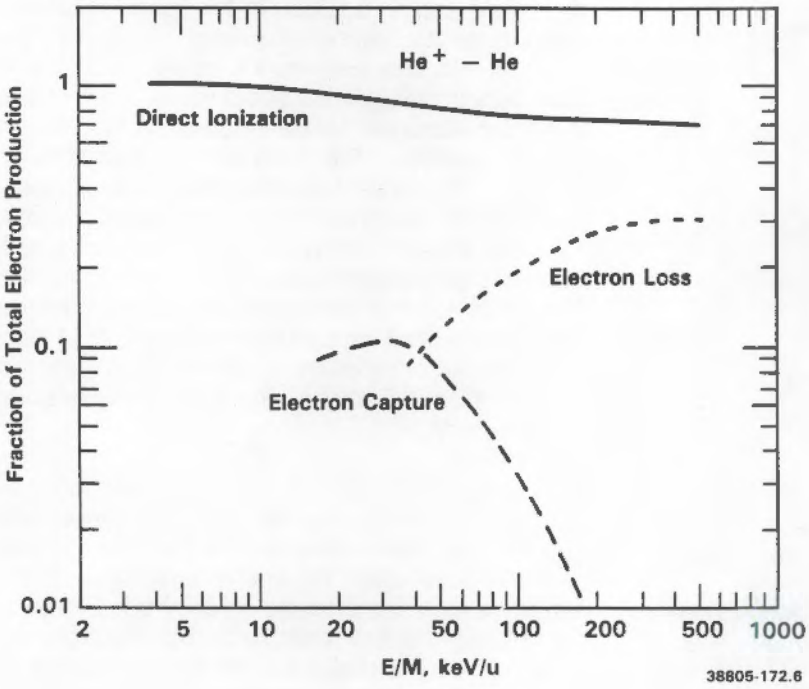

FIGURE 2. The Fraction of the Total Free-Electron Production Resulting from Direct Ionization, Electron Capture, and Electron Loss in He^+ - He, Ar Collisions

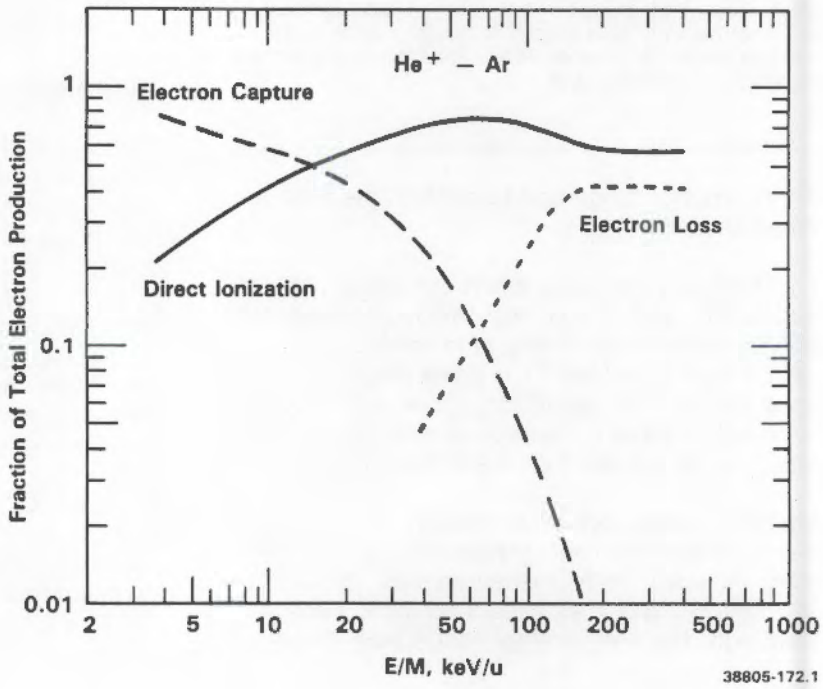

Ionization/Dissociation of Simple Molecules

R. D. DuBois

Using the expertise gained from our work on multiple ionizations of atoms, studies of ionization/dissociation of simple molecules by hydrogen and helium beams were initiated during the past year. The experimental approach is identical to that used in the multiple-ionization studies, i.e., coincidences between extracted charged target ions and projectile ions are measured. From this information, cross sections for ionization, electron capture and loss, and dissociation into one or more charged fragments are obtained.

During the past year, considerable effort was expended in improving the time resolution of our time-of-flight system and in calibrating the various detectors in order to obtain absolute cross sections. Also, establishing an efficient data-accumulation procedure was investigated.

As an example of preliminary data obtained thus far, Figure 1 shows a target ion spectra obtained for 200 keV $H^\circ + D_2O \rightarrow H^+ +$ fragment collisions. The various charged D_2O fragments are identified as well as various nitrogen and oxygen fragments originating from the background chamber pressure. In Figure 1b, the autocorrelation spectra for $H^\circ + D_2O \rightarrow H^+ + D^+ +$ charged fragment collisions are shown. Evidence of D_2O dissociating into various charged fragment combinations, e.g., $D^+ + DO^+$, $D^+ + O^+$, $D^+ + O^{2+}$, is seen. Efforts are in progress to improve the data-accumulation process and to better characterize the experimental apparatus.

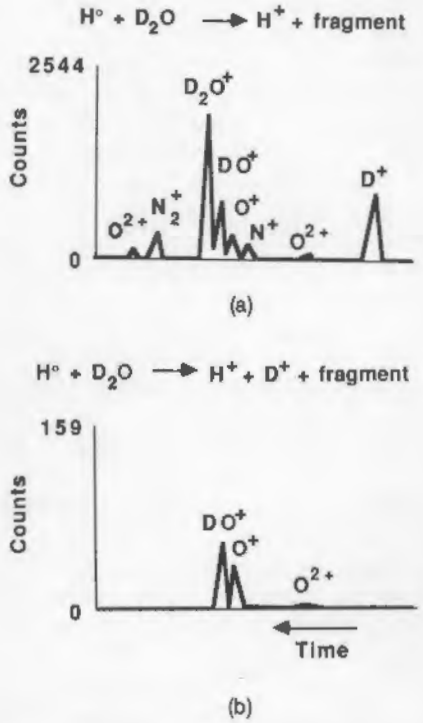

FIGURE 1. Time-of-Flight Recoil Ion Spectra for 200 keV $H^+ + D_2O$ Electron-Loss Collisions. Figure 1a is the total recoil ion spectra, whereas Figure 1b is the charged fragments in coincidence with a D^+ fragment ion.

Prediction of Secondary-Electron Energy Spectra

J. H. Miller and W. E. Wilson

The energy spectrum of secondary electrons is an important part of the database needed to understand the physicochemical stage of radiation damage to living matter. We are developing semiempirical methods to calculate these spectra that are based on the close relationship between photoionization and the ejection of electrons in glancing collisions of target molecules with fast charged particles. The value of this approach should increase as more data on optical properties of biologically important molecules become available from experiments with sources of synchrotron light.

Our model can be expressed mathematically in the following form:

$$\frac{d\sigma_k}{d\epsilon} = \frac{4\pi a_o^2 z^2}{T} \frac{R^2}{E_k} \frac{df_k}{d\epsilon} \ln(T/R) + f(\epsilon) \frac{d\sigma_k^{BEA}}{d\epsilon} \qquad (1)$$

where $d\sigma_k$ is the differential cross section for ejection of electrons with energy between ϵ and $\epsilon + d\epsilon$ from the kth electronic subshell of a molecule by collisions with a structureless particle of charge z and velocity v. The Bohr radius, a_o, and the Rydberg energy, R, are fundamental constants equal to 0.529 Å and 13.6 eV, respectively, and T is the kinetic energy of an electron with velocity v. The energy lost by the projectile in the collision is $E_k = I_k + \epsilon$ with I_k being the ionization potential of the kth subshell. The partial optical oscillator strength, which is proportional to the cross section for photoionization of the kth subshell, is denoted by $df_k/d\epsilon$, and $d\sigma_k^{BEA}/d\epsilon$ is the binary encounter approximation (BEA) to single differential cross sections (SDCS) for ionization of subshell k.

This model combines two methods for calculating SDCS that are valid in different regions of the secondary-electron energy spectrum. The term in Equation (1) that is proportional to $\ln(T)/T$ predominates when the velocity of the projectile is large and the secondary-electron energy is small. Collisions with large impact parameter and small momentum transfer make the largest contribution to the cross section for ejection of low-energy secondary electrons by a fast projectile. For these distant collisions, a dipole approximation to the interaction between the target and the projectile is valid. Since this dipole approximation is equivalent to the interaction of the target with photons, the optical oscillator strength of the target determines the energy distribution of electrons ejected by this mechanism.

Glancing collisions are not effective in producing high-energy secondary electrons and the coefficient of the $\ln(T)/T$ term in Equation (1) decreases rapidly with increasing secondary-electron energy. Hence, most collisions that produce fast secondary electrons can be approximated as a binary encounter between the projectile and the ejected electron. The binding of electrons in the target plays a minor role in the cross section for these close collisions. The BEA treats the ejected electron as initially free but with a velocity distribution determined by the electronic state of the target before the collision. These initial velocity distributions can be calculated from the ground-state wave functions of the target; however, a hydrogenic velocity distribution parameterized by the average kinetic energy of electrons in a subshell is more compatible with the binary encounter level of approximation (Vriens 1967).

The function $f(\epsilon)$ in Equation (1) allows us to make a smooth transition between the low- and high-energy approximations. The physical significance of this function can be better understood if we consider the limit of small energy losses by fast projectiles where Equation (1) summed over subshells reduces to

$$\frac{d\sigma}{d\epsilon} = \frac{4\pi a_o^2 z^2}{T} [A(\epsilon) \ln(T/R) + B(\epsilon)] \quad (2)$$

with

$$A(\epsilon) = \Sigma_k \frac{R^2}{kE_k} \frac{df}{d\epsilon} k \quad (3)$$

and

$$B(\epsilon) = f(\epsilon) \Sigma_k n_k \left(1 + \frac{4U_k}{3E_k}\right) \left(\frac{R}{E_k}\right)^2 \quad (4)$$

where n_k is the number of electrons in the subshell and U_k is their average kinetic energy. This result is identical to the first two terms of Bethe's asymptotic expansion of the first Born approximation (Inokuti 1971). That approach to deriving Equation (2) shows that $B(\epsilon)$ is independent of projectile properties. Hence, it is consistent with the Bethe theory to assume that our interpolation function f is independent of T. Cross sections for ejection of fast secondary electrons depend on the projectile velocity in two ways. One of these is the $1/T$ dependence of the Rutherford cross section and the other is related to the kinematics of the collision. We find that both are adequately given by the BEA so that no additional T dependence is needed in $f(\epsilon)$.

The traditional method for determining coefficients of the Bethe expansion is to construct plots of T times $d\sigma/d\epsilon$ as a function of $\ln(T)$. If these plots are linear, then $A(\epsilon)$ and $B(\epsilon)$ can be calculated from the slope and y intercept, respectively. This is usually not the most effective way to use the available experimental data for the following reasons: 1) experimental data at a fixed secondary-electron energy over a wide range of projectile velocities are rare; hence, estimation of A and B from Fano plots can involve large uncertainty; 2) optical data that can be used to calculate $A(\epsilon)$ are available for many targets of radiological importance and provide information about the target that should be used in estimating the B coefficient; and 3) the work of Professor Rudd at the University of Nebraska and DuBois at PNL have substantially improved the database of total cross sections for ionization by proton impact. These data should also contribute to prediction of SDCS.

For these reasons, we depart from the traditional approach and determine $f(\epsilon)$ by fitting total-ionization cross sections under the assumption that $A(\epsilon)$ is known from photoionization measurements. This approach has the advantage that no differential ionization data are needed for application of the model to a particular target. Obviously, this is not an *ab initio* prediction of SDCS, which remains a formidable challenge for most biologically important molecules; however, the model has sufficient theoretical basis to be used with reasonable confidence when experimental SDCS are not available or are difficult to obtain.

This predictive aspect of our model is illustrated for ionization of water molecules by electron impact in a paper that appeared recently in *Physical Review A* (Hollman et al. 1988).

Since we assume that $f(\epsilon)$ is independent of k, the model can be used to predict SDCS for ionization of individual subshells of the target if sufficient optical data are available to determine partial optical oscillator strengths. The SDCS for individual subshells are important in track-structure application since the final state of the residual ion may be correlated with the energy of ejected electrons. However, this aspect of the model cannot be rigorously tested at the present time because most differential ionization measurements implicitly sum over final states of the target. Total dissociative ionization cross sections provide a weak test of this aspect of the model since the dependence on secondary-electron energy of the contribution from various subshells to excitation of a given dissociative ionization channel in glancing collisions can be deduced from optical data (Tan et al. 1978). We assume that a similar partition of energy transfer over dissociative channels applies to close collisions. Table 1 compares predictions of our model with experimental data on dissociative ionization of water molecules by electron (Schutten et al. 1966) and proton impact. The difference in the branching ratio for H^+ production observed with the two projectiles is not expected on the basis of the first Born approximation, which should be applicable in this case due to the high velocity of the ions. Our model calculations agree better with the proton-impact data from PNL.

In summary, we have developed semiempirical techniques to calculate cross sections that are differential in the energy of secondary electrons for ionization of individual subshells of atomic and molecular targets. The model endeavors to make optimum use of the rapidly expanding database of photoionization cross sections. Results predicted by the model show good agreement with experimental data.

TABLE 1. Branching Ratios for Dissociative Ionization of Water Vapor

	H_2O+	OH^+	H^+	O^+
Electron impact[a]	0.62	0.16	0.20	0.02
Proton impact	0.65	0.20	0.11	0.03
Theory	0.72	0.16	0.10	0.02

(a) Schutten et al. 1966

References

Hollman, K. W., G. W. Kerby III, M. E. Rudd, J. H. Miller, and S. T. Manson. 1988. "Differential Cross Sections for Secondary Electron Production by 1.5-keV Electrons in Water Vapor." *Phys. Rev. A* 38:3299-3302.

Inokuti, M. 1971. "Inelastic Collisions of Fast Charged Particles with Atoms and Molecules: The Bethe Theory Revisited." *Rev. Mod. Phys.* 43:297-347.

Schutten, J., F. J. de Heer, H. R. Moustafa, A.J.H. Boerboom, and J. Kistemaker. 1966. "Gross- and Partial-Ionization Cross Sections for Electrons on Water Vapor in the Energy Range 0.1-20 keV." *J. Chem. Phys.* 44:3924-3928.

Tan, K. H., C. E. Brion, Ph. E. van der Leeuw, and M. J. van der Wiel. 1978. "Absolute Oscillator Strengths (10-60 eV) for the Photoabsorption, Photoionization and Fragmentation of H_2O." *Chem. Phys.* 29:299-309.

Vriens, L. 1967. "Binary-Encounter Proton-Atom Collision Theory." *Proc. Phys. Soc.* 90:935-944.

Microscopic Dosimetry of Photon-Irradiated Oocytes

W. E. Wilson and J. H. Miller, in collaboration with T. Straume and R. L. Dobson of Lawrence Livermore National Laboratory (LLNL)

Mouse immature oocytes are among the most radiosensitive cells known. Their killing has been studied for exposures to x-rays, gamma rays, tritium, neutrons, and heavy ions. Though the immature oocytes are at least 50 times more sensitive to x and gamma irradiation than most other cells, they do not exhibit a significant linear energy transfer (LET) effect. Recent studies propose that the radiosensitive target for cell killing is the oocyte membrane (Straume et al. 1987).

In order to achieve a better understanding of the microscopic radiation dosimetry of this complex target, we have undertaken extensive Monte Carlo electron track structure calculations in oocyte-like sites. Since mutagenesis is an important end point in many oocyte studies, we are interested in correlated depositions in the compound target. Our assumed ideal geometry is two concentric spheres of 12 and 8 μm in diameter representing, respectively, the cell and its nucleus and a 10-nm-thick shell on the outer sphere representing the

oocyte cell membrane. The microdosimetric computations assume a continuum secondary-electron spectrum computed for a 250-kVp photon field.

Single-event specific-energy distributions for the cell, cellular membrane, and nucleus were calculated for monoenergetic electrons between 10 and 95 keV. The distributions for the nucleus and the cell are very similar in shape, whereas, the distributions for the cell membrane are quite different from these other two targets (see Figure 1). Single-event distributions for a continuum

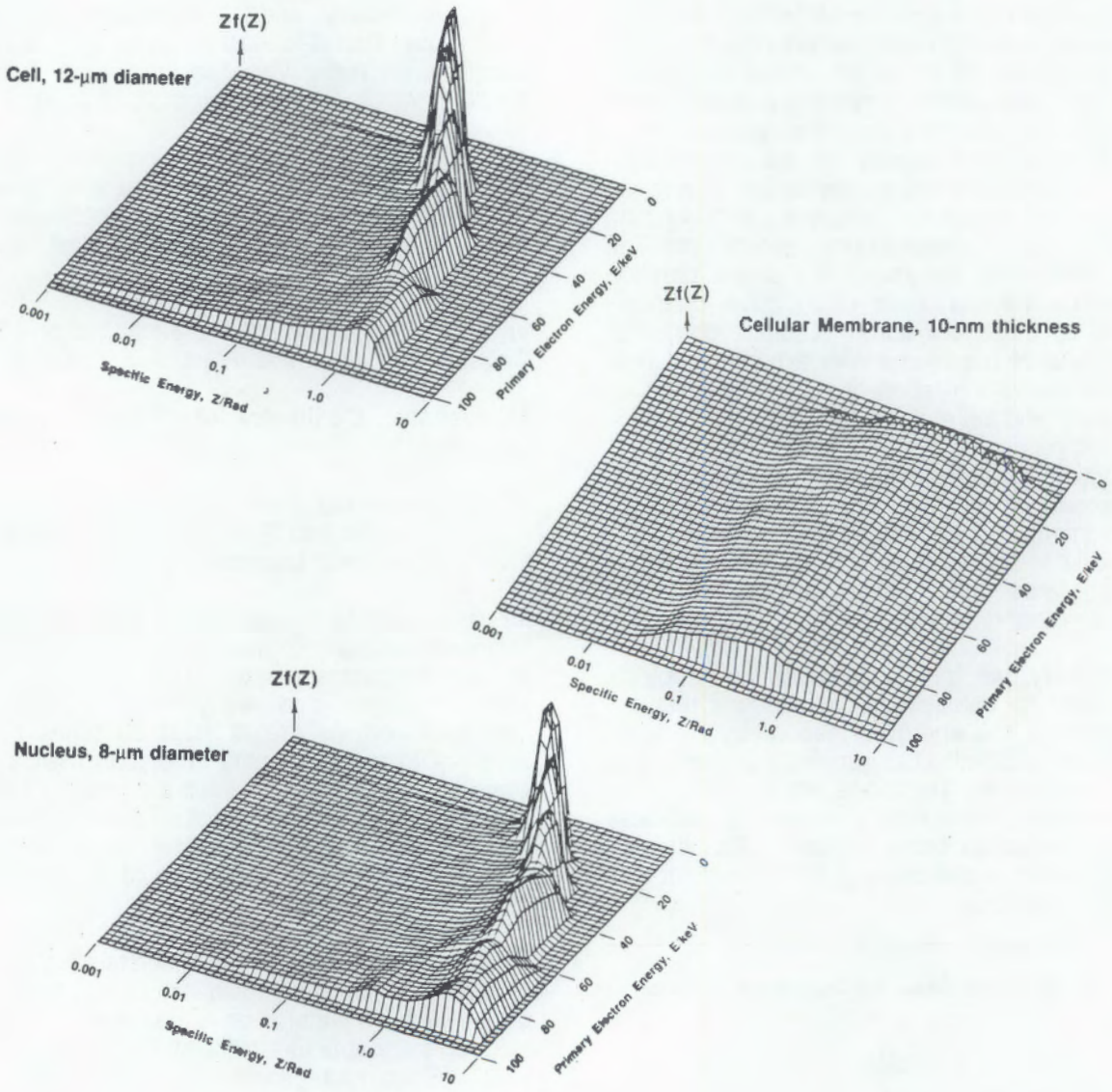

FIGURE 1. Single-Event Distributions in Specific Energy for Monoenergetic Electrons of Energy E in keV Irradiating a Simulated Oocyte-Like Target. The assumed target geometry consists of a 12-μm-diameter sphere, bounded by a 10-nm-thick shell (membrane), and contains an 8-μm-diameter spherical nucleus.

source spectrum are constructed by integrating these surfaces over electron energy, weighted by the source spectrum, and the total event frequency. The resulting single-event distributions, Figure 2, are conditional on the cell being hit exactly once. The results indicate that the nucleus and the membrane are each independently hit approximately 30% of the time. The unconditional frequency-mean specific energies are 1.39, 3.95, and 3.93 mGy for the cell, nucleus, and membrane, respectively. Higher dose, multiple-event distributions will be deduced by convolution of the single-event results.

Reference

Straume, T., R. L. Dobson, and T. C. Kwan. 1987. "Neutron RBEs and the Radiosensitive Target for Mouse Immature Oocyte Killing." *Radiat. Res.* 111:47-57.

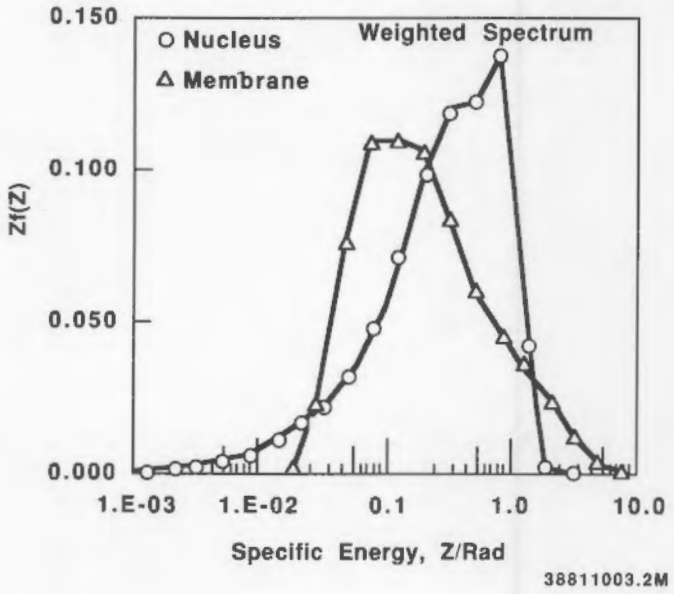

FIGURE 2. Single-Event Distributions in Specific Energy for the Oocyte Nucleus and the Membrane for a Continuous Source Spectrum. These results are computed by integrating the surfaces in Figure 1 over electron energy weighted by the source spectrum and by the total event frequency.

Radiation Dosimetry

Dosimetry

The primary goal underlying the Radiation Dosimetry task is to understand the connections between the physical events produced by the interaction of ionizing radiation with matter and their biological consequences. Dosimetry concentrates on the physical aspects of the problem, utilizing fundamental physical data to describe the interactions and organizing the results in ways that can be correlated with the biological effects. Special mathematical and experimental techniques are being developed to explore the differences in the energy deposition characteristics of various radiations in an effort to understand the effects of these radiations in radiobiology research and in the environment. Experimental tests of specific aspects of track structure calculations are conducted to test the completeness of these models and the adequacy of the input data. Comparisons with other methods of characterizing the energy deposition by charged particles such as the homogenous track models were also carried out. In addition, this program develops specialized dosimeters needed for the execution of these experimental tests of track structure and for the proper dosimetry of special radiation beams used in biophysical studies.

Microdosimetry of Fast Heavy Ion Beams

N. F. Metting, L. H. Toburen, and L. A. Braby

The initial spatial pattern of ionization produced as charged particles slow down in matter plays a significant role in the subsequent evolution of radiation damage. In biological systems, the local density of energy deposition in volumes of subcellular dimensions may be the dominant factor in determining the relative biological effectiveness (RBE) of different radiation types. In high-linear energy transfer (LET) radiobiology, homogeneous track structure models have been the most widely used to estimate the local energy density in and around high-energy heavy ion tracks (Zhang, Dunn, and Katz 1985; Chatterjee and Schaefer 1976). These models predict that the energy density should decrease as approximately $1/b^2$, where b is the radial distance from the path of the charged particle. However, recent measurements (made at the BEVALAC accelerator) of the ionization distributions in small volumes as a function of the radial distance from the path of very fast heavy ions have shown marked differences between the calculated average and the measured local ionization density (Metting 1987). To further investigate this phenomena, in 1987 we initiated a series of measurements at the UNILAC accelerator in Darmstadt in collaboration with the research groups of Dr. G. Kraft, Gesellschaft für Schwerionenforschung (GSI), Darmstadt, and Dr. H. Schmidt-Böcking, University of Frankfurt, West Germany. A brief description of these measurements of the distributions of energy deposited in small simulated tissue volumes in and near the path of fast heavy ions was presented in last year's annual report (Metting et al. 1987). During the past year we have continued analysis of the data accumulated in those measurements.

Data accumulated during measurements at the UNILAC accelerator were a result of one week-long experiment with a 5.9-MeV/amu uranium ion beam and one week-long experiment in which 13.0-, 13.8-, 16.2-, and 17.2-MeV/amu germanium ion beams were studied. The primary emphasis during the past year has been analysis of the germanium beam data. As described in our previous report (Metting et al. 1987), ionization distributions were measured using a small grid-walled proportional counter in a large propane-filled chamber through which the ion beam passed. For the measurements with germanium ions, two simulated site diameters were used: 0.5 μm and 1.0 μm. The amount of energy deposited in the grid-walled proportional counter, either by direct interactions of the incident ion or those of its secondary electrons, was determined by pulse height analysis of the proportional counter output. The pulse height was calibrated to energy deposited by using alpha particles of known stopping power from an ^{241}Am source. For measurements with the germanium beams, radial distances from 0 (beam passing through the center of the proportional counter) to about 8-μm simulated tissue were possible. Although larger radial distances could be reached with the proportional counter, experimental uncertainties at those greater distances have made interpretation of the results unreliable.

An example of the pulse height distributions obtained for ionization measured in a simulated 0.5-μm diameter, "tissue-equivalent" volume at several distances from a 13.8-MeV/amu germanium ion's path is shown in Figure 1. As the

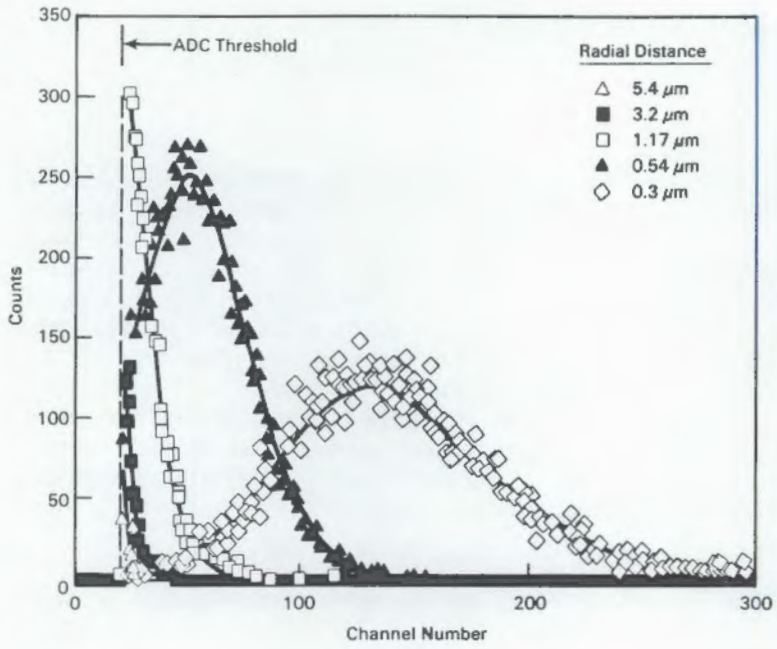

FIGURE 1. Pulse Height Distributions Observed for Different Positions of the Proportional Counter Relative to the Path of a 13.8-MeV/amu Germanium Ion

proportional counter was moved to greater distances from the beam, the pulse height decreased reflecting the smaller number of energy deposition events that occurred within the counter volume. In order to determine the mean energy deposited at each position of the detector, which is used for comparison to model calculations, it was necessary to extrapolate these distributions to zero energy. This was accomplished by a simple horizontal line fitted to the low energy end of the spectra. This is consistent with the expected shape of the proportional counter pulse height spectra for energy deposition resulting in production of 50 to 100 ion pairs in the counter volume; approximately 80 ion pairs would be expected at the threshold setting. In addition, wide variations in the form of this extrapolation were tested and found to have little effect on the mean value derived from the distributions.

Data for the mean energy deposited in 1.0- and 0.5-μm-diameter sites at various positions from a 13.8-MeV/amu germanium ion's path are shown in Figure 2 along with model calculations (Zhang, Dunn, and Katz 1985; Chatterjee and Schaefer 1976; Varma, Baum, and Kliauga 1978). Good agreement between measured $\bar{Z}(b)$ and calculated D(b) is observed for small radial distances with data for the larger site being in agreement with the predicted average values to somewhat larger values of b. The flattening of the measured distributions at the larger radial distances is representative of sites that receive energy from passage of a single electron, or photon, i.e., the minimum amount of energy a site of this size will receive if it is hit. Note that the plotted value, $\bar{Z}$ [or D(b)] is the energy absorbed per mass of the simulated site. Thus, comparable energy absorbed in a larger site would result in a smaller $\bar{Z}$ because of the larger mass of material in that volume. If the measured values are converted to energy loss per unit length in traversing the proportional counter (not shown), the two site sizes give the same values, as expected. The model calculations shown in Figure 2 represent the *average* amount of energy deposition expected at a specified distance from a charged particle track. The difference between the measured and calculated values at large b represents the decreasing probability that any particular ion will deposit energy in a given small volume. The ratio of energy deposition events per particle is also determined in these measurements. When this ratio is used to calculate the *average* energy deposited per ion, the results are in excellent agreement with the calculated averages.

Data for germanium beams of two different energies are shown in Figure 3, along with previous measurements (Metting 1987) for much higher energy iron ions. Note that the same trend is observed for the radial distribution of energy deposited by each ion, although the magnitude of the energy deposited at the greater distances from the ion path decreases with increasing ion velocity. It should also be noted that the iron ion data represent energy deposited in a 1.3-μm-diameter site; thus the plotted quantity, $\bar{Z}$, is somewhat reduced relative to the 0.5-μm germanium data, owing to the energy-per-unit-mass

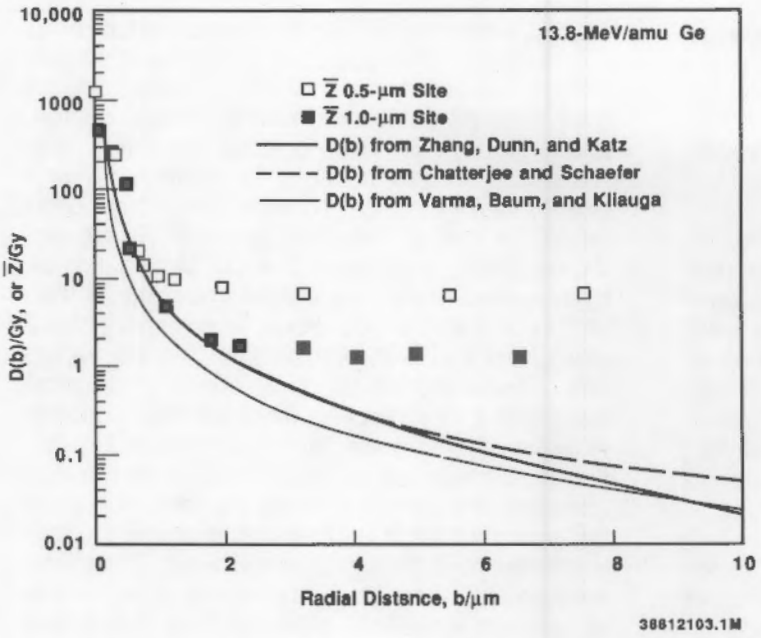

FIGURE 2. Radial Distributions of the Mean Energy Deposited in 0.5- and 1.0-μm-Diameter Tissue-Equivalent Sites by 13.8-MeV/amu Germanium Ions. The theoretical calculations of the average energy deposited are from the work of Zhang, Dunn, and Katz 1985; Chatterjee and Schaefer 1976; and Varma, Baum, and Kliauga 1978.

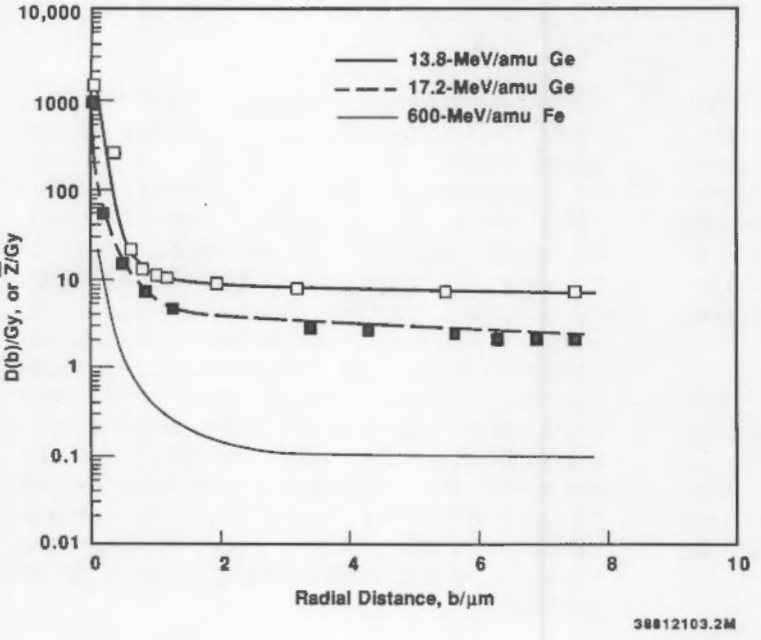

FIGURE 3. Radial Distributions of the Mean Energy Deposited in a 0.5-μm-Diameter Tissue-Equivalent Site by 13.8- and 17.2-MeV/amu Germanium Ions. Also shown are previously published distributions of the mean energy deposited in a 1.3-μm-diameter site by 600-MeV/amu iron ions (Metting 1987).

definition of $\bar{Z}$. If one compares the actual energy deposited for these three ions, rather than comparing the respective $\bar{Z}$, the ratio of values obtained in the plateau region approximately reflects the stopping power of the maximum-energy electrons ejected by each energy ion.

Although these data represent a preliminary analysis of only part of the data obtained from the UNILAC measurements, there seems to be convincing evidence that sizable discrepancies exist between model calculations of average dose at distances greater than a few micrometers from an ion track and measurements of the actual energy deposited in volumes of subcellular dimensions.

References

Chatterjee, A., and H. J. Schaefer. 1976. "Microdosimetric Structure of Heavy Ion Tracks in Tissue." *Radiat. Environ. Biophys.* 13:215-227.

Metting, N. F. 1987. "A Comparison of Microscopic Dose with Average Dose Near High Energy Heavy Ions." *Nucl. Instrum. Meth.* B24/25:1050-1053.

Metting, N. F., L. A. Braby, L. H. Toburen, G. Kraft, M. Scholz, F. Kraske, H. Schmidt-Böcking, R. Dörner, and R. Seip. 1987. "Microdosimetry of Fast Heavy Ion Beams." In *Physical Sciences*, part 4 of *Pacific Northwest Laboratory Annual Report for 1987 to the DOE Office of Energy Research*. PNL-6500, Pt. 4, pp. 33-36, Pacific Northwest Laboratory, Richland, Washington.

Varma, M. N., J. W. Baum, and P. Kliauga. 1978. "Microdosimetric Results Obtained by Proportional Counter and Ionization Chamber Methods: A Comparison." In *Proceedings of the Sixth Symposium on Microdosimetry*, eds. J. Booz and H. G. Ebert, pp. 227-237. Harwood Academic Publishers Ltd, Brussels.

Zhang, C., D. E. Dunn, and R. Katz. 1985. "Radial Distributions of Dose and Cross Sections for the Inactivation of Dry Enzymes and Viruses." *Radiat. Protect. Dosim.* 13:215-218.

Relationship Between $\bar{Q}$ Defined in Terms of y for 1-μm Sites and Initial Radiation Damage[a]

L. A. Braby, W. E. Wilson, and N. F. Metting

It has been proposed that the microdosimetric quantity lineal energy (y) be substituted for linear energy transfer (LET) in a new definition of Q (ICRU 1986). The advantages to such a system include the fact that y can be measured directly (LET must be calculated from the mass, charge, and velocity of the ionizing particle), that reasonably simple relationships between y and relative biological effectiveness (RBE) have been found for many biological systems (Bond and Varma 1983), and that y is more closely related to the actual energy deposition in cell nuclei than LET is for those radiations where energy loss, straggling, and delta-ray escape may be important. These include most radiations of practical importance in protection from external sources. However, there are also disadvantages to a definition of Q based on y. Such a definition requires choosing the diameter of the site for which y will be specified. It is unlikely that a single site size is relevant to all biological systems and endpoints. Furthermore, data on the biological effectiveness of unusual radiations such as very soft x-rays (Goodhead 1977) and molecular ions (Kellerer et al. 1980) show that the initial damage responsible for common biological effects is governed by energy deposition in very small sites, on the order of 10 nm.

Current experimental techniques are limited to a minimum simulated site diameter of about 300 nm by the requirements of the gas-gain mechanism. For low-energy charged particles (range comparable to or less than the simulated site diameter), the energy deposited approaches the energy of the charged particle, and y depends directly on the site size. However, these short track radiations are relatively minor problems in radiation protection; x-rays below a few keV do not penetrate the body and neutrons below 100 keV are important primarily when the source is well shielded. This discussion will deal only with radiations which transfer energy via charged particles with range larger than the diameter simulated by the detector. For these long track radiations, y is a slowly varying function of the site size.

The primary tool for studying the energy deposition in small sites is track structure simulation by Monte Carlo techniques. Using suitable atomic cross section data, the position of each ionization produced by a charged particle and its secondaries can be calculated (Wilson and Paretzke 1980). The most noticeable characteristics of such tracks are the occurrence of occasional clumps of

(a) Summary of paper prepared for presentation at the International Radiation Protection Association meeting held in Sidney, Australia, May 1987.

ionizations and delta rays which often carry significant quantities of energy away from the path of the primary ion. The results of soft x-ray and molecular-ion experiments suggest that the concentration of several ions in a small cluster may be responsible for the biochemical changes which initiate the biological effect. These clusters can be caused by the random occurrence of ionization along an ion or delta-ray track, by the overlap of two or more elements of a track (for example, a delta-ray track turning and crossing the primary ion track), or from the decreasing mean free path for ionization near the end of an electron's range. Thus the question of the relationship between measurements in a relatively large site and effects in sites a few nanometers in diameter can be divided into two parts: the ionization produced by the primary ion and that produced by delta-ray events.

Figure 1 shows the ratio of the mean lineal energy in a 10-nm site to the mean in a 1000-nm site as a function of proton energy. It is evident that the lineal energy in the small site is less than in the large site. This is due primarily to transport of energy outside the small site by delta rays. Furthermore, the ratio is relatively constant down to a few million electron volts, indicating that energy deposited in micrometer-diameter sites can be used as a reasonable indicator of mean energy deposited in much smaller sites. At the lower energies, the range of delta rays is short and less energy is transported outside a small site. In this region, the overlap of ionizations produced by the primary particle and those produced by the delta rays becomes more significant; but even in the extreme case, the ratio of means changes by only about 50% and the stopping power changes by approximately a factor of ten.

If it is the relatively large energy-deposition events that are relevant biologically, then one must consider the shape of the distribution of events in addition to their means. Distribution functions shown in Figure 2 give the probability that an is a steep curve. For small sites the curve is less steep and crosses the large site curve at about 0.7. Thus, for protons from 0.5 to 20 MeV crossing 10-nm sites, the effect of increasing the site size is simply to narrow the distribution of energy-deposition events and increase the mean lineal energy by including some delta-ray ionizations, which would occur outside a smaller site. The difference between those curves is less for event sizes greater than the median than it is for the smaller events. Thus, for the portion of the energy-deposition distribution assumed to be most relevant to the production of biological damage, the large events in small volumes, the energy deposition measured in larger sites would provide a better indication of biological effectiveness than would be suggested by a simple comparison of mean values.

Approximately one-third of the energy deposited in matter by protons with initial energy greater than 3 MeV is carried beyond a 5-nm radius

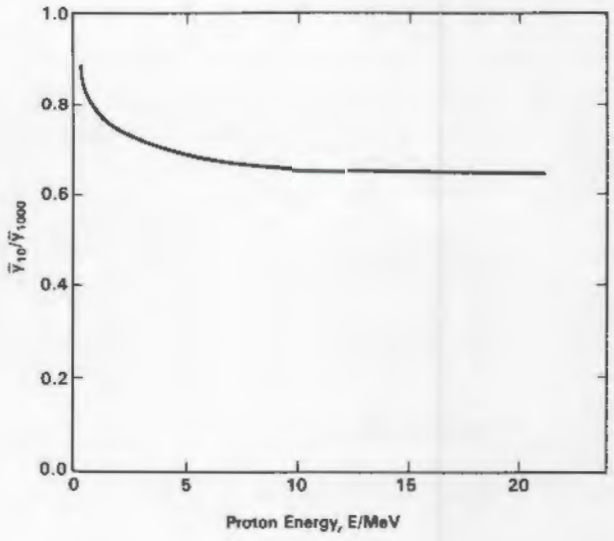

FIGURE 1. The Ratio of Lineal Energy in 10-nm- and 1000-nm-Diameter Sites Is Nearly Constant for Protons Above 5 MeV

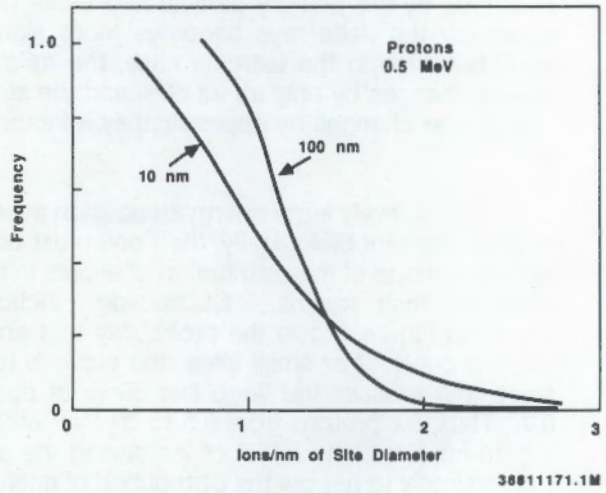

FIGURE 2. The Distribution Functions for Protons Crossing Through the Centers of 10-nm and 1000-nm Sites Cross at Approximately the Same Probability for a Wide Range of Energies. Energy deposition in the large site is an adequate indication of large events in the small site.

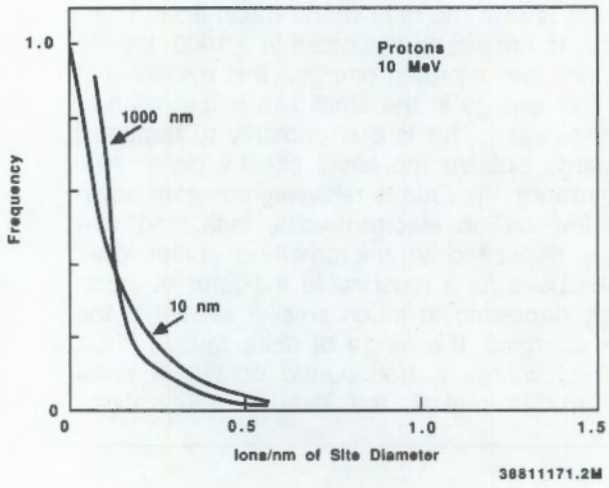

around its track by secondary electrons (delta rays). Experimental work using relatively large simulated site sizes (Glass and Roesch 1972) suggests that if only delta rays interact with a site, the energy deposition is nearly independent of the primary ion energy as well as the distance from the site to the track. This can be understood based on the characteristics of electron tracks. An electron can transfer any fraction of its energy to another electron in a collision, so a characteristic distribution of electron energies develops after monoenergetic electrons have undergone only a few collisions. Thus, electron spectra differ only with respect to the frequency of the highest-energy electrons, and since these have low stopping power, they contribute very little to the energy-deposition distribution. To illustrate this for very small sites, the lineal energy in random 10-nm-diameter sites irradiated by electrons of different initial energies is illustrated in Figure 3. It is evident that the distribution of delta-ray events is essentially independent of the initial particle energy. Thus the energy deposition in large sites, which is a good indication of the total amount of energy transferred by delta rays, can be used to estimate the amount of biological damage caused through this mechanism as well as that caused by the primary ionizations.

References

Bond, V. P., and M. N. Varma. 1983. "A Stochastic, Weighted Hit Size Theory of Cellular Radiobiological Action." In *Radiation Protection*, eds. J. Booz and H. G. Ebert, Commission of the European Communities.

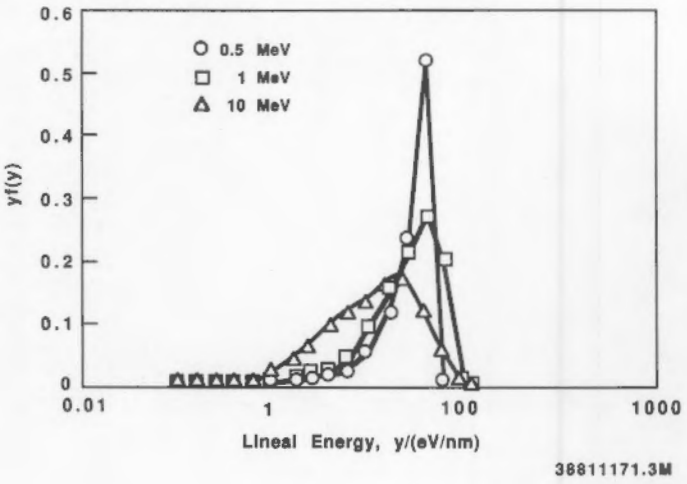

FIGURE 3. Calculated Lineal-Energy Distributions in Small Sites Are Similar for a Wide Range of Initial Electron Energies

Glass, W. A., and W. C. Roesch. 1972. "Measurement of Ionization Distribution in Tissue-Equivalent Gas." *Radiat. Res.* 49:477-494.

Goodhead, D. T. 1977. "Inactivation and Mutation of Cultured Mammalian Cells by Aluminum Characteristic Ultrasoft X-Rays." *Int. J., Radiat. Biol.* 32:43-70.

International Commission on Radiation Units and Measurements (ICRU). 1986. "The Quality Factor in Radiation Protection." Report 40 ICRU, Bethesda, Maryland.

Kellerer, A. M., Y. P. Lam, and H. H. Rossi. 1980. "Biophysical Studies with Spatially Correlated Ions, 4. Analysis of Cell Survival Data for Diatomic Deuterium." *Radiat. Res.* 83:511-528.

Wilson, W. E., and H. G. Paretzke. 1980. "Calculation of Ionization Frequency Distributions in Small Sites." *Radiat. Res.* 81:326-335.

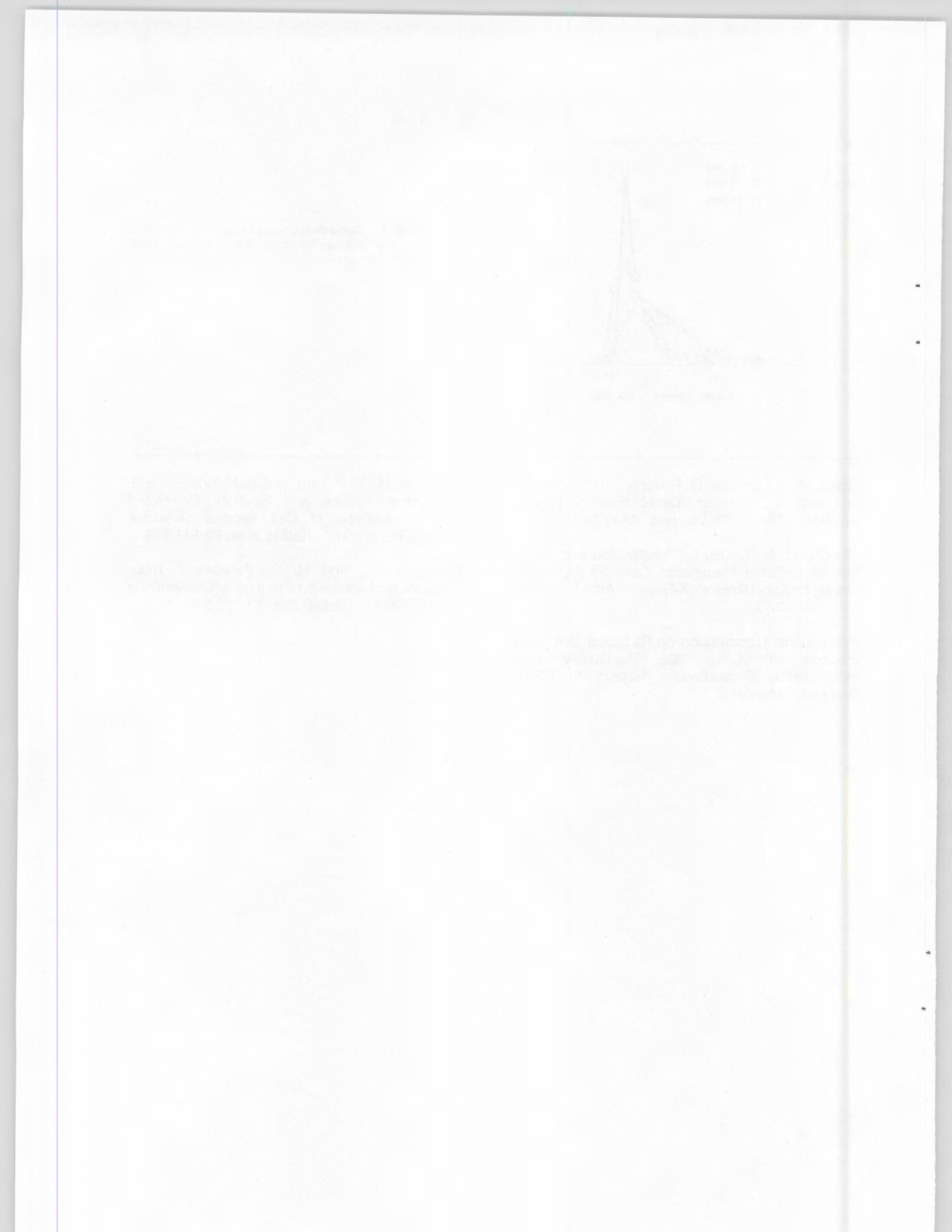

Testing Cell Response Models

The effects of ionizing radiation on living systems begin with the physical processes of energy deposition and develop through many stages of chemical reaction and biological response. The dosimetry task attempts to test alternative models that may organize the available data into a self- consistent system. In the Modeling Cellular Response program, models that are characteristic of specific biochemical mechanisms or groups of mechanisms are contrasted in order to determine whether they produce different consequences at the cellular level. When differences that would be statistically significant at the precision of realistic experiments are found, suitable experiments are designed. In general, experiments using a well-characterized cell line are preferred, since more can be learned about specific mechanisms and their interactions by studying one system in detail.

Mathematical modeling and cellular studies complement each other. New experimental techniques in molecular biology sometimes result in discovery of new mechanisms. When these mechanisms are included in models, the resulting changes in the predicted effects of specific irradiation regimes inspire new experiments. Often the results of these experiments show deviations from the predictions, which in turn suggest other mechanisms to be tested. For example, we have recently found that mechanisms such as enzyme pool depletion, concentration-dependent misrepair, and sublethal damage interaction are not adequate to account for the observed interaction of dose and repair time on the reproductive survival of plateau-phase Chinese hamster ovary (CHO) cells. Other mechanisms, such as the effect of chromosome structure on the accessibility of damage to repair, are being investigated to determine whether they play a role.

Multiple Split-Dose Repair in Plateau-Phase Mammalian Cells[a]

J. M. Nelson, L. A. Braby, and N. F. Metting

Repair of ionizing radiation damage is a major contributing factor altering the response of cells irradiated at low doses and dose rates. Understanding the nature of such time-dependent processes is essential to understanding the action of the radiation itself. Changes in survival probability, which are nonlinear with dose, are observed in both split-dose and delayed-plating experiments. The increase in survival resulting from splitting a dose into two or more fractions separated by variable time intervals was first observed in *Chlamydomonas reinhardi* (Jacobson 1957) and later studied in considerable depth using mammalian cells (Elkind and Sutton 1959); this increase contributes to a shoulder on the survival curve. Since it was originally assumed to result from enzymatic repair of rather innocuous nonlethal lesions which could become lethal only if they were allowed to combine or interact with additional damage, repair observed in split-dose measurements was called "sublethal damage repair."

We have used split-dose experiments to investigate the kinetics of repair in terms of enhancement of reproductive survival of starved plateau-phase CHO cells. The results of these experiments demonstrate two distinct components of repair, one having a characteristic time of about 53 min for the removal of a lesion, the other, about 18 h. The rate at which each component removes damage and the fraction of the total damage that each removes appears to be independent of the initial amount of damage produced, i.e., dose. This lack of dose dependence is not consistent with some simple models of ionizing radiation damage and repair, such as those which assume saturation of a repair process or depletion of enzyme pools. It is recognized that survival depends on dose; however, these interaction models assume that the amount of damage removed, rather than the fraction of damage removed is independent of dose. In addition, the relationship between the amounts of each type of damage affected and the doses involved appears to be consistent with models which assume that only a portion of the initial damage is directly accessible to the repair systems or that the initial damage consists of a mixture of potentially lethal and sublethal lesions, repaired by processes sharing a common rate-limiting step.

Our paper describes the experimental techniques and analytical methods by which these conclusions were obtained. It also describes the growth characteristics and details of our stationary-phase CHO cultures, which have provided the test

(a) Summary of a paper submitted to *Radiation Research*

system capable of measuring the longer characteristic repair times.

References

Elkind, M. M., and H. Sutton. 1959. "X-Ray Damage and Recovery in Mammalian Cells in Culture." *Nature* 184:1293-1295.

Jacobson, B. S. 1957. "Evidence for Recovery from X-ray Damage in *Chlamydomonas*." *Radiat. Res.* 7:394-406.

Relative Split-Dose and Delayed-Plating Effects Following Low Doses of X-Radiation

J. M. Nelson, L. A. Braby, and N. F. Metting

If we assume that the dose dependence observed in the shoulder region of a mammalian cell survival curve results from the removal or alteration of radiation damage by biochemical processes within the cell, then we must accept that survival, and perhaps other endpoints, are affected by both the accuracy of these damage modification processes, and the consequences of unrepaired damage which remains behind. Saturation models assume that damage is lethal unless it has been repaired. Interaction models, including the accumulation models and the lethal-potentially-lethal (LPL) model (Curtis 1985), assume that part of the damage becomes lethal or irreparable through its interaction with additional damage. Damage production is assumed to be proportional to dose for both categories of models. Therefore, we conclude that the lower the dose, the lower the opportunity (and consequently, probability) for damage interaction; the expression of damage not involving interaction should dominate at lower doses.

Since processes involving damage interaction strongly influence split-dose survival, while processes such as repair saturation are most readily observed in delayed-plating experiments, it is conceptually possible to identify sublethal and potentially lethal damage and to distinguish between them by comparing cellular repair capacity under these two experimental conditions. Last year we began comparing survival of plateau-phase Chinese hamster ovary (CHO) cells following split-dose and delayed-plating procedures at increasingly lower doses. At that time we reported that neither damage nor repair was detectable by either the split-dose or delayed-plating procedure, i.e., clonogenic survivals were not statistically different from controls following doses of 1 Gy or less (Braby, Nelson, and Metting 1987). These findings were based on a rather limited number of preliminary experiments and were plagued with technical complications as described in that report. Nevertheless, even by these early studies it was apparent that the increase in effectiveness of delayed-plating repair, predicted by models incorporating binary misrepair, did not occur in our stationary-phase CHO cells; this finding remains. After gaining control of the problems referred to above, we have continued these low-dose studies, the most recent of which have been done at doses as low as 0.25 Gy.

For these experiments, clonogenic cell survival is determined following two fractions separated by a variable repair interval (split-dose), a single dose followed by the same repair interval (delayed-plating), and a single dose with no time allowed for repair prior to subculture (prompt-plating), for a variety of different doses. These results are plotted in Figure 1 for doses ranging from 0.50 to 8.0 Gy. Mean values are surrounded by error bars indicating ±1 standard deviation (68% confidence limits). In all experiments, the time available for repair was 24 h and doses were given at 1 Gy/min.

At each dose, the effects of damage repair are observed after both the split-dose and delayed-plating procedures, as measured by the enhanced survival relative to cells plated immediately following the exposure. These experiments consistently demonstrate a greater reduction in lethal effects following the split-dose procedure, compared to the delayed-plating procedure, indicating that damage removal during the interfraction interval of a split-dose experiment is more effective than that during the post-irradiation interval of a delayed-plating experiment.

Data such as these suggest that damage interaction is considerably more important in these stationary cells than some modelers have assumed. Such interaction would lead either to the production of lethal products or would render such lethal products irreparable. As can be seen, however, the observed differences are small and become significant only when several experiments are considered together.

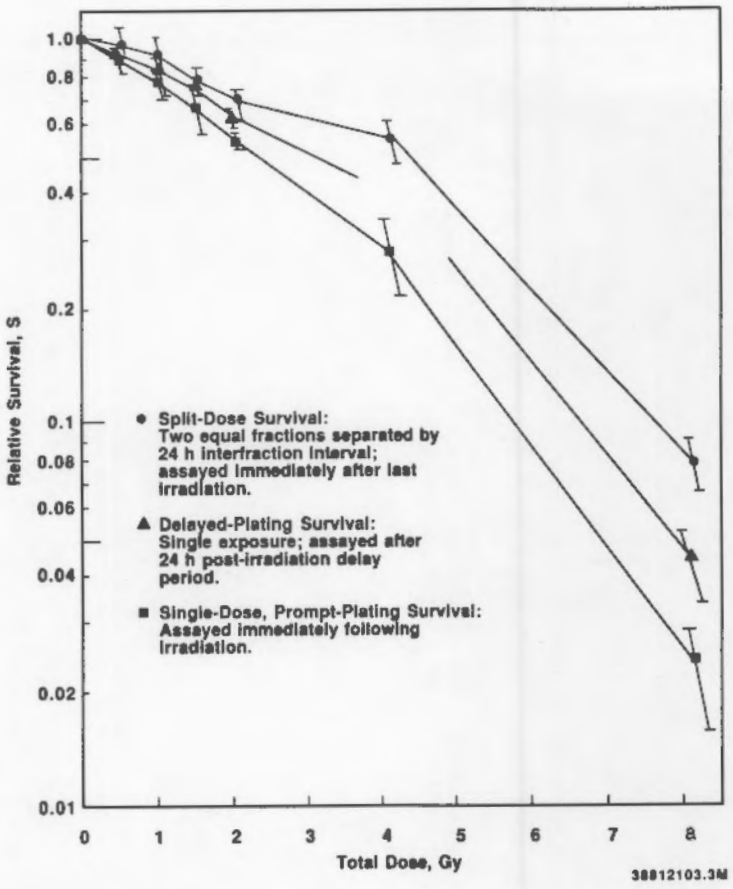

FIGURE 1. Survival of Plateau-Phase CHO Cells After Receiving the Same Dose Administered According to Split-Dose, Delayed-Plating, and Prompt-Plating Techniques. The greater effectiveness of split-dose over delayed-plating repair can be seen at all doses from 0.50 Gy to 8.0 Gy.

References

Braby, L. A., J. M. Nelson, and N. F. Metting. 1987. "The Modification of Damage Following Low Doses." In *Physical Sciences*, part 4 of *Pacific Northwest Laboratory Annual Report for 1987 to the DOE Office of Energy Research*. PNL-6500, Pt. 4, Pacific Northwest Laboratory, Richland, Washington.

Curtis, S. B. 1985. "Lethal and Potentially Lethal Lesions Induced by Radiation--A Unified Repair Model." *Radiat. Res.* 106:252-270.

Radiation Biophysics

The Radiation Biophysics project conducts specific radiobiological studies to test various aspects of the mathematical models developed in the Modeling Cellular Response program. These studies are designed to determine whether specific mathematical expressions, intended to characterize the expected effects of biochemical mechanisms on cellular response, are consistent with the behavior of selected biological systems. Cultured cells are used for these experiments. Since stringent requirements are usually placed on the cellular system, special techniques and culture conditions are used to minimize biological variability. Cells which have ceased progression through the cell cycle are required to study the effects of dose protraction during long-interval split-dose or low-dose-rate studies. In another case, cells of a given age, i.e., from a specific position in the cell cycle, are required to determine changes in biochemical mechanisms which might be associated with observed cell-cycle effects. These carefully characterized cell populations are providing data on the extent of repair following low doses of radiation and on changes in the types of damage that can be repaired as the cells progress toward mitosis.

Other experiments test mechanisms of physical and chemical damage to deoxyribonucleic acids (DNA) and regulation of the repair of that damage. Particular attention has been given to investigating mechanisms leading to the effects of intracellular pools of DNA precursors, collectively referred to as deoxynucleotide triphosphates (dNTPs), on the induction of mutations in Chinese hamster ovary (CHO) cells. Our results suggest that the relative sizes of dNTP pools are involved in the regulation of the rate of DNA synthesis and further, that changes in these pool sizes can dramatically affect the mutagenicity of DNA-damaging agents. This appears to be related to the extent to which DNA damage is repaired before replication, a conclusion based on the observation that an increase in certain dNTP pools can restore the normal mutation induction response to a repair-deficient mutant strain of CHO-K1 cells.

Modulation by Deoxycytidine of DNA Precursor Pools, DNA Synthesis, and the Ultraviolet Sensitivity of a Repair-Deficient CHO Cell Line[a]

C. N. Newman and J. H. Miller

The presence of 2-mM deoxycytidine (CdR) in the growth medium of CHO cells increased the deoxycytidine triphosphate (dCTP) and deoxythymidine tri-phosphate (dTTP) pools in the cell line CHO-K1 and a radiation-sensitive mutant, xrs-5, derived from it. We also observed significant differences in alkaline-sucrose gradient profiles of pulsed-labeled DNA from unirradiated CHO-K1 and xrs-5 cells. For the latter cell line, a sizable fraction of the DNA synthesized during 5 or 10 min of growth subsequent to a 5-min radiolabeling period was found to cosediment with large chromosomal DNA. This characteristic of xrs-5 was dramatically reduced by the presence of 2-mM CdR in the culture medium and the resistance of the mutant to cell killing and mutation induction by ultraviolet (UV) light was increased to nearly that of the parent cell line under these culture conditions. The presence of 2-mM CdR in the growth medium had no effect on the x-ray sensitivity of either CHO-K1 or xrs-5.

If the increased sensitivity of xrs-5 to x-rays and UV light relative to wild-type CHO-K1 is conferred by a single genetic change, then the differential effect of 2-mM CdR in the growth medium on the two cell lines must be related to the coupling between the pathways for the repair of DNA damage induced by the two agents. One possible mechanism for coupling these pathways is that repair of UV-induced pyrimidine dimmers that are closely spaced on opposite strands of the double helix may require rejoining of a DNA double-strand break (DSB). Since xrs-5 may be deficient in the repair of DSBs (Kemp, Sedgwick, and Jeggo 1984), this mechanism should increase the UV sensitivity to xrs-5 relative to that of CHO-K1. The effect of 2-mM CdR on alkaline-sucrose gradient profiles of pulsed-labeled DNA from xrs-5 can be interpreted as a reduction in the rate of replication-fork movement. This change in the pattern of DNA replication, which may be related to changes in the size of DNA precursor pools, could also affect the batch size of the nucleotide excision repair pathway. If the batch size in xrs-5 is reduced by the presence of 2-mM CdR, then removal of UV photoproducts on opposite stands would be less likely to produce a DSB and the

(a) Summary of an invited paper for a special issue of *Mutation Research* on Genetic Aspects Deoxynucleotide Metabolism.

mutant should be less sensitive to the lethal and mutagenic effects of UV light under these culture conditions.

It is also possible that the sensitivity of xrs-5 to both UV light and x-rays results from independent genetic alterations, only one of which is affected by the presence of CdR in the growth medium. This seems unlikely since the probability of selecting a double mutant is extremely low when no selective pressure favoring UV sensitivity was applied (Jeggo, Kemp, and Holiday 1982).

Nevertheless, we are attempting to isolate revertants of xrs-5 with normal x-ray sensitivity. Measuring the UV sensitivity of these revertants will test the independence of the mutant phenotypes.

References

Jeggo, P. A., L. M. Kemp, and R. Holiday. 1982. "The Application of the Microbial 'Tooth-Pick' Technique to Somatic Cell Genetics, and Its Use in the Isolation of X-Ray-Sensitive Mutants of Chinese Hamster Ovary Cells." *Biochimie.* 64:713-715.

Kemp, L. M., S. G. Sedgwick, and P. A. Jeggo. 1984. "X-Ray Sensitive Mutants of Chinese Hamster Ovary Cells Defective in Double-Strand Break Rejoining." *Mutat. Res.* 132:189-196.

Techniques for Monitoring DNA Synthesis

J. M. Nelson, N. F. Metting, M. Nowicki, and L. A. Braby

One of the unexpected results of our studies of the survival of irradiated plateau-phase Chinese hamster ovary (CHO) cells is the slow rate of one of the repair processes observed in split-dose experiments. Although multiple repair rates are commonly observed in a variety of cell systems, the characteristic times for repair are usually ~1 h or less. The ~17-h time we have observed is therefore of special interest. Based on experiments to date, we believe that this characteristic time reflects a rate-limiting step in one or more enzymatic repair processes. However, other possibilities, such as a change in the radiation sensitivity induced by the first fraction of the split-dose irradiation, could also lead to the observed increase in cell survival with interval between doses. Such a change in sensitivity would occur if irradiation causes a fraction of the noncycling cells to progress out of G_2 phase, through mitosis, into G_1 phase, or to begin DNA synthesis and move to a new and more resistant position within S phase. We have investigated these possibilities using a variety of techniques, including cell-cycle distribution analysis by flow cytometry and analysis of the dose-response curves following the initial dose. We have not been able to detect any indication of a change in radiation sensitivity or in the distribution of cells within the cell-cycle. However, the techniques used have limited sensitivity and could not detect a small shift of the population from one phase to another or even within S phase.

The choice of techniques to study changes in the cell-cycle age distribution is necessarily limited because the cells are held in plateau phase by nutrient depletion and addition of even trace amounts of most compounds to the medium could initiate progression through the cycle. One recently developed technique which is compatible with maintaining the cells in stationary phase is the use of fluorescent-labeled antibodies to bromodeoxyuradene (BUdR) for detecting the amount of DNA synthesis occurring in cells while they are held in BUdR-containing medium. BUdR can be added to the cultures after they reach plateau phase but well before irradiation without concern for additional effects such as the radiation damage which would be produced by tritium-labeled compounds. Any perturbation of the plateau phase induced by addition of the BUdR should reach equilibrium before the test irradiation, and its effect can be subtracted out of the results. However, implementation of this technique requires precise flow cytometric measurements and customization of the antibody-staining technique to the specific cell type and culture conditions.

The flow cytometer which we assembled a few years ago had to be moved this year in order to make room for some of the molecular biology experiments, so we took advantage of the opportunity to upgrade the alignment mechanism and the mounting of the detectors. The system now operates reliably with very little maintenance or alignment work, and provides a coefficient of variation of better than 3.5%. This is more than sufficient for the detection of very small changes in BUdR incorporation. Unfortunately, the DNA of plateau-phase CHO cells proved to be resistant to acid denaturation and a long search was required to find the required conditions for thermal denaturation to provide optimum binding of the antibody. The technique has now been established and will be used in conjunction with the next series of repair studies to evaluate the amount of DNA synthesis occurring following single and both between and after split doses.

Mechanisms of Radiation Mutagenesis

J. H. Miller, C. N. Newman, T. L. Morgan,
E. W. Fleck, and J. M. Nelson

We have used exploratory research funds for several years to investigate the molecular characteristics of mutations induced at the hypoxanthine-guanine phosphribosyl transferase (HGPRT) locus in Chinese hamster ovary (CHO) cells by x-ray exposure. The primary tool of these experimental studies is Southern blot analysis (Southern 1975). In this procedure, DNA extracted from either mutant or wild-type cells is digested with restriction enzymes, subjected to gel electrophoresis, transferred to nitrocellulose, and probed with labeled sequences from the gene of interest. When this experimental technique is applied to mutations induced in mammalian cells by ionizing radiation, deletion of genetic information is the most frequent type of mutation found and in many cases these deletions encompass the entire locus under investigation.

We used plateau-phase CHO cells (Nelson, Todd, and Metting 1984) to investigate the dependence of these molecular characteristics of x-ray-induced mutations on dose, dose fractionation, and delayed plating. Our exposure conditions and the results obtained for the total frequency of induced mutations are shown in Table 1. Increasing the exposure level from 2 to 4 Gy caused the induced mutation frequency to increase by about a factor of 4. We are currently investigating this dose response in greater detail and comparing it to the dose dependence of mutation induction at the HGPRT locus in exponentially growing CHO cells. Preliminary results suggest that the plateau-phase cells are hypermutable relative for growing cultures. Table 1 also shows that holding plateau-phase cells in a nonproliferating state for 24 h after radiation exposure does not significantly affect mutation induction at the HGPRT locus. However, splitting the 4-Gy exposure into equal fractions separated by 24 h reduces the frequency of induced mutations by about 25%. These results are similar to the findings of Thacker and Stretch (1983) and are generally interpreted as evidence for induction of repairable submutagenic lesions which are converted to unrepairable precursors of mutations by further interaction of the cells with x-rays.

Table 2 summarizes the results of our Southern blot analysis of 89 mutant clones. A mutant is classified as a full deletion if no HGPRT-specific bands were detected. If mutant and wild-type DNA show the same banding pattern on Southern blots for all restriction digest (at least two in all cases), then the mutant is classified as "no change." Most of the mutations in this class probably result from deletions that are too small to be resolved by our experimental technique. Mutations that exhibit a banding pattern of HGRPT-specific sequences that are different from the wild type are classified as "alterations." Most of the mutations in the last category are probably intragenic deletions; however, terminal deletions that may be as large as the full deletions and mutations produced by insertion and/or rearrangement of HGPRT-specific sequences could also contribute to this class of mutations.

The distinction between "alteration" and "no change" is dependent on the resolution of gel electrophoresis and the choice of restriction enzymes. The classification of a mutant as a full deletion is less dependent on these experimental parameters. For this reason and for simplicity, we have limited our statistical analysis of the data in

TABLE 1. Total Induced Frequencies

Exposure	Induced Mutations, per 10^6 surviving cells
2.0 Gy	27 ± 6
4.0 Gy	96 ± 9
4.0 Gy (24 h delayed plating)	104 ± 22
4.0 Gy (2.0 Gy + 24 h + 2.0 Gy)	70 ± 11

TABLE 2. Mutation Spectrum

Exposure	Number of Clones of Each Mutation Type: Full	Alteration	No Change	Total
2.0 Gy	9 (43%)	8 (38%)	4 (19%)	21
4.0 Gy	20 (69%)	7 (24%)	2 (7%)	29
4.0 Gy (24 h delayed plating)	9 (70%)	2 (15%)	2 (15%)	13
4.0 Gy (2.0 Gy + 24 h + 2.0 Gy)	16 (62%)	8 (31%)	2 (7%)	26
Totals	54 (61%)	25 (28%)	10 (11%)	89

Table 2 to comparison of the fraction of full deletions produced under the different exposure conditions. This fraction increased as the dose in single-exposure immediate-plating experiments increased (9/21 at 2 Gy versus 20/29 at 4 Gy). Chi-square analysis shows that this difference is significant at the 90% confidence level ($p = 0.09$). It is unlikely that this difference is due to contamination of isolates by spontaneous mutants since the spontaneous background is about one-fifth of the total mutation frequency observed after a 2-Gy exposure. Splitting the 4-Gy exposure into equal fractions separated by 24 h shifts the mutation spectrum in the same direction as decreasing the dose to 2 Gy, but the magnitude of the effect is smaller and not statistically significant. As was the case for the total induced frequency, we observed no effect of delayed plating on the spectrum of x-ray-induced mutations.

Since all of the 4-Gy exposures produced essentially the same spectrum of mutations, it is reasonable to pool these data for comparison with the fraction of full deletions induced by the 2-Gy exposure. Pooling the 4-Gy data gives a p value of 0.056 to the dose dependence of the mutation spectrum. To explain this effect we propose that two mechanisms of mutation induction are operating in our cell system. One of these produces mostly intragenic deletions and predominates at low exposure levels. The other mechanism favors multilocus deletions and becomes more important as the dose increases. The nonlinear dose dependence of the total induced mutation frequency should place additional constraints on this model; however, more data at the molecular level are crucial for understanding the dose dependence of the mutation spectrum. The observation that intragenic deletions in our system tend to cluster near the center of the HGPRT locus is a step in this direction.

References

Nelson, J. M., P. W. Todd, and N. F. Metting. 1984. "Kinetic Differences Between Fed and Starved Chinese Hamster Ovary Cells." *Cell Tiss. Kinet.* 17:411-425.

Southern, E. M. 1975. "Detection of Specific Sequences Among DNA Fragments Separated by Gel Electrophoresis." *J. Mol. Biol.* 98:503-517.

Thacker, J., and A. Stretch. 1983. "Recovery from Lethal and Mutagenic Damage During Postirradiation Holding and Low-Dose-Rate Irradiation of Cultured Mammalian Cells." *Radiat. Res.* 96:380-392.

Modeling Cellular Response to Genetic Damage

The objective of this project is to understand the mechanisms that underlie cellular responses to physical and chemical carcinogens with particular emphasis on the role of damage to deoxyribonucleic acids (DNA) in cell killing and mutation induction by ionizing radiation. Our approach is multilevel in that it combines kinetic modeling of cellular response with molecular modeling of the interaction of radiation with living matter. The current focus of the project is investigation of mechanisms and effects of interaction between damaged molecules in cells that have absorbed energy from the radiation exposure. At the cellular level these interactions appear to affect the dose and dose-rate dependence of cell killing by radiation with low linear energy transfer (LET) through accumulation of damage. For high-LET radiation, the interaction between damaged molecules in the same particle track seems to manifest as lesions that are unrepairable or prone to misrepair. Computer simulation of particle tracks by Monte Carlo methods is our basic tool for investigating radiation damage in cells at the molecular level. The current focus of these studies is energy transfer along DNA chains and its effect on the quality and quantity of radiation-induced DNA damage. Our results in this area suggest that sites of damage in DNA that are separated by as much as 100 base pairs may interact in ways that influence the free-radical yield.

Modeling Radiation-Induced DNA Damage

J. H. Miller, W. E. Wilson, and
C. E. Swenberg[a]

Spatial patterns of energy deposition by ionizing radiation have a large effect on the yield of reactive species in the absorbing medium. Our efforts to model the effect of track structure on radical production in simple condensed matter were reviewed in the invited paper "Track Effects in High-LET Radiation Chemistry," which will be published in a special issue of *Radiation Physics and Chemistry* on early events in radiation chemistry. One of the goals of the Modeling Cellular Response project is to understand how these physicochemical aspects of radiation exposure are related to the relative biological effectiveness of radiations with different LET. Computer simulation of damage to DNA by high-LET radiation is one approach to investigating these phenomena. Our contributions to this type of research were reviewed in the paper "Modeling the Biological Effectiveness of High-LET Radiation," which will be published in *Health Physics*. The basic hypothesis underlying this type of modeling is that some types of damage or some combinations of damage are impossible to repair or more likely to be repaired erroneously. This increase in the amount of "refractory" damage with increasing LET of the radiation exposure is generally associated with an increase in the importance of the linear term in the linear-quadratic model of survival dose response. Thus, modeling the LET dependence of cellular responses leads us to consider types of interaction that occur between molecules damaged by the same particle track and the relationship of this interaction to subsequent cellular processing of the damage which determines its refractory quality.

The computational techniques currently being used to model DNA damage by high-LET radiation are based on the assumption that energy deposited in mammalian chromatin produces localized chemical changes. Recent experiments with oriented DNA fibers exposed to neutrons (Arroyo et al. 1986) suggest that this assumption may not be valid. Arroyo and coworkers reported that the yield of neutron-induced free radicals in DNA at 77K is dependent on the orientation of the molecule relative to the neutron flux. We are investigating the hypothesis that these unusual observations are due to intramolecular energy transfer in DNA (Miller et al. 1988a and 1988b). Our results suggest that energy transport over distances greater than 100 base pairs is necessary to explain an orientation dependence of radical yields comparable to that reported by Arroyo et al. Conventional mechanisms of energy migration such as exciton transfer cannot account for transport of energy over distances this large in DNA of heterogeneous base composition. Hence we speculate that coherent transfer of vibrational

(a) Armed Forces Radiobiology Research Institute, Bethesda, Maryland

energy may be involved and we modeled this mechanism by a large asymmetry in thermal diffusion coefficients. A more realistic model based on the induction of solitons by radiation exposure (Bednar 1985) is being developed.

References

Arroyo, C. M., A. J. Carmichael, C. E. Swenberg, and L. S. Myers, Jr. 1986. "Neutron-Induced Free Radicals in Oriented DNA." *Int. J. Radiat. Biol.* 50:789-793.

Bednar, J. 1985. "Electronic Excitations in Condensed Biological Matter." *Int. J. Radiat. Biol.* 48:147-166.

Miller, J. H., W. E. Wilson, C. E. Swenberg, L. S. Myers, Jr., and D. E. Charlton. 1988a. "Modeling Radical Yields in Oriented DNA Exposed to High-LET Radiation." *Radiat. Phys. Chem.* 32:349-353.

Miller, J. H., W. E. Wilson, C. E. Swenberg, L. S. Myers, Jr., and D. E. Charlton. 1988b. "Stochastic Model of Free Radical Yields in Oriented DNA Exposed to Densely Ionizing Radiation." *Int. J. Radiat. Biol.* 53:901-907.

Comparison of Models for the Effect of Split Dose and Delayed Plating on Cell Survival After Radiation Exposure

L. A. Braby, J. M. Nelson, and H. D. Thames[a]

Mathematical models of the response of biological systems to irradiation serve not only as input to the process of estimating risks and setting radiation exposure limits, but also as tools for organizing information and helping to design experiments which clarify our understanding of the mechanisms of damage induction and cellular response. The survival dose response of many cellular systems exposed to ionizing radiation is consistent with the "alpha-beta" model $S = \exp(\alpha D + \beta D^2)$, where S is the surviving fraction after a dose D, and α and A3 β are adjustable parameters. However, there is considerable disagreement over the nature of the mechanisms that lead to this relationship and the way the coefficients will vary with radiation quality and the dose rate or other dose protraction schemes. One fundamental uncertainty concerns the consequences of unrepaired damage: Is all damage lethal unless repaired, or is part of it cumulative (innocuous unless it combines with additional damage) in nature? If all damage is lethal unless it is repaired, what processes limit the extent of repair?

Some models of cellular radiation response are based on the concept that absorption of energy in critical subcellular targets, such as nucleic acids, produces lesions that will be lethal or mutagenic unless they are successfully repaired by cellular enzymatic functions. These models attribute the shoulder that is frequently observed on the survival dose response to depletion of this repair capacity. They explain the enhancement of survival that usually results from protraction of the radiation exposure or holding cells in a nonproliferating state after irradiation to an increase in the time available to repair damage before some critical phase of metabolism in growing cells makes it unrepairable. We have investigated several variations on this hypothesis that involve a degree of misrepair, fixation, or interaction of potentially lethal damage that is proportional to the square of its concentration. All of the models considered thus far predict that survival following delayed plating will exceed the survival following a split-dose exposure with the time between exposures equal to the holding time in the delayed-plating experiment. This prediction is contrary to our observations with plateau-phase Chinese hamster ovary (CHO) cells that survival following a split dose exceeds that of cells given a single dose and a delay before entering the cell cycle.

One of the difficulties in making these comparisons among potentially lethal damage models is the fact pointed out by Curtis (1985) that the time available for repair after replating cannot be directly measured. We are currently conducting experiments in our laboratory with the repair inhibitor adenine-9B-0-arabino furanoside (β ara-A) that may provide information on the amount of damage repaired after replating, if the drug does not also alter the production of specific types of damage. However, since the amount of repair after replating should be similar in split-dose and delated-plating survival studies, it seems unlikely that this uncertainty in the application of models based on the concept of potentially lethal damage can explain the deviation of these models from experimental observations. Currently, the only type of model that explains the higher survival of plateau-phase CHO cells following a split-dose exposure than a comparable delayed-plating treatment is a model that allows for accumulation of damage by interaction of sublethal damage.

(a) M. D. Anderson Hospital, Houston, Texas

Reference

Curtis, S. B. 1985. "Lethal and Potentially Lethal Lesions Induced by Radiation--A Unified Repair Model." *Radiat. Res.* 106:252-270.

Interpreting Survival Observations Using Phenomenological Models[a]

J. M. Nelson, L. A. Braby, and N. F. Metting

It is generally accepted that the dose-rate dependence observed in the shoulder region of the mammalian cell survival curve results from the modification of some fraction of the original damage by biochemical processes within the cell. Although most models assume that enzymatic removal of repairable damage is at least partly responsible for the shoulder at all dose rates, it is still not known whether the same processes are involved at low and high dose rates. It is also not clear what role these processes play in determining the effects of ionizing radiations of different stopping powers. Nevertheless, survival and perhaps other endpoints appear to depend on both the accuracy of the biochemical processes involved in removal or fixation of radiation-induced defects and on the consequences of the unprocessed damage remaining within the cells at any given time.

According to repair-saturation models, if all of the damage produced were lethal or potentially lethal (capable of killing the cell unless repaired), then the curvature observed as a shoulder on survival curves would have to have resulted either from the saturation of one or more repair processes or from a misrepair process which depends on the square of the concentration of damage. Another group of models assumes that some fraction of the damage is not necessarily lethal or potentially lethal, but can be made so only by interacting with additional sublethal damage. The assumptions of these interaction models also lead to a shoulder on the survival curve, but it would be the repair of this sublethal damage that is responsible for the observed dose-rate and split-dose effects. Each of the different mechanisms by which repair might affect the shape of the survival curve reflects a possible mechanism underlying the linear energy transfer (LET) effect. An increase in biological effectiveness with increasing LET would be expected if there was either sublethal damage interaction or a concentration-dependent misrepair process. The repair-saturation concept, at least in its simplest form, should be LET independent. If repair saturation were solely responsible for the dose-effect relationship and an increase in effectiveness with increasing LET could be identified, then there must have been additional damage which was produced as a consequence of the higher energy deposition densities. This leads to the inescapable conclusion that regardless of the model considered, we must assume two or more different types of damage.

We have demonstrated two distinct components of radiation damage repair in plateau-phase CHO cells and have attempted to study each of these independently using split-dose, dose-rate, and delayed-plating techniques. Analysis of the rate of repair shows one component with a mean repair time of less than 1 h and the other, about 18 h. The repair rates and fractions of damage repaired appear independent of the initial amounts of damage produced. Although the two processes may share some common steps in the biochemical sequence, there is strong evidence to indicate that they involve different types of initial damage. Our data have been compared with the predictions of several different phenomenological models. These results do not appear compatible with models which assume simple types of mechanisms, such as the saturation of a rapid repair process or the interaction of pairs of sublesions. Our data are, however, consistent with more complex models which consider combinations of both sublethal and potentially lethal damage or multiple step processes. Unfortunately, since these more complex models involve more parameters, simple agreement with dose-effect curves or repair kinetics can provide only a very weak test of their validity. More complex tests, such as determining dose dependence of the repair capacity, must be used to provide more definitive tests of these models. Such tests facilitate our understanding of the role that biochemical and cellular processes play in modifying radiation damage as a function of dose, dose rate, and radiation quality.

(a) Summary of a paper in the proceedings of the conference "Quantitative Mathematical Models in Radiation Biology," J. Kiefer, ed., published by Springer-Verlag, Heidelberg, 1988.

Publications and Presentations

Publications

Bean, R. M., B. L. Thomas, E. K. Chess, J. G. Pavlovich, and D. L. Springer. 1988. "Quantitative Determination of Polycyclic Aromatic Hydrocarbon Adducts to Deoxyribonucleic Acid Using GC/MS Techniques." Accepted for publication in *Polynuclear Aromatic Hydrocarbons: 11th International Symposium*, Lewis Publishers, Chelsea, Michigan.

Bean, R. M., B. L. Thomas, D. A. Dankovic, D. B. Mann, G. A. Ross, and D. L. Springer. 1988. "Analysis of Classical and Nonclassical Adducts." In *Proceedings of the Twenty-Seventh Hanford Symposium on Health and the Environment*, Richland, Washington (in press).

Braby, L. A., N. F. Metting, W. E. Wilson, and C. A. Ratcliffe. "Characterization of Space Radiation Environment in Terms of the Energy Deposition in Functionally Important Volumes." Conference on High Energy Radiation Background in Space, November 1987, submitted to American Institute of Physics Conference Proceedings Series.

Braby, L. A., and W. D. Reece. "Use of Charged-Particle Microbeams to Study Mechanisms by Carcinogenesis." Submitted to *Nucl. Instrum. Methods*.

Cannon, B. D., T. J. Whitaker, G. K. Gerke, and B. A. Bushaw. 1988. "Anomalous Linewidths and Peak-Height Ratios in 137-Ba Hyperfine Lines." *Appl. Phys.* B47:201-206.

Chess, E. K., B. L. Thomas, D. J. Hendron, and R. M. Bean. 1988. "Mass Spectral Characterization of Derivatized Metabolites of Benzo[a]pyrene." *Biomed. Environ. Mass Spectrometry* 15:485-493.

Dankovic, D. A., D. L. Springer, D. B. Mann, B. L. Thomas, L. G. Smith, and R. M. Bean. 1988. "Preparation of Microgram Quantities BAP-DNA Adducts Using Rat Hepatocytes *In Vitro*." Accepted for publication in *Carcinogenesis*.

DuBois, R. D. "Multiple Ionization in He^+-Rare Gas Collisions." *Phys. Rev. A* (in press).

DuBois, R. D., and L. H. Toburen. "Single and Double Ionization of Helium by Neutral to Fully Stripped Ion Impact." *Phys. Rev. A* (in press).

Hollman, K. W., G. W. Kerby III, M. E. Rudd, J. H. Miller, and S. T. Manson. "Differential Cross Sections for Secondary Electron Production by 1.5 keV Electrons in Water Vapor." *Phys. Rev. A* (in press).

Inokuti, M., M. A. Dillon, J. H. Miller, and K. Omidvar. 1987. "Analytic Representation of Secondary-Electron Spectra." *J. Chem. Phys.* 12:6967-6972.

Manson, S. T., and J. H. Miller. 1987. "Electron Ejection Cross Sections in Electron and Ion Impact Ionization: Ab Initio and Semiempirical Calculations." *Int. J. Quantum Chem.* 21:297-306.

Miller, J. H., W. E. Wilson, S. T. Manson, and M. E. Rudd. 1987. "Differential Cross Sections for Ionization of Water Vapor by High-Velocity Bare Ions and Electrons." *J. Chem. Phys.* 86:157-162.

Miller, J. H., W. E. Wilson, C. E. Swenberg, L. S. Myers, Jr., and D. E. Charlton. 1988a. "Modeling Radical Yields in Oriented DNA Exposed to High-LET Radiation." *Radiat. Phys. Chem.* 32:349-353.

Miller, J. H., W. E. Wilson, C. E. Swenberg, L. S. Myers, Jr., and D. E. Charlton. 1988b. "Stochastic Model of Free Radical Yields in Oriented DNA Exposed to Densely Ionizing Radiation at 77K." *Int. J. Radiat. Biol.* 53:901-907.

Miller, J. H., and W. E. Wilson. "Modeling the Biological Effectiveness of High-LET Radiation." Twenty-Sixth Hanford Life Sciences Symposium, October 1987, *Health Phys.* (in press).

Miller, J. H., and W. E. Wilson. "Track Effects in High-LET Radiation Chemistry." *Radiat. Phys. Chem.* (in press).

Nelson, J. M., L. A. Braby, N. F. Metting, and W. C. Roesch. "Analyzing the Role of Biochemical Processes in Determining Response to Ionizing Radiations." Twenty-Sixth Hanford Life Sciences Symposium, October 1987, paper submitted to *Health Phys.*

Nelson, J. M., L. A. Braby, N. F. Metting, and W. C. Roesch. 1988. "Interpreting Survival Observations Using Phenomenological Models." In *Quantitative Mathematical Models in Radiation Biology*, ed. J. Kiefer, pp. 125-134. Springer-Verlag, Heidelberg.

Nelson, J. M., L. A. Braby, N. F. Metting, and W. C. Roesch. "Multiple Split-Dose Repair in Plateau-Phase Mammalian Cells." Submitted to *Radiat. Res.*

Newman, C. N., H. Hagler, K. Poston, and J. H. Miller. 1988. "Modulation of DNA Precursor Pools, DNA Synthesis, and Ultraviolet Sensitivity of a Repair-Deficient CHO Cell Line by Deoxycytidine." *Mutat. Res.* 200:201-206.

Schlachter, A. S., E. M. Bernstein, M. W. Clark, R. D. DuBois, W. G. Graham, R. H. McFarland, T. J. Morgan, D. W. Mueller, K. R. Stalder, J. W. Stearns, M. P. Stockli, and J. A. Tanis. 1988. "Multiple-Electron Capture in Close Nearly Symmetric Ion-Atom Collisions." *J. Phys. B: At. Mol. Opt. Phys.* 21:L291-L297.

Springer, D. L., D. A. Dankovic, B. L. Thomas, K. L. Hopkins, R. M. Bean, and D. D. Mahlum. 1988. "Metabolism and DNA Binding of BAP in the Presence of Complex Organic Mixtures." In *Health and Environmental Research on Complex Mixtures*, DOE Symposium Series 62, eds. R. H. Gray, E. K. Chess, P. J. Mellinger, R. G. Riley, and D. L. Springer, pp. 369-378. National Technical Information Service, Springfield, Virginia.

Toburen, L. H. "Atomic and Molecular Processes of Energy Loss by Energetic Charged-Particles." To be published as an IAEA TECDOC (in press).

Toburen, L. H. "Spatial Patterns of Ionization in Charged Particle Tracks." Submitted to *Nucl. Instrum. and Methods*.

Whitaker, T. J., B. A. Bushaw, and B. D. Cannon. 1988. "Laser-Based Techniques Improve Isotope Analysis." In *Laser Focus/Electro Optics*, pp. 88-101.

Wilson, W. E., N. F. Metting, and H. G. Paretzke. 1988. "Microdosimetric Aspects of 0.3- to 20-MeV Proton Tracks. I. Crossers." *Radiat. Res.* 115:389-402.

Presentations

Braby, L. A., and W. D. Reece. 1988. "Controlling Dose to Individual Cells." PNL-SA-16029A, presented at the Twenty-Seventh Hanford Life Sciences Symposium, Richland, Washington.

Braby, L. A., and W. D. Reece. 1988. "Use of Charged Particle Microbeams to Study Mechanisms of Carcinogenesis." PNL-SA-16077A, invited paper presented at the 10th Conference on the Application of Accelerators in Research and Industry, Denton, Texas.

Braby, L. A., W. E. Wilson, and N. F. Metting. 1988. "Relationship Between $\bar{Q}$ Defined in Terms of y for 1 μm Sites and Initial Radiation Damage." PNL-SA-14760A, presented at the 7th International Radiation Protection Association-7 Congress, Sydney, Australia.

Bushaw, B. A. 1988. "Trace Isotopic Analysis by High Resolution Ionization Spectroscopy." Invited presentation at the 4th International Laser Science Conference, Atlanta.

Bushaw, B. A., B. D. Cannon, G. K. Gerke, G. R. Janik, and T. J. Whitaker. 1988. "High-Resolution Ionization Spectroscopy for Isotopic Analysis." Invited presentation at the Lasers '88 Conference, Lake Tahoe, Nevada.

Bushaw, B. A., and G. K. Gerke. 1988. "Trace Isotopic Analysis by Double-Resonance Ionization with cw-Lasers and Graphite Furnace Atomization." Presented at the 4th International Symposium on Resonance Ionization Spectroscopy, Gaithersburg, Maryland.

Bushaw, B. A., and T. J. Whitaker. 1988. "Laser Measurements of Pb-210." Presented at OHER Radon Contractors Workshop, Lawrence Berkeley Laboratory, Berkeley, California.

Carr, F. 1988. "Chernobyl Database." Poster session presented at the 33rd Annual Meeting of the Health Physics Society, Boston.

Carr, F. 1988. "Chernobyl Database." Poster session presented at the 36th Annual Meeting of the Radiation Research Society, Philadelphia.

DuBois, R. D. 1988. "Single and Double Ionization of Helium by Hydrogen Atom Impact." PNL-SA-16078A, presented at the 10th Conference on the Application of Accelerators in Research and Industry, Denton, Texas.

Metting, N. F., L. H. Toburen, L. A. Braby, G. Kraft, M. Scholz, F. Kraske, H. Schmidt-Böcking, R. Dörner, and R. Seip. 1988. "Microdosimetry at the UNILAC." PNL-SA-15416A, presented at the 36th Annual Radiation Research Society Meeting, Philadelphia.

Miller, J. H., W. E. Wilson, S. T. Manson, and M. E. Rudd. 1988. "Differential Cross Sections for Electron-Impact Ionization of Water." PNL-SA-15430A, presented at the 36th Annual Radiation Research Society Meeting, Philadelphia.

Morgan, T. L., E. W. Fleck, and J. H. Miller. 1988. "Molecular Characterization of Mutants at the HGPRT Locus in Plateau-Phase Chinese Hamster Ovary Cells Irradiated with 250 KVP X-Rays." PNL-SA-15434A, presented at the 36th Annual Radiation Research Society Meeting, Philadelphia.

Morgan, T. L., E. W. Fleck, B.J.F. Rossiter, and J. H. Miller. 1988. "Molecular Characterization of Mutants at the HGPRT Locus in Chinese Hamster Ovary Cells Irradiated with X-Rays." PNL-SA-16045A, presented at the XVIth International Congress of Genetics, Toronto.

Morgan, T. L., E. W. Fleck, B.J.F. Rossiter, and J. H. Miller. 1988. "Use of Mammalian Cells to Investigate the Genetic Consequences of DNA Damage Induced by Ionizing Radiation." PNL-SA-15899A, presented at the 27th Hanford Life Sciences Symposium, Richland, Washington.

Nelson, J. M., L. A. Braby, and N. F. Metting. 1988. "Importance of Repair to Cellular Radiation Survival." PNL-SA-15663A, presented at the 12th Annual Meeting of the Cell Kinetics Society, Omaha, Nebraska.

Nelson, J. M., L. A. Braby, N. F. Metting, and W. C. Roesch. 1988. "Relative Split-Dose and Delayed-Plating Effects Following Low Doses of X-Radiation." PNL-SA-15417A, presented at the 36th Annual Radiation Research Society Meeting, Philadelphia.

Smith, R. D. 1988. "Electrophoresis-Mass Spectrometry." Presented at the Nineteenth Ohio Valley Chromatography Symposium, Hueston Woods State Park, Ohio.

Smith, R. D., C. J. Barinaga, and H. R. Udseth. 1988. "Electrospray Ionization Phenomena and the Interface of Capillary Zone Electrophoresis and Mass Spectrometry." Presented at the 36th ASMS Conference on Mass Spectrometry and Allied Topics, San Francisco.

Smith, R. D., H. K. Jones, and J. L. Fulton. 1988. "Reverse Micelles in Supercritical Fluid Chromatography." Presented at the 39th Pittsburgh Conference on Analytical Chemistry, New Orleans.

Smith, R. D., H. K. Jones, B. W. Wright, and J. L. Fulton. 1988. "Reverse Micelles in Supercritical Fluid Chromatography." Presented at the 1988 Workshop on Supercritical Fluids, Park City, Utah.

Smith, R. D., J. A. Loo, C. J. Barinaga, and H. R. Udseth. 1988. "An Improved Interface for Capillary Zone Electrophoresis-Mass Spectrometry." Presented at the 36th ASMS Conference on Mass Spectrometry and Allied Topics, San Francisco.

Smith, R. D., H. R. Udseth, and C. J. Barinaga. 1988. "Capillary Zone Electrophoresis-Mass Spectrometry." Presented at the Bay Area Chromatography Colloquim, Foster City, California.

Smith, R. D., H. R. Udseth, and C. J. Barinaga. 1988. "Capillary Zone Electrophoresis-Mass Spectrometry." Presented at the 39th Pittsburgh Conference on Analytical Chemistry, New Orleans.

Smith, R. D., H. R. Udseth, and C. G. Edmonds. 1988. "Capillary Zone Electrophoresis-Mass Spectrometry." Presented at the International Symposium in LC/MS, Freiburg, W. Germany.

Smith, R. D., H. R. Udseth, J. A. Loo, C. J. Barinaga, and C. G. Edmonds. 1988. "Developments in Combined Capillary Zone Electrophoresis-Mass Spectrometry." Presented at 1988 FACSS Meeting, Boston.

Smith, R. D., B. W. Wright, and H. R. Udseth. 1988. "SFC/MS and CZE/MS: High Efficiency Separation Techniques Combined with Mass Spectrometry." Presented at the 39th Pittsburgh Conference on Analytical Chemistry, New Orleans.

Tingey, J. M., R. D. Smith, and J. L. Fulton. 1988. "Solvatochromic Studies of Reverse Micelles in Supercritical Fluids." Presented at the ACS Symposium, Toronto.

Toburen, L. H. 1988. "Atomic and Molecular Processes of Energy Loss by Energetic Charged Particles." PNL-SA-15817A, invited paper presented at the International Atomic Energy Agency (IAEA) Advisory Group Meeting on Atomic and Molecular Data for Radiotherapy, Vienna.

Toburen, L. H. 1988. "Ion-Atom Collision Processes: A Radiological Physics Prospective." PNL-SA-15660A, presented at the University of Nevada-Reno.

Toburen, L. H. 1988. "Spatial Patterns of Ionization in Charged-Particle Tracks." PNL-SA-16036A, invited paper presented at the 10th Conference on the Application of Accelerators in Research and Industry, Denton, Texas.

Udseth, H. R., H. T. Kalinoski, and R. D. Smith. 1988. "Applications of SFC-MS to Toxins and Compounds of Biological Interest." Presented at the 36th ASMS Conference on Allied Topics, San Francisco.

Wilson, W. E., J. H. Miller, and D. B. Olsen. 1988. "Microscopic Dosimetry of Photon Irradiated Oocytes." PNL-SA-15418A, presented at the 36th Annual Radiation Research Society Meeting, Philadelphia.

Wright, B. W., H. R. Udseth, and R. D. Smith. 1988. "Recent Applications of SFC-MS." Presented at the 1988 Workshop on Supercritical Fluids, Park City, Utah.

Author Index

Author Index

Distribution

Distribution

FOREIGN

G. E. Adams, Director
Medical Research Council
Radiobiology Unit
Harwell, Didcot
Oxon OX11 ORD
ENGLAND

D. C. Aumann
Institut für Physikalische Chemie
Universität Bonn
Abt. Nuklearchemie
Wegelerstrasse 12
5300 Bonn 1
FEDERAL REPUBLIC OF GERMANY

M. R. Balakrishnan, Head
Library & Information Services
Bhahda Atomic Research Centre
Central Complex
Trombay, Bombay - 400 085
INDIA

G. W. Barendsen
Laboratory for Radiobiology
AMC, FO 212
Meibergdreef 9
1105 AZ Amsterdam
THE NETHERLANDS

A. M. Beau, Librarian
Département de Protection Sanitaire
Commissariat á l'énergie Atomique
BP No. 6
F-92265 Fontenay-aux-Roses
FRANCE

G. Bengtsson,
Director-General
Statens Stralskyddsinstitut
Box 60204
S-104 01 Stockholm
SWEDEN

D. J. Beninson
Gerencía de Protección Radiológica y Seguridad
Comisión Nacional de Energía Atómica
Avenida del Libertador 8250
2° Piso Of. 2330
1429 Buenos Aires
ARGENTINA

J. Booz
KFA Jülich Institut für Medezin
Kernsforschungsanlage Jülich
Postfach 1913
D-5170 Jülich
FEDERAL REPUBLIC OF GERMANY

A. Brink
SASOL-One Limited
P.O. Box 1
Sasolburg 9570
REPUBLIC OF SOUTH AFRICA

M. J. Bulman, Librarian
Medical Research Council
Radiobiology Unit
Harwell, Didcot
Oxon OX11 ORD
ENGLAND

Cao Shu-Yuan, Deputy Head
Laboratory of Radiation Medicine
North China Institute of Radiation Protection
P.O. Box 120
Tai-yuan, Shan-Xi
THE PEOPLE'S REPUBLIC OF CHINA

M. Carpentier
Commission of the European Communities
200 rue de la Loi
J-70 6/16
B-1049 Brussels
BELGIUM

Chen Xing-An
Laboratory of Industrial Hygiene
Ministry of Public Health
2 Xinkang Street
Deshengmenwai, Beijing
THE PEOPLE'S REPUBLIC OF CHINA

R. Clarke
National Radiological Protection Board
Harwell, Didcot
Oxon OX11 ORQ
ENGLAND

Commission of the European Communities
DG XII - Library SDM8 R1
200 rue de la Loi
B-1049 Brussels
BELGIUM

Deng Zhicheng
North China Institute of Radiation Protection
Tai-yuan, Shan-Xi
THE PEOPLE'S REPUBLIC OF CHINA

Director
Commissariat á l'énergie Atomique
Centre d'Etudes Nucléaires
Fontenay-aux-Roses (Seine)
FRANCE

Director
Commonwealth Scientific and Industrial Research Organization
Aspendal, Victoria
AUSTRALIA

Director
Laboratorio di Radiobiologia Animale
Centro di Studi Nucleari Della Casaccia
Comitate Nazionale per l'Energia Nucleare
Casella Postale 2400
I-00100 Roma
ITALY

D. Djuric
Institute of Occupational and Radiological Health
11000 Beograd
Deligradoka 29
YUGOSLAVIA

L. Feinendegen, Director
Institut für Medezin
Kernsforschungsanlage Jülich
Postfach 1913
D-5170 Jülich
FEDERAL REPUBLIC OF GERMANY

G. B. Gerber
Radiobiology Department
Commission of the European Communities
200 rue de la Loi
B-1049 Brussels
BELGIUM

D. Goodhead
Medical Research Council
Radiobiology Unit
Harwell, Didcot
Oxon OX11 ORD
ENGLAND

T. Jaakkola
University of Helsinki
Department of Radiochemistry
Unioninkatu 35, 00170
Helsinki 17
FINLAND

Jiang Shengjie, Standing Vice President
Chinese Nuclear Society
P.O. Box 2125
Beijing
THE PEOPLE'S REPUBLIC OF CHINA

K. E. Lennart Johansson
National Defense Research Institute
FOA 45 1
S-901-82 Umeå
SWEDEN

A. M. Kellerer
Institut für Medezin Strahlenkunde
Universität Würzburg
Versbacher Strasse 5
D-8700 Würzburg
FEDERAL REPUBLIC OF GERMANY

H.-J. Klimisch
BASF Aktiengesellschaft
Abteilung Toxikologie, Z470
D-6700 Ludwigshafen
FEDERAL REPUBLIC OF GERMANY

A. Kövér
Nuclear Ressearch Institute of Hungary
Hungarian Academy of Science
P.O. Box 51
H-4001 Debrecen
HUNGARY

G. H. Kraft
c/o GSI Postbox 110541
Planck Str.
D-6100 Darmstadt
FEDERAL REPUBLIC OF GERMANY

T. Kumatori, Director
National Institute of Radiological Sciences
9-1, Anagawa-4-chome
Chiba-shi 260
JAPAN

J. R. A. Lakey, Director
Department of Nuclear Sciences & Technology
Royal Naval College, Greenwich
London SE10 9NN
ENGLAND

H. P. Leenmouts
National Institute of Public Health & Environmental Hygiene
P.O. Box 1
NL-3720 BA Bilthoven
THE NETHERLANDS

Li De-Ping
Professor and Director of North China Institute of Radiation Protection, NMI
Tai-yuan, Shan-Xi
THE PEOPLE'S REPUBLIC OF CHINA

Librarian
Centre d'Etudes Nucléaires de Saclay
P.O. Box 2, Saclay
Fig-sur-Yvette (S&O)
FRANCE

Librarian
CSIRO
314 Albert Street
P.O. Box 89
East Melbourne, Victoria
AUSTRALIA

Librarian
HCS/EHE
World Health Organization
CH-1211 Geneva 27
SWITZERLAND

Librarian
Kernforschungzentrum Karlsruhe
Institut für Strahlenbiologie
Postfach 3640
D-75 Karlsruhe 1
FEDERAL REPUBLIC OF GERMANY

Librarian
Max-Planck-Institut für Biophysics
Forstkasstrasse
D-6000 Frankfurt/Main
FEDERAL REPUBLIC OF GERMANY

Librarian
Medical Research Council
Radiobiology Unit
Chilton
Oxon OX11 ORD
ENGLAND

Librarian
Ministry of Agriculture, Fisheries & Food
Fisheries Laboratory
Lowestoft, Suffolk NR33 OHT
ENGLAND

Librarian
National Institute of Radiological Sciences
9-1, Anagawa-4-chome
Chiba-shi 260
JAPAN

Librarian
Supervising Scientist for the Alligator Rivers Region
Level 23, Bondi Junction Plaza
P.O. Box 387
Bondi Junction NSW 2022
AUSTRALIA

Library
Atomic Energy Commission
Risø, Roskilde
DENMARK

Library
Atomic Energy Commission of Canada, Ltd.
Whiteshell Nuclear Research Establishment
Pinawa, Manitoba ROE 1L0
CANADA

Library
Department of Meteorology
University of Stockholm
Arrhenius Laboratory
S-10691 Stockholm
SWEDEN

Ma Fubang, Director
Chief Engineer
Institute of Atomic Energy
P.O. Box 275
Beijing
THE PEOPLE'S REPUBLIC OF CHINA

A. M. Marko, Director
Atomic Energy Commission of Canada, Ltd.
Biology and Health Physics Division
Chalk River Nuclear Laboratories
P.O. Box 62
Chalk River, Ontario
KOJ 1JO
CANADA

R.G.C. McElroy
Atomic Energy Commission of Canada, Ltd.
Dosimetric Research Branch
Chalk River, Ontario K0J1J0
CANADA

J. C. Nénot, Deputy Director
Département de Protection
Centre d' Etudes Nucléaires
BP No. 6
F-92260 Fontenay-aux-Roses
FRANCE

H. G. Paretzke
GSF Institut für Strahlenschutz
Ingolstadter Landstrassé 1
D-8042 Neuherberg
FEDERAL REPUBLIC OF GERMANY

O. Pavlovski
Institute of Biophysics
Ministry of Public Health
Givopisnaya 46
Moscow D-182
USSR

D. H. Perison
Atomic Energy Research Establishment
Health Physics and Medical Division B.
364 Harwell, Didcot
Berkshire
ENGLAND

V. Prodi
Department of Physics
University of Bologna
Via Irnerio 46
I-40126 Bologna
ITALY

Reports Librarian
Harwell Laboratory, Bldg. 465
UKAEA
Harwell, Didcot
Oxon OX11 ORB
ENGLAND

P. J. A. Rombout
Inhalation Toxicology Department
National Institute of Public Health and Environmental Protection
P.O. Box 1
NL-3720 BA Bilthoven
THE NETHERLANDS

M. Rzekiecki
Commissariat à l'énergie Atomique
Centre d'Etudes Nucleaires de Cadarache
BP No. 13-St. Paul
Les Durance
FRANCE

H. Smith
International Commission on Radiological Protection
P.O. Box 35
Didcot
Oxon OX11 ORJ
ENGLAND

J. W. Stather
National Radiological Protection Board
Building 383
Chilton, Didcot
Oxon OX11 ORQ
ENGLAND

M. J. Suess
Regional Officer for
Environmental Hazards
World Health Organization
8, Scherfigsvej
DK-2100 Copenhagen
DENMARK

Sun Shi-quan, Head
Radiation-Medicine
Department
North China Institute of
Radiation Protection, MNI
P.O. Box 120
Tai-yuan, Shan-Xi
THE PEOPLE'S REPUBLIC
OF CHINA

J. W. Thiessen
Radiation Effects Research
Foundation
5-2 Hijiyama Park
Minami-Ku
Hiroshima 732
JAPAN

D. Van As
Atomic Energy Board
Private Bag X 256
Pretoria 0001
REPUBLIC OF SOUTH
AFRICA

Vienna International Centre
Library
Gifts and Exchange
P.O. Box 100
A-1400 Vienna
AUSTRIA

Wang Hengde
North China Institute of
Radiation Protection
P.O. Box 120
Tai-yuan, Shan-Xi
THE PEOPLE'S REPUBLIC
OF CHINA

Wang Renzhi
Institute of Radiation
Medicine
11# Tai Ping Road
Beijing
THE PEOPLE'S REPUBLIC
OF CHINA

Wang Ruifa, Associate
Director
Laboratory of Industrial
Hygiene
Ministry of Public Health
2 Xinkang Street
P.O. Box 8018
Deshengmenwai, Beijing
100088
THE PEOPLE'S REPUBLIC
OF CHINA

Wei Lü-Xin
Laboratory of Industrial
Hygiene
Ministry of Public Health
2 Xinkang Street
Deshengmenwai, Beijing
100088
THE PEOPLE'S REPUBLIC
OF CHINA

B. C. Winkler, Director
Licensing
Raad Op Atomic
Atoomkrag Energy Board
Privaatsk X 256
Pretoria 0001
REPUBLIC OF SOUTH
AFRICA

Wu De-Chang
Institute of Radiation
Medicine
27# Tai Ping Road
Beijing
THE PEOPLE'S REPUBLIC
OF CHINA

DOMESTIC

W. R. Albers
EH-12, GTN
Department of Energy
Washington, DC 20545

D. Anderson
ENVIROTEST
1108 NE 200th Street
Seattle, WA 98155-1136

J. A. Auxier
IT/Radiological Services
Laboratory
1550 Bear Creek Road
P.O. Box 549
Oak Ridge, TN 37831

F. Badgley
13749 NE 41st Street
Seattle, WA 98125

R. E. Baker
8904 Roundleaf Way
Gaithersburg, MD
20879-1630

R. M. Baltzo
Radiological Safety Division
University of Washington
Seattle, WA 98105

R. W. Barber
EH-131, GTN
Department of Energy
Washington, DC 20545

A. D. Barker
Battelle Columbus
Laboratories
505 King Avenue
Columbus, OH 43201

N. F. Barr
ER-72, GTN
Department of Energy
Washington, DC 20545

J. R. Beall
ER-72, GTN
Department of Energy
Washington, DC 20545

D. Beirman
Central Intelligence Agency
Attn: OIR/DSD/DB
Washington, DC 20505

W. R. Bibb
Energy Programs and
Support Division
Department of Energy
P.O. Box B
Oak Ridge, TN 38731

L. C. Brazley, Jr.
NE-22, GTN
Department of Energy
Washington, DC 20545

D. J. Brenner
Radiological Research Lab
College of Physicians and Surgeons
Columbia University
630 W. 168th Street
New York, NY 10032

G. Burley
Office of Radiation Programs, ANR-458
Environmental Protection Agency
Washington, DC 20460

W. W. Burr, Chairman
Medical & Health Sciences Division
Oak Ridge Associated Universities
P.O. Box 117
Oak Ridge, TN 37830

L. K. Bustad
College of Veterinary Medicine
Washington State University
Pullman, WA 99164-7010

R. J. Catlin
Electric Power Research Institute
3412 Hillview Avenue
P.O. Box 10412
Palo Alto, CA 94303

A. Chatterjee
Lawrence Berkeley Laboratory
MS 29-100
1 Cyclotron Road
Berkeley, CA 94720

N. Cohen
New York University Medical Center
P.O. Box 817
Tuxedo, NY 10987

Council on Environmental Quality
722 Jackson Place, NW
Washington, DC 20503

J. F. Decker
ER-1, FORS
Department of Energy
Washington, DC 20585

Department of Energy
Environment & Health Division
P.O. Box 5400
Albuquerque, NM 87115

G. DePlanque, Director
Department of Energy-EMEL
375 Hudson Street
New York, NY 10014

DOE Office of Scientific and Technical Information (10)

H. Drucker
Argonne National Laboratory
9700 South Cass Avenue
Argonne, IL 60439

G. D. Duda
ER-72, GTN
Department of Energy
Washington, DC 20545

A. P. Duhamel
ER-74, GTN
Department of Energy
Washington, DC 20545

W. H. Ellett
BRER--National Research Council, MH-370
2101 Constitution Avenue, NW
Washington, DC 20418

R. J. Engelmann
11701 Karen
Potomac, MD 20854

S. J. Farmer
17217 77th Avenue W.
Edmonds, WA 98020

W. R. Garrett
Oak Ridge National Laboratory
P.O. Box 2008
Oak Ridge, TN 37831

T. F. Gesell
Idaho Operations Office
Department of Energy
785 DOE Place
Idaho Falls, ID 83402-4149

R. D. Gilmore, President
Environmental Health Sciences, Inc.
Nine Lake Bellevue Building
Suite 104
Bellevue, WA 98005

G. Goldstein
ER-74, GTN
Department of Energy
Washington, DC 20545

G. H. Gronhovd
Grand Forks Energy Research Center
Department of Energy
Box 8213, University Station
Grand Forks, ND 58202

E. J. Hall
Radiological Research Laboratory
Columbia University
630 West 168th Street
New York, NY 10032

J. W. Healy
51 Grand Canyon Drive
White Rock, NM 87544

F. Hutchinson
Department of Molecular Biophysics & Biochemistry
Yale University
260 Whitney Avenue
P.O. Box 6666
New Haven, CT 06511

D. S. Ingle
Dayton Area Office
DOE - Albuquerque Operations Office
P.O. Box 66
Miamisburg, OH 45342

M. Inokuti
Argonne National Laboratory
9700 South Cass Avenue
Argonne, IL 60439

H. Ishikawa, General Manager
Nuclear Safety Research Association
P.O. Box 1307
Falls Church, VA 22041

A. W. Johnson
Vice President for Academic Affairs
San Diego State University
San Diego, CA 92182

J. F. Johnson
Kenworth Truck Co.
P.O. Box 1000
Kirkland, WA 98033

L. J. Johnson
Idaho National Engineering Lab
IRC MS 2203
P.O. Box 1625
Idaho Falls, ID 83415

G. Y. Jordy, Director
ER-30, GTN
Department of Energy
Washington, DC 20545

G. A. Kolstad
ER-15, GTN
Department of Energy
Washington, DC 20545

R. T. Kratzke
EH-131, GTN
Department of Energy
Germantown, MD 20545

Librarian
Brookhaven National Laboratory
Research Library, Reference
Upton, Long Island, NY 11973

Librarian
Colorado State University
Documents Department--The Libraries
Ft. Collins, CO 80523

Librarian
Electric Power Research Institute
3412 Hillview Avenue
P.O. Box 10412
Palo Alto, CA 94303

Librarian
Health Sciences Library, SB-55
University of Washington
Seattle, WA 98195

Librarian
Lawrence Livermore National Laboratory
University of California
Technical Information Dept., L-3
P.O. Box 808
Livermore, CA 94550

Librarian
Los Alamos National Laboratory
Report Library, MS P364
P.O. Box 1663
Los Alamos, NM 87545

Librarian
Oregon Regional Primate Research Center
505 NW 185th Avenue
Beaverton, OR 97006

Librarian
Washington State University
Pullman, WA 99164-6510

Library
Serials Department (#80-170187)
University of Chicago
1100 East 57th Street
Chicago, IL 60637

J. N. Maddox
ER-73, GTN
Department of Energy
Washington, DC 20545

J. R. Maher
ER-65, GTN
Department of Energy
Washington, DC 20545

C. R. Mandelbaum
ER-32, GTN
Department of Energy
Washington, DC 20545

S. Marks
c/o U.S. Marine Corp. Air Station
ABCC/RERF
FPO
Seattle, WA 98764-5000

H. M. McCammon
ER-75, GTN
Department of Energy
Washington, DC 20545

R. O. McClellan, President
Chemical Industry Institute of Toxicology
P.O. Box 12137
Research Triangle Park, NC 27709

C. B. Meinhold
Radiological Sciences Division
Bldg. 703M
Brookhaven National Laboratory
Upton, Long Lsland, NY 11973

M. L. Mendelsohn
Biomedical and Environmental Research Program
Lawrence Livermore National Laboratory, L-452
University of California
P.O. Box 5507
Livermore, CA 94550

C. Miller
P.O. Box 180
Watermill, NY 11976

S. M. Nealey
Battelle - Seattle
4000 NE 41st Street
Seattle, WA 98105

N. S. Nelson
Office of Radiation Programs, ANR-461
Environmental Protection Agency
401 M Street, SW
Washington, DC 20460

W. R. Ney, Executive Director
National Council on Radiation Protection and Measurements
7910 Woodmont Avenue
Suite 1016
Washington, DC 20014

Nuclear Regulatory Commission
Advisory Committee on Reactor Safeguards
Washington, DC 20555

M. J. O'Brien
Radiation Safety Office, GS-05
University of Washington
Seattle, WA 98195

R. H. Poirier
Battelle Memorial Institute
505 King Avenue
Columbus, OH 43201-2693

R. G. Rader
ER-33, GTN
Department of Energy
Washington, DC 20545

D. P. Rall, Director
National Institutes of Environmental Health Sciences
P.O. Box 12233
Research Triangle Park, NC 27709

L. A. Rancitelli
Battelle Memorial Institute
505 King Avenue
Columbus, OH 43201-2693

J. Rasey
Division of Radiation Oncology
University of Washington Medical School
Seattle, WA 98195

C. R. Richmond
Oak Ridge National Laboratory
4500N, MS-62523
P.O. Box 2008
Oak Ridge, TN 37831-6253

J. S. Robertson
ER-73, GTN
Department of Energy
Washington, DC 20545

S. L. Rose
ER-73, GTN
Department of Energy
Washington, DC 20545

R. D. Rosen, Tech. Librarian
Environmental Measurements Laboratory
Department of Energy
376 Hudson Street
New York, NY 10014

L. Sagan
Electric Power Research Institute
3412 Hillview Avenue
P.O. Box 10412
Palo Alto, CA 94304

R. A. Scarano
Mill Licensing Section
Nuclear Regulatory Commission
Washington, DC 20545

M. Schulman
ER-70, GTN
Department of Energy
Washington, DC 20545

A. Sharkey
Pittsburgh Energy Technology Center
P.O. Box 10940
Pittsburgh, PA 15236

R. Shikiar
Battelle - Seattle
4000 NE 41st Street
Seattle, WA 98105

P. H. Silverman
Lawrence Berkeley Laboratory
Donner Laboratory, Room 466
University of California
Berkeley, CA 94720

W. K. Sinclair, President
National Council on Radiation Protection
7910 Woodmont Avenue
Suite 1016
Bethesda, MD 20814

D. H. Slade
ER-74, GTN
Department of Energy
Washington, DC 20545

J. N. Stannard
University of California
17441 Plaza Animado #132
San Diego, CA 92128

R. W. Starostecki
NE-40, GTN
Department of Energy
Washington, DC 20545

E. T. Still
Kerr-McGee Corporation
P.O. Box 25861
Oklahoma City, OK 73125

J. Stroman
Library
Department of Energy/NIPER
P.O. Box 2128
Bartlesville, OK 74005

Technical Information
Service
Savannah River Laboratory
Room 773A
E. I. duPont de Nemours &
Company
Aiken, SC 29801

R. G. Thomas
ER-72, GTN
Department of Energy
Washington, DC 20545

P. W. Todd
Center for Chemical
Engineering
National Bureau of
Standards (773.10)
325 Broadway
Boulder, CO 80303

E. J. Vallario
15228 Red Clover Drive
Rockville, MD 20853

M. N. Varma
ER-74
Department of Energy
Washington, DC 20545

C. R. Vest
Battelle, Pacific Northwest
Laboratory
Washington Operations
370 L'Enfant Promenade,
Suite 900
901 D Street, SW
Washington, DC 20024

G. J. Vodapivc
DOE - Schenectady Naval
Reactors Office
P.O. Box 1069
Schenectady, NY 12301

G. L. Voelz
Los Alamos National
Laboratory
MS-K404
P.O. Box 1663
Los Alamos, NM 87545

B. W. Wachholz
Radiation Effects Branch
National Cancer Institute
EPN, Room 530
8000 Rockville Pike
Bethesda, MD 20892

R. A. Walters
Assistant to the Associate
Director
Los Alamos National
Laboratory
MS-A114
P.O. Box 1663
Los Alamos, NM 87545

C. G. Welty, Jr.
EH-123, GTN
Department of Energy
Washington, DC 20545

W. W. Weyzen
Electric Power Research
Institute
3412 Hillview Avenue
P.O. Box 10412
Palo Alto, CA 94303

W. E. Wilson, Associate
Director
Nuclear Radiation Center
Washington State University
Pullman, WA 99164

F. J. Wobber
Department of Energy
14 Goshen Court
Gaithersburg, MD
20879-4403

R. W. Wood
PTRD, OHER
ER-74, GTN
Department of Energy
Washington, DC 20545

D. Woodall, Manager
Physics Group
EG&G Idaho, INEL
P.O. Box 1625
Idaho Falls, ID 83415

Zhu Zhixian
Laboratory for
Energy-Related Health
Research
University of California
Davis, CA 95616

ONSITE

DOE Richland Operations Office (2)

E. C. Norman/D. L. Hoff
M. W. Tiernan

Tri-Cities University Center

J. Cooper, Librarian

Hanford Environmental Health

D. B. Breitenstein

Westinghouse Hanford Co.

D. E. Simpson

Pacific Northwest Laboratory (92)

W. J. Apley
S. T. Autrey
R. W. Baalman (5)
J. F. Bagley
W. J. Bair (15)
N. E. Ballou
R. M. Bean
L. A. Braby
B. A. Bushaw
L. L. Cadwell
B. D. Cannon
F. Carr, Jr.
D. B. Cearlock
E. K. Chess
T. D. Chikalla
T. T. Claudson
D. A. Dankovic
J. M. Davidson
D. W. Dragnich
R. D. DuBois
C. G. Edmonds
C. E. Elderkin
D. R. Fisher
J. S. Fruchter
G. K. Gerke
N. E. Geusic
W. A. Glass
R. H. Gray
R. Harty
D. H. Hendren
J. R. Johnson

B. J. Kelman
E. A. Lepel
J. A. Mahaffey
D. B. Mann
N. F. Metting
J. H. Miller
J. T. Munley
J. M. Nelson
J. F. Park
K. A. Parnell
R. W. Perkins
W. D. Reece
G. F. Schiefelbein
L. C. Schmid
C. L. Simpson
R. D. Smith
J. K. Soldat
D. L. Springer
J. A. Stottlemyre
T. S. Tenforde (2)
B. L. Thomas
L. H. Toburen
R. J. Traub
H. R. Udseth
B. E. Vaughan
T. J. Whitaker
R. E. Wildung
W. R. Wiley
J. R. Williams
W. E. Wilson
N. A. Wogman
B. W. Wright
C. W. Wright
Health Physics Department Library
Life Sciences Library (2)
Publishing Coordination
Technical Report Files (5)